

TABLE OF CONTENTS

	Page
INTRODUCTION	1
CHAPTER 1 DENSE DEPLOYMENT OF SMALL-CELLS: MOTIVATIONS AND CHALLENGES	5
1.1 Small-cell networks: a necessary paradigm shift	5
1.1.1 Explosion of data traffic in wireless networks	5
1.1.2 Small-cell heterogeneous network deployment	5
1.1.2.1 Small-cells overview, motivations and operation	5
1.1.2.2 The access modes of small-cells	8
1.1.3 Role in 5G and success factors of network densification	8
1.1.4 Conclusion and discussions	11
1.2 Technical challenges of dense deployment of small-cells	12
1.2.1 Co-existence with macro-cellular network and interference management in small-cells based networks	12
1.2.1.1 Co-tier interference	12
1.2.1.2 Cross-tier interferences	13
1.2.2 Mobility management and handover	13
1.2.3 Neighbouring and self-organizing small-cells networks	15
1.2.4 Conclusion and discussions	16
1.3 Interference and resource management in small-cells heterogeneous networks	16
1.3.1 Interference avoidance and spectrum partitioning in two-tier networks	17
1.3.1.1 Spectrum arrangement in multi-tier systems	18
1.3.1.2 Fractional frequency reuse in HetNets	20
1.3.2 Interference and resource management approaches for OFDMA-based HetNets : a literature review	22
1.3.2.1 Resource Allocation Optimization Problems	22
1.3.2.2 Power Control under Co-channel Assignment	24
1.3.3 Resource management in self-organizing small-cells networks	26
1.3.3.1 Distributed and Cognitive approaches for Self-Organizing Small-cells HetNets	26
1.3.3.2 Cluster based resource management in OFDMA Small-Cells Networks	29
1.3.4 Call admission control in small-cells HetNets	30
1.4 Game theoretic approaches for resource management in HetNets	33
1.4.1 Applications of game theory in wireless communications and networking	33
1.4.2 Coalitional and canonical games and their applications	35
1.5 Recent opportunities: small-cells deployment in the mmWave spectrum	37

1.6	Conclusion of chapter I and proposed research plan	43
CHAPTER 2 QOS-AWARE ADMISSION CONTROL FOR OFDMA FEMTOCELL NETWORKS UNDER FRACTIONAL FREQUENCY-BASED ALLOCATION		
		45
2.1	Introduction	45
2.1.1	Motivation and prior related work	45
2.1.2	Main contribution and organization	47
2.2	System model of the proposed FFR	47
2.2.1	QoS constraints	48
2.3	LTE resource blocks specifications	50
2.4	Admission control policy	52
2.5	Performance analysis	53
2.5.1	Mobility and handover in out of the two-tier network	54
2.5.1.1	Teletraffic flow coefficients	54
2.5.1.2	Calculation of handoff arrival rates	56
2.5.2	Stationary analysis of Markov chains $\Delta_{M1}(t)$ and $\Delta_{M2}(t)$	56
2.5.2.1	Calculation of transition rates	57
2.5.2.2	Calculation of the blocking probabilities	59
2.5.3	Stationary analysis of Markov chains Γ_{F1} and Γ_{F2}	60
2.6	Numerical results	61
2.6.1	Results on the best parameters for resource partitionning	61
2.6.2	Performance results in terms of blocking probability	61
2.7	Conclusion	65
CHAPTER 3 COALITIONAL GAMES FOR JOINT CO-TIER AND CROSS-TIER COOPERATIVE SPECTRUM SHARING IN DENSE HETEROGENEOUS NETWORKS		
		67
3.1	Introduction	67
3.1.1	Motivations and prior related works	67
3.1.2	Main contributions and organization	70
3.2	Problem formulation and motivations	72
3.3	System model	73
3.3.1	Interference set detection	73
3.4	Cross-tier macrocell-smallcells cooperation as coalitional games	76
3.4.1	Proposed game theory approach	76
3.4.2	Definition and formulation of the game	78
3.4.3	Non-emptiness of the core and stability of the grand coalition	79
3.4.4	The proposed canonical game	80
3.4.4.1	Imputation value for the canonical game	80
3.4.5	The proposed coalition structure game	85
3.4.5.1	The weighted Owen value as the imputation value of the CS game	86
3.5	Simulation results and analysis	90

3.5.1	Computational complexity	91
3.5.2	Comparison with other schemes of the art	92
3.5.3	Comparison with other types of access	93
3.5.4	Comparison with other cooperative game solutions	94
3.5.5	Impact of interference degree and user demands	96
3.5.6	Performance analysis of the proposed Weighted Solidarity value	98
3.5.7	Performance evaluation in terms of fairness	99
3.6	Conclusion	103
CHAPTER 4	TOWARDS 1GBPS IN ULTRA-DENSE SYSTEMS : A SPATIAL FREQUENCY REUSE MODEL FOR SMALL- CELLS BASED MMWAVE NETWORKS	105
4.1	Introduction	105
4.1.1	Motivations and prior work	106
4.1.2	Main contributions and organization	107
4.2	System model	109
4.3	Tractable framework on coverage probability	109
4.3.1	Coverage analysis of the macro-tier	112
4.3.1.1	In the macro-tier center zone	112
4.3.1.2	In the macro-tier edge zone	114
4.3.2	Coverage analysis of the smallcell-tier	115
4.3.2.1	Center zone of small-cells	115
4.3.2.2	Edge zone of small-cells	116
4.4	Single user-throughput analysis	116
4.5	Performance evaluation with accurate large-scale distant-dependent pathloss models	117
4.5.1	Path loss model for millimeterwave bands	119
4.5.2	Proposed algorithm for BS association and SINR computation	120
4.5.3	Instantaneous rate computation of a typical user	120
4.6	Numerical results	121
4.6.1	Validation of the proposed model	122
4.6.2	Coverage comparison with other systems	124
4.6.3	Results on user throughput analysis	126
4.6.4	Simulation results on throughput using the accurate path loss models	129
4.7	Conclusion	132
CHAPTER 5	DISCUSSION AND RECOMMENDATIONS	135
5.1	Discussion on future challenges for resource management in 5G networks	135
5.2	Recommendations and potential approaches for further research	138
GENERAL CONCLUSION	141

APPENDIX I APPENDIX OF CHAPTER 3143
APPENDIX II APPENDIX OF CHAPTER 4147
BIBLIOGRAPHY149

LIST OF TABLES

	Page
Table 1.1	Different types of elements in HetNets and their specifications 7
Table 1.2	Different types of interferences in OFMDA-based two-tier networks..... 12
Table 2.1	Frequency measures and number of elements 51
Table 2.2	Key parameters and variables 55
Table 3.1	Numerical values..... 90
Table 3.2	Mean Fairness Index103
Table 4.1	Parameters for alpha plus beta model path loss model120
Table 4.2	Numerical values for the analytical and system-simulation evaluation.....123

LIST OF FIGURES

	Page
Figure 1.1	Cisco forecast of global mobile data traffic from 2015 to 2020 6
Figure 1.2	Global mobile traffic growth by device type..... 6
Figure 1.3	Scenario of co-tier interferences 13
Figure 1.4	Scenario of cross-tier interferences 14
Figure 1.5	Fractional frequency reuse scheme 21
Figure 1.6	Soft frequency reuse scheme 22
Figure 1.7	An exemple of co-tier interference management in cognitive radios 28
Figure 1.8	Transition diagram for the new call bounding scheme 32
Figure 1.9	Trend of commercially available wireless systems: increasing carrier frequency and bandwidth enable increasing data rates..... 38
Figure 1.10	Rain attenuation in mmWave frequencies 39
Figure 1.11	Atmospheric absorption across mm-wave frequencies in dB/km 40
Figure 1.12	Flow chart illustrating the existing resource allocation techniques and situating the contributions of this thesis 44
Figure 2.1	Interference management scheme using an adjusted FFR3 model 49
Figure 2.2	LTE Physical Layer Structure 51
Figure 2.3	Blocking probability of calls connecting to a MBS and FBS in center area versus the percentage of bandwidth allocated to the center macro-area 63
Figure 2.4	Blocking probability of calls connecting to a MBS and FBS in edge area versus the percentage of bandwidth allocated to the center macro-area 63
Figure 2.5	Blocking probability of calls connecting with MBS and FBS in center area versus the outdoor traffic density 64

Figure 2.6	Blocking probability of calls connecting with MBS and FBS in edge area versus the outdoor traffic density	64
Figure 3.1	An illustration of a scenario leading to the proposed coalition formation and coalition structure game	74
Figure 3.2	An illustration of a scenario leading to the proposed coalition formation and canonical game	75
Figure 3.3	General flow chart describing the formation of the coalition structures and the classification of the two game.....	77
Figure 3.4	A snapshot of a dense small-cell networks. The SBSs are modelled by a Poisson process represented by green points. The center red square represents the MBS, the blue triangles represent the MUEs: those with a red point in the centre are served by the MBS; those with a blue point are served by the SBS offering the best SINR. The blue lines represent the link between a SBS and its hosted MUE	91
Figure 3.5	Throughput Cumulative Distribution Function for users of both types: Comparison of the centralized approach, the F-Aloha method and the proposed framework	93
Figure 3.6	Throughput Cumulative Distribution Function for users of both types: Comparison of the proposed framework with the open-access mode and the traditional hybrid-access mode $\delta = 0.8$	94
Figure 3.7	Throughput Cumulative Distribution Function for users of both types: Comparison of the proposed framework with other coalitional games	96
Figure 3.8	Throughput Cumulative Distribution Function for all MUEs of the system: Comparison of the centralized approach, the shapley value, the owen value and the proposed framework	97
Figure 3.9	Throughput Cumulative Distribution Function for all SUEs of the system: Comparison of the centralized approach, the shapley value, the owen value and the proposed framework	98
Figure 3.10	Throughput Cumulative Distribution Function for SBSs inside a union only: Comparison of the centralized approach, the Shapley value, the Owen value and the proposed framework	99

Figure 3.11 Throughput Cumulative Distribution Function for MUEs inside a union only: Comparison of the centralized approach, the Shapley value, the Owen value and the proposed framework100

Figure 3.12 Average gain of the payoff as a function of the interference degree with the hybrid access as basis of comparison ($\delta = 0.8$)100

Figure 3.13 Average gain of the payoff as a function of the level of demand with the hybrid access as basis of comparison ($\delta = 0.8$)101

Figure 3.14 Number of canonical games and CS games played at each iteration of the system for two levels of interferences101

Figure 3.15 Throughput Cumulative Distribution Function for the users of a system participating to a canonical game when the satiation axiom is violated: Comparison of the proposed weighted solidarity value (with the computed weights in algorithm 3.1) and the Solidarity value102

Figure 4.1 Propagation loss in mmWaves frequency bands 28 GHz and 73 GHz using large-scale path loss model108

Figure 4.2 Frequency reuse for millimeterwave bands in small cells based networks110

Figure 4.3 Validation of the proposed analytical model: Analytical coverage probability versus simulated coverage analysis in the macro-tier124

Figure 4.4 Validation of the proposed analytical model: Analytical coverage probability versus simulated coverage analysis in the small-tier125

Figure 4.5 Validation of the proposed analytical model: Analytical coverage probability versus simulated coverage analysis for users from both tiers125

Figure 4.6 Coverage probability for macro-tier (center and edge) under the proposed model compared to no frequency reuse and microwaves systems $\lambda_2 = 100 * \lambda_1$ SBSs deployed127

Figure 4.7 Coverage probability for smallcell-tier under the proposed model compared to no frequency reuse and microwaves systems $\lambda_2 = 100 * \lambda_1$ SBSs deployed127

Figure 4.8 Overall coverage probability under the proposed model compared to no frequency reuse and microwaves systems. $\lambda_2 = 100 * \lambda_1$ SBSs deployed128

Figure 4.9 Overall user throughput distribution (CCDF curves) for different small-cells densities128

Figure 4.10 Small-cell user throughput distribution (CCDF curves) for different small-cells densities129

Figure 4.11 CDF of the achieved throughput for different small cells densities130

Figure 4.12 CDF of the achieved throughput for an LTE system (no mimo and mimo 4*4) for purpose of comparison with the performances of the proposed model Fig.9131

Figure 4.13 Median throughput achieved vs radius ratio (inner/outer) of small-cells132

Figure 4.14 Median throughput achieved vs radius ratio(inner/outer) of macrocells132

LIST OF ABBREVIATIONS

ASC	Agence Spatiale Canadienne
CDF	Cumulative Distribution Function
CSG	Closed Subscribers Group
EnodeB	Evolved Node B
ETS	École de Technologie Supérieure
FBS	Femtocell Base Station
FFR	Fractional Frequency Reuse
FUE	Femtocell User Equipment
HeNB	Home eNodeB
HetNet	Heterogeneous Network
ICIC	Inter-Cell Interference Coordination
IoT	Internet of Things
LTE-A	Long Term Evolution Advanced
LTE	Long Term Evolution
M2M	Machine-to-Machine
MBS	Macrocell Base Station
MeNB	Macro eNodeB
MIMO	Multiple Input Multiple Output
mmWave	Millimeter-wave

MUE	Macrocell User Equipment
NFV	Network Function Virtualization
OFDMA	Orthogonal Frequency-Division Multiple Access
PDF	Probability Density Function
QoE	Quality of Experience
QoS	Quality of Service
SBS	Small-cell Base Station
SCN	Small-cell Network
SDN	Software Defined Networks
SINR	Signal-to-Interference-plus-Noise-Ratio
SFR	Soft Frequency Reuse
SON	Self-Organizing Network
SUE	Small-cell User Equipment

INTRODUCTION

Mobile phones have been one of the fastest-growing consumer technologies in history. While digital mobile phones were introduced in the 1990s, they have grown today to reach more than 6.4 billion and we expect to exceed 50 billion of connected devices across the world by 2020. The astonishing advances of smart phone devices, multimedia applications, social networks led to the explosive growth of traffic and demand for higher data rates and pose several new challenges to the next generation of mobile networks. To accommodate this ever-increasing trend the wireless industry is facing the crucial necessity of increasing the capacity of mobile networks.

In addition to massive Multiple Input Multiple Output (MIMO) systems, millimeter-wave (mmWave) communications, Network Function Virtualization (NFV) and Software Defined Networks (SDN), one of the enabling key technologies to fulfil these requirement is small-cells network densification. Small-cells networks have emerged as an attractive paradigm to provide coverage and capacity in dense networks, and hold great promise for the next generation of wireless communications systems.

Indeed, small-cells Heterogeneous Networks (HetNets) are an important part of operator's strategy to add capacity through dense deployments of low-cost, short-ranged small-cells allowing an aggressive reuse of cellular spectrum. In 2016, small-cells were servicing up to 25% of all mobile traffic. The further deployment of small-cells in rural zones and their extreme densification in urban areas are currently the big hope to resolve the challenge facing the wireless industry of having to increase the capacity of mobile devices by 1000 times (Americas, 2013), and to provide ubiquitous network coverage and a better QoS.

However, the successful rollout and operation of ultra-dense small-cells networks are still facing significant technical challenges and issues among which radio resource management (i.e., interference management, admission control, spectrum allocation) is the most significant.

Thesis organization

This thesis is organized in five chapters as follows:

Chapter 1, presents the technical challenges and the motivations of the dense deployment of small-cells in cellular networks. An overview of the radio resource management problem in multi-tier networks is provided as well as a literature review on the existing methods for radio interference mitigation and resource allocation in HetNets.

The three following chapters cover our research studies investigating three different ways to address the two main challenges of dense small-cells networks: radio interference and resource management.

In Chapter 2, a fractional frequency reuse model is developed in order to cope with cross-tier interference and especially with the deadzone problem caused by the co-existence of small-cells and macrocells tiers. To overcome the capacity limitation inherent with lower frequency reuse, flexibility in the resource sharing of non-used subchannels is allowed through call admission control and overflowing policies. This chapter is mostly based on our published conference paper (Hajir & Gagnon, 2015).

Chapter 3 covers a cooperative approach in self organizing small-cells networks allowing small-cells and the underlying macrocell tier to collaborate and find an agreement for the common resource allocations while offering high overall throughput, fairness and lower complexity in the system. This chapter is a summary of our research based on our published conference (Hajir *et al.*, 2016b) and journal paper (Hajir *et al.*, 2016a)

Chapter 4 is driven by the recent mmWave measurement campaigns and coverage analysis studies showing that roughly three times more small-cells are required to accommodate 5G networks compared to existing 3G and 4G systems. Hence, a frequency reuse model for mmWave

small-cells network is investigated and a model for the system coverage analysis is proposed. This chapter is based on our submitted conference (Hajir & Gagnon, 2017a) and journal paper (Hajir & Gagnon, 2017b). Some of the results of this research study have been presented as part of a poster competition at ACM MobiCom 2016 in New York, where we were rewarded the runner-up best poster award.

The results obtained in this research and the related published or submitted papers to international conferences and journals are listed in the following:

Journal papers:

- Coalitional games for joint co-tier and cross-tier cooperative spectrum sharing in dense heterogeneous networks (Hajir *et al.*, 2016a);
- Towards 1Gbps in ultra-dense systems : a spatial frequency reuse model for small-cells based mmWave Networks (Hajir & Gagnon, 2017b).

Conference papers:

- QoS-aware admission control for OFDMA femtocell networks under fractional frequency reuse allocation (Hajir & Gagnon, 2015);
- Solidarity-based cooperative games for resource allocation with macro-users protection in HetNets (Hajir *et al.*, 2016b);
- Spatial Reuse Model for mmWave frequencies in ultra-dense small-cells networks (Hajir & Gagnon, 2017a).

CHAPTER 1

DENSE DEPLOYMENT OF SMALL-CELLS: MOTIVATIONS AND CHALLENGES

1.1 Small-cell networks: a necessary paradigm shift

1.1.1 Explosion of data traffic in wireless networks

By 2020, 20 billion mobile devices will be connected across the world. Globally, mobile data traffic has doubled in each of the 10 previous years and there are strong indications that this trend will continue and amplify in the next years as (Cisco, Feb. 2014) forecasted in Figure 1.1. Monthly global mobile data traffic will reach 30.6 exabytes by 2020. As shown in Figure 1.2, the emergence of several new technologies such as cloud-based services, the Internet of Things (IoT), Machine-to-Machine communications (M2M), smarter and faster devices, will fuel this trend.

5G wireless networks will emerge between 2020 and 2030 and will have to support massive capacity, connections for at least 100 billion devices, 10 Gbps user experience and very low latency. As a result of the rapid penetration of smart phones, tablets and bandwidth-intensive applications, user data traffic is increasing in an exponential manner. This unprecedented trend lead industries and researchers in academia to look for new technologies capable of supporting high capacity and connectivity.

1.1.2 Small-cell heterogeneous network deployment

1.1.2.1 Small-cells overview, motivations and operation

The proliferation of mobile devices and mobile Internet usage in the past years has led to an increase in the demand for higher capacity and data rates. Recent studies show that the number of mobile-connected devices will exceed the number of people on Earth reaching 10 billion mobile-connected devices and generating a monthly global mobile data traffic of more than

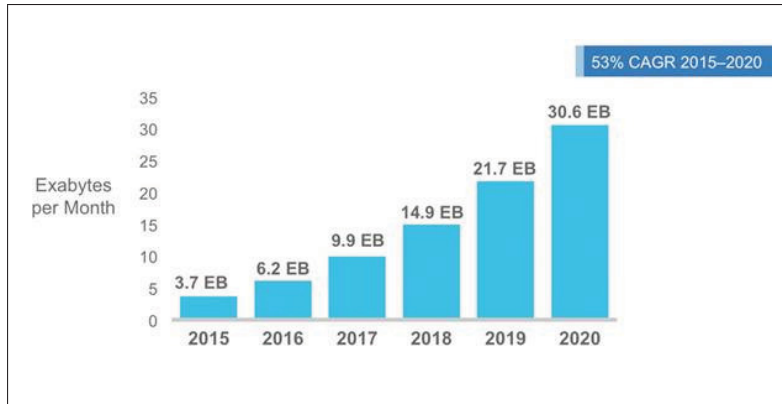


Figure 1.1 Cisco forecast of global mobile data traffic from 2015 to 2020
Taken from Cisco (2016)

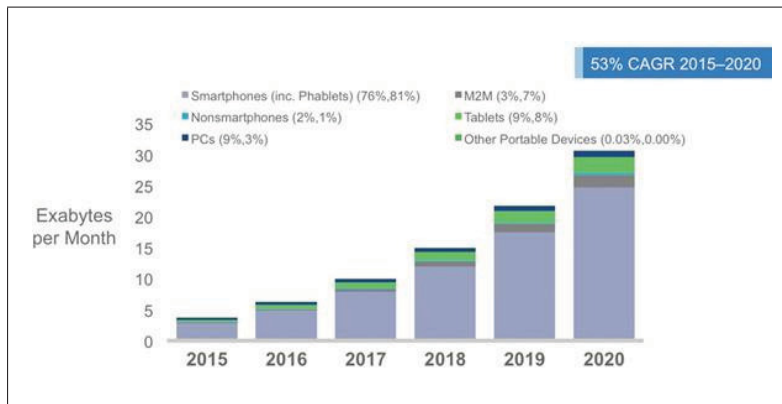


Figure 1.2 Global mobile traffic growth by device type
Taken from Cisco (2016)

15 exabytes (Cisco, Feb. 2014). To address this demand in growth for more cellular services and higher data rates, several technologies and standards have been developed. Typically, innovation is aimed at reaching two objectives: one, improving indoor coverage; and two, increasing the network capacity in future generations of wireless communications systems.

One solution is to enhance the network coverage and capacity by placing transmitters and receivers closer together. In recent years, a HetNet-based deployment model that permits to exploit this strategy is being explored by mobile operators and the research community. A Het-

Net is defined as to a multi-tier cellular network in which the existing homogeneous network is overlaid with additional smaller base stations.

Small-cells are low-power and short-ranged access points operating in licensed spectrum that play an essential role in the improvement of cellular coverage and capacity for homes, enterprises, urban and rural spaces. They include technologies as femtocells, picocells, microcells and metrocells as depicted in Table 1.1.

Femtocells are short-ranged (10-30m) and low-powered (10-100mW) access points, connecting the users to the cellular networks via broadband communications links (DSL, optic fiber) (Saquib *et al.*, 2012). They can also be deployed by the user themselves by plugging-in the devices that can act as wireless routers. This deployment is supported by the fact that more than 50% of voice calls and more than 70% of data traffic are originating indoors. This strategy allows for a higher data rate and increased reliability for users, as well as a reduced amount of traffic on an expensive macrocell network for the operator.

Table 1.1 Different types of elements in HetNets and their specifications

Type of Node	Macrocell	Picocell	Femtocell	Wi-Fi
Coverage	300-2000m	40-100m	10-40m	100-200m
Users location	Outdoor	Outdoor-Indoor	Indoor	Indoor
Power of transmission	40 W	200 mW-2 W	10-100mW	100-200 mW
Backhaul	S1 interface	X2 interface	Internet IP	Internet IP
Deployment	Operator	Operator	Subscriber	Customer
Cost (approx.)	\$60,000/yr	\$10,000/yr	\$200/yr	\$100/yr
QoS	High	High	High	Best-effort

The advantages of the deployment of small-cells overlaying the homogeneous macrocell network are numerous. They are deployed to offload the traffic from the macrocells, improve indoor coverage and cell-edge user performance and enhance spectral efficiency in mobile networks. This last advantages is essential since small-cells enable more subscribers to use the same pool of radio resources via spatial reuse. This allows for a significant improvement of

system capacity and spectrum efficiency. Likewise, given the short distance between the transmitter and the receiver, it is possible to achieve greater signal strength and better QoS.

1.1.2.2 The access modes of small-cells

Among the different types of existing small-cells, some operate under specific access modes that we describe in this subsection. Unlike the MBS accessible to any subscriber of the wireless communication provider, the SBSs that are paid and deployed by the end user may operate under an open, closed or hybrid access mode.

In the open access mode, all customers of the operator have the right to use the resources of any small-cell. As demonstrated in (Lopez-Perez *et al.*, 2009), open access mode improves the overall capacity of the network since macrocell users can connect to nearby femtocells when their resources are not sufficient but the increase of handoff and signalling is major.

In the closed access mode, only the users belonging to the Closed Subscriber Group (CSG) are allowed to connect to the SBSs. Hence, in this mode, access to a SBS is restricted to a handful of pre-registered subscribers. In closed access mode, the power of transmission in small-cells is perceived as interferences to nearby macrocell users.

In the hybrid access mode, a limited amount of small-cells resources are available to all users while the rest are dedicated to CSG users or a certain priority is applied in the access to the small-cell resources in order to protect the subscribed users.

1.1.3 Role in 5G and success factors of network densification

From 1G to 5G each generation is a class of standards associated with typical major technological advances that enable to do use cases. Historically, in 1981 the analog voice with Advanced Mobile Phone System (AMPS) known as 1G, in 1991 digital voice with the apparition of Global System for Mobile Communications (GSM) and Interim Standard 95 (IS-95) known as 2G, the internet data appeared in 2000 with Wideband Code Division Multiple Ac-

cess (WCDMA) and CDMA2000 known as 3G, broadband data in 2008 with Long Term Evolution (LTE) and Worldwide Interoperability for Microwave Access (WiMax) known as 4G and by 2020 we expect the release of 5G that will be built upon both new radio access technologies (RAT) and evolved existing wireless technologies (LTE, High Speed Packet Access (HSPA), GSM and Wi-Fi). This fifth generation 5G has four main classes of fundamental requirements:

- Ability to support massive capacity and massive connectivity: the amount of data the network can serve will need to increase roughly by 1000x from 4G to 5G;
- High data rates: 1Gbps data rate user in average with a 100 Mbps edge rate and tens of Gbps peak rate;
- Extreme low latency : about 1ms roundtrip latency in order to support virtual and enhanced reality, novel cloud-based technologies and other services and applications requiring fast procedure response times;
- Energy and cost saving: low energy consumption and low cost infrastructures are expected for 5G mobile networks.

Beyond radio link improvements, the network topology is changing drastically, essentially with the ultra-dense deployment of small-cells overlaying the existing larger cells, for both outdoor and indoor communications and in different types and sizes. Small-cell densification to give contiguous coverage in the network is believed to be the most promising solution to meet the requirements of 5G and the 1000 X traffic growth.

It is understood from the previous sections that small-cells densification of networks is driven by the increase of demand but we have not yet properly defined the densification concept. As Martin Cooper acknowledged, the advances of wireless system capacity are due to three main factors: increase in the number of wireless infrastructure nodes, increased use of radio spectrum, and improvement in link efficiency. The throughput of a user in a cellular system is

upper-bounded by a variation of Shannon's the well-known capacity :

$$C = m \left(\frac{W}{n} \right) \log_2 \left(1 + \frac{S}{I+N} \right) \quad (1.1)$$

where W denotes the spectrum bandwidth, n the number of users sharing the given bandwidth, m the number of streams between the transmitter and receiver, S the desired signal power, I the interference power and N the noise power at the receiver. This fundamental equation illustrates the key features of cellular system performance and will allow us to explain the densification of wireless networks.

If we want to increase the capacity, we can clearly increase W by using additional spectrum. Or, we can decrease the value of n through cell splitting, by deploying more base stations, hence decreasing the number of users operated by each cell. And finally, we can increase m by using a larger number of antennas at the base station and user devices. These three main concepts are widely investigated for the performances of 5G through mmWave frequencies, small-cells densification and massive MIMO.

Network densification is often defined as a combination of spatial densification (i.e., the increase of the ratio $\frac{m}{n}$) and spectral aggregation (i.e., the increase of W):

- spatial densification: increase of number of antennas, increase of the density of small-cells;
- spatial aggregation: increase of the bandwidth, use spatial aggregation and spectrum reuse.

In (Andrews *et al.*, 2014), the BS densification gain $\rho(\lambda_1, \lambda_2)$ is defined as the effective increase in data rates relative to the increase in network density. Let R_1 be an initial data rate (5% edge data rate or aggregate data rate) obtained with an initial network density of λ_1 , and let R_2 be a data rate obtained with a greater network density λ_2 , then the densification gain $\rho(\lambda_1, \lambda_2)$ can be quantified as:

$$\rho(\lambda_1, \lambda_2) = \frac{(R_2 - R_1)/R_1}{\lambda_2 - \lambda_1}/\lambda_1 \quad (1.2)$$

With proper co-tier and cross-tier interference management and load balancing techniques, the increase of cell densification can lead to an increase of ρ that reaches in the best case the value 1.

In millimeterwave communication, $\rho \gg 1$ is possible. In (Larew *et al.*, 2013), it has been shown that increasing the number of BS from 36 to 96 in a kilometre square urban area, increased the 5% cell-edge rate from 24.5 Mbps up to 1396 Mbps, giving a value of the densification gain $\rho = 9.9$.

Hence, small-cells deployment is essential to achieve network densification. This deployment has several favourable side-effects: decreasing the transmitter-receiver distance hence increasing the value of the received signal S , decreasing the value n by distributing the traffic load of a given geographical area among the different deployed cells and finally increasing the value of W by ensuring a higher bandwidth through spectrum reuse.

1.1.4 Conclusion and discussions

We have seen in this chapter how data traffic will undergo an exponential increase in the next following years with the emergence of new devices, technologies and needs. We also have seen how the various wireless communications efforts are to couple with the deployment of dense small-cell networks in order to fulfil the capacity and data-rate requirements of the future generations of connected world. However, the advantages of small-cells deployment come with several technical challenges that will be crucial to suppress or at least mitigate in order to fully benefit from the appealing features of small-cells networks. The next section is dedicated to identify these technical challenges and further details regarding the limits they represent to fully reach the appeal of these networks.

1.2 Technical challenges of dense deployment of small-cells

1.2.1 Co-existence with macro-cellular network and interference management in small-cells based networks

The major technical challenges associated with the deployment of small cell networks are the cross-tier and intra-tier interference problems i.e, the interference management between neighbouring small-cells and between small-cells and macrocells respectively. Therefore, when small-cells use the same bandwidth as macrocells, it becomes primordial to employ an efficient interference management technique. There exist six types of interferences in a two-tier small-cells macrocell network. These interferences can either be co-tier or cross-tier, in the uplink or the downlink and among MBSs, MUEs, FBSs and FUEs as summarized in Table 1.2.

Table 1.2 Different types of interferences in OFMDA-based two-tier networks

Aggressor	Victim	Interference type	Transmission mode
Macrocell UE	Small-cell BS	Cross-tier	Uplink
Macrocell BS	Small-cell UE	Cross-tier	Downlink
Small-cell UE	Macrocell BS	Cross-tier	Uplink
Small-cell BS	Macrocell UE	Cross-tier	Downlink
Small-cell UE	Small-cell BS	Co-tier	Uplink
Small-cell BS	Small-cell BS	Co-tier	Uplink

1.2.1.1 Co-tier interference

This type of interferences occurs among users belonging to the same tier of the network. In this case the interference caused to a small-cell is due to the transmission of a neighbouring small-cell as we can see in the illustration in Figure 1.3.

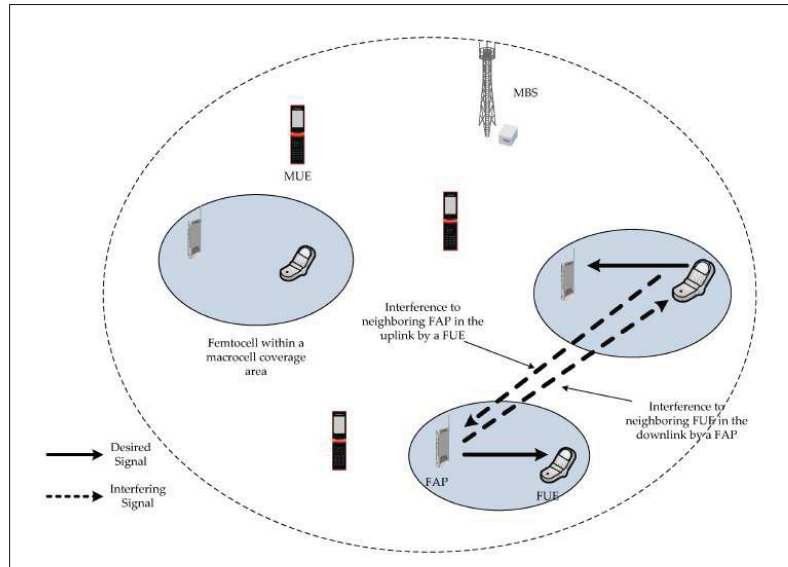


Figure 1.3 Scenario of co-tier interferences
Taken from Hatoum *et al.* (2011)

1.2.1.2 Cross-tier interferences

This type of interferences occurs among users belonging to different tiers of the network. These interferences can occur either in the uplink or the downlink transmissions as depicted in Figure 1.4.

1.2.2 Mobility management and handover

The dense deployment of small-cells overlaying macrocells in urban areas, introduces a major new challenge to 5G networks design. With the emergence of several mobile devices and applications, an efficient handover mechanism when users move in and out the cells is primordial since it directly impacts the perceived quality of experience (QoE) of the end user.

The handover success rates should be maintained at a level of 97% to 99%. The handover is not necessarily triggered by the mobility of the users. We can classify the handover processes into two categories. The first one, often called a coverage handover, is a handover process in order to maintain the connectivity of the mobile user when it is moving in a geographic area.

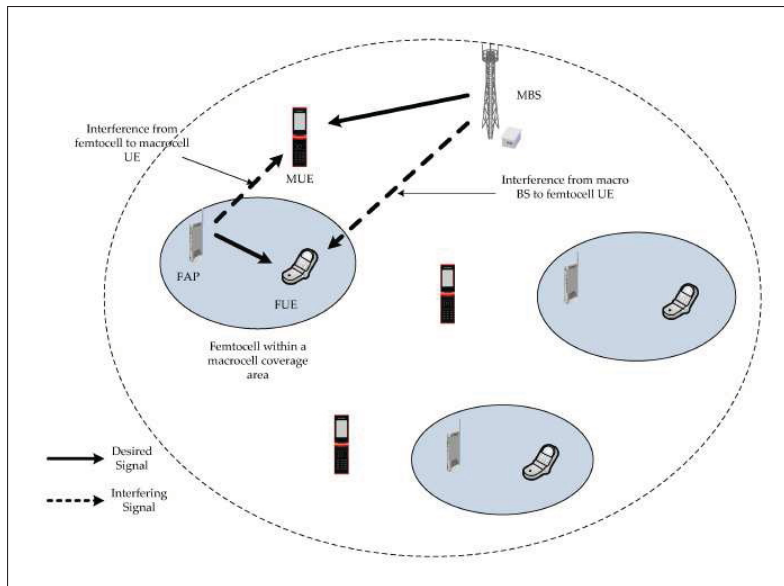


Figure 1.4 Scenario of cross-tier interferences
Taken from Hatoum *et al.* (2011)

The second type of handover, often called the vertical handover, takes place for load balancing of cells with overlapping coverage to ensure that data rates demanded by an ongoing service are met.

Mobility management can be categorised into three different groups:

- Inbound mobility: from a serving MBS to a target SBS;
- Outbound mobility: from a serving SBS to a target MBS;
- Inter small-cells mobility: from a serving SBS to a target SBS.

In a two-tier small-cell macrocell deployment, several scenarios cause challenging handover processes. This is particularly the case when a dense small-cells network is deployed, with a reduced coverage area of each cell and various access modes in urban areas. First of all, the open access modes of small cells allow public users to connect to nearby small cells, but since coverage of the small-cells is reduced and the mobility of users is high numerous handovers might take place, therefore seriously affecting the QoS of users. Secondly, the same spectrum

is shared by macrocells and small-cells, if the handoff boundary between cells is based on the received SINR, some users located close to a SBS might switch to the MBS. Hence creating high uplink interferences to the nearby small-cell. A proper handover decision mechanism is needed in this case.

To reduce the number of handovers, it has been proposed to consider a cluster of small-cells as a virtual macrocell, where the frequencies used by a user in the first small-cell of the cluster is reserved to its use in each other small-cell of the virtual cell (Sen *et al.*, 1999). In (Bonald *et al.*, 2009; Borst *et al.*, 2006) authors investigate the impact of inter and intra-cell mobility on capacity, throughput and fairness, and show that when the BSs interact and collaborate the mobility tend to enhance the capacity of the network. Seamless continuity with the macrocell network through a better mobility and handover management is primordial to the requirement of 5G networks and should be considered in the interference and frequency planning.

1.2.3 Neighbouring and self-organizing small-cells networks

Since small-cells may be directly deployed by the users, in some cases without any coordination from the macrocell, the two concepts of neighbouring cells and self-organizing networks (SON) are essential for successful small-cells deployments.

A self-organization is a concept used in many different fields and the technical specifications of SONs have been standardized in LTE and LTE-A systems by 3GPP in release 8 and 9 (standard3gpp). The basis of a self-organizing system is its *autonomous and intelligent adaptivity*, *i.e., its ability to respond to external environment changes* (Anpalagan *et al.*, 2015). Another important property of SONs, is the distributed control where each node in the network has to take individual decisions on its own. In particular, for small-cells networks self-organizing features allow them to detect the environment changes and take decisions by interacting locally with each others.

The neighbouring concept is closely related to SON operations. Indeed, self-organization of a cell usually takes the parameters of neighbouring cells into account. For instance, self-

organized inter-cell interference mitigation requires neighbouring cells informations to reduce coverage overlap while supporting seamless handovers. Two types of neighbouring concept are possible. Firstly, a centralized scheme where a global entity acting as a head cluster is in charge of gathering informations from the neighbouring cells and optimizes the relevant parameters based on these informations. Secondly, a distributed scheme where the neighbouring cells communicate directly with each other and optimize their own parameters based on local sensing and optimizing techniques.

In conclusion, neighbouring small cells are deployed by the users in residential areas or in small businesses. Since the end users do not have any understanding of cellular technology or network optimization, it is essential that these small cells support a sophisticated set of SON features that allow them to configure and optimize themselves continuously.

1.2.4 Conclusion and discussions

We have seen in this first section how the deployments of small-cells are primordial to cope with the exponential increase of data rates demands and to fulfil the requirements of 5G. However, several challenges arise from the dense deployment of these unplanned access points. The co-existence of small-cells with the underlying macro-tier and the ultra-dense deployment of overlapping cells are the main issue since the interference induced to the users from both tiers and the scarcity of the spectrum requires new interference and resource management techniques. The mobility management and handover problems have also been explored as well as the need for developing new framework capable of supporting self-organizing features for future small-cells networks.

1.3 Interference and resource management in small-cells heterogeneous networks

In Orthogonal Frequency-Division Multiple Access (OFDMA) based small-cell networks, the multi-user version of OFDMA provides diversity in time, frequency and users, thus orthogonal sub-carriers can be assigned to small-cells and macrocells. In OFDMA-based networks,

radio resource allocation, call admission control (CAC) and power control are crucial to provide service to a maximum of users from all tiers and support its QoS requirements. Resource management in small-cells OFDMA heterogeneous networks can be grouped in three categories: decentralized resource allocation approach (cooperative and non-cooperative), centralized spectrum allocation and power control, and call admission control. Different methods for interference avoidance and spectrum allocation have been summarized in (Lopez-Perez *et al.*, 2009). We present in this section the state of the art in resource allocation and optimization for two-tier networks. In the following sub-sections a better insight will be given to three main concepts used in this thesis.

1.3.1 Interference avoidance and spectrum partitioning in two-tier networks

Several papers intend to solve the existing co-channel interference issue in LTE, LTE-A and the next generations of heterogeneous networks. All the techniques presented in this section fall into one of the four categories below that we will describe briefly:

- Time domain techniques;
- Frequency domain techniques;
- Space domain techniques;
- Other techniques.

First, the most used and recent technique is the Time domain (TDM) enhanced inter-cell interference coordination (eICIC) technique (Pedersen *et al.*, 2012), that involves restricting the macro-layer subframe transmission to a fraction of the total subframes. Small-cell base stations can transmit during the fraction of subframes when the macro-tier is not transmitting, also known as almost blank subframes. Time and phase synchronization are made over the X2 interface between the macrocell and small-cells employing TDM eICIC.

In general, time domain techniques allow system's users to be protected by scheduling MUEs and SUEs in time domain. This technique is based on muting the interfering layer subframes while scheduling the users of the interfered layer for reducing the co-tier interference in the network.

Small-cell range extension is another time-domain technique where the coverage of small-cells is extended temporarily (Ghosh *et al.*, 2012), since the enhancement of the systems overall capacity is done by offloading users to the small-cells tier. A cell-specific positive bias is applied to the interfered UE in order to increase the reference signal received power (RSRP) value from the interfering SBS, resulting on this UE selecting the SBS instead of the MBS.

Second, frequency domain techniques involve scheduling users in the frequency domain. The available bandwidth is split into several disjoint portions which are assigned to different tiers or cell regions. Among these techniques we can cite Inter-Cell Interference Coordination (ICIC) methods that have been proposed in LTE release 9 (Wang & Pedersen, 2012), such as fractional frequency reuse, soft frequency reuse, dynamic frequency partitioning etc.

Third, space domain techniques involve interference cancellation through coordinated beamforming or joint transmission. Coordinated multi-point (CoMP) is a space domain method, wherein multiple base stations cooperate in a way to mitigate inter-cell interference and to serve multiple users simultaneously (Clerckx *et al.*, 2011).

Finally, the fourth category encompasses several methods, algorithms, technologies for the optimization and control of transmission characteristics (power and frequency) for interference mitigation or cancellation in two-tier networks. Several of these methods will be investigated in this section, and specially the ones that directly concern the research we have carried out.

1.3.1.1 Spectrum arrangement in multi-tier systems

Spectrum sharing among macrocells and small-cells in a network are generally classified into two groups. One method used to suppress the cross-layer interferences is to split the spectrum

in two parts: one dedicated to the macrocell users and the other to the small-cell users, this is the orthogonal channel assignment. The drawback of this method is the low spectrum reuse as it has been shown in (Ghosh *et al.*, 2010). Therefore, co-channel assignment of the macrocell and femtocell layers seems more efficient and profitable for operators, although far more intricate from the technical point of view.

Indeed, if the spectrum is shared by entities from different tiers with different levels of power transmission, the network system will meet several challenges related to the interferences issue. First, the deadzone problem induced by a MUE's larger power inhibiting the uplink of nearby small cells. The deadzone problem in the downlink is also critical when the signal received by a MUE located in the boundary of the cell is corrupted by the downlink transmission of surroundings SBSs. Second, the inappropriate scheduling: because of the dynamic scheduling of HeNBs and the constant change of co-channel interference, cooperation is needed among macrocell BS and HeNBs.

Under a co-channel approach, Wu *et al.* (2009) develop a new scheme for femtocell-aware spectrum arrangement. The paper describes a method to coordinate the use of the spectrum between macrocells and femtocells. This is done by a scheduling algorithm, through the gathering information from the MBS about the femtocells spectrum use. The MBS creates a pool of MUEs that may interfere with nearby HeNBs. A certain part of the spectrum is dedicated to those MUEs, while the other part of the spectrum is shared by FUEs and MUEs. This can help to reduce significantly the uplink cross-tier interference (Saqib *et al.*, 2012).

In (Estrada *et al.*, 2013), the authors determine the distance d_{im} between an MBS and a MUE as a radius surrounding the MBS inside which the MUEs may suffer from high degradations from the FBSs. They identify the number of FBSs than can reuse the subcarriers allocated to the macro-tier according to d_{im} , without degrading the MUEs QoS. The performance analysis is achieved in terms of spectrum efficiency, throughput and outage probability of MUEs and FUEs are compared to the existing models.

Both co-channel and split-spectrum approaches are studied in this thesis and different methods are proposed to reduce interference and enhance capacity. In the next sub-section, we present the most commonly used orthogonal spectrum allocation approach: fractional frequency reuse.

1.3.1.2 Fractional frequency reuse in HetNets

In order to explain the principle of frequency reuse, it is essential to start by reminding one of the fundamentals of cellular networks. When only a single transmitter is available in a large area, a high power of transmission is necessary to reach every user in the given area. Hence, one single transmission is possible per frequency which reduces significantly the number of users possibly supported by the network over the geographic of the single transmitter coverage area. To overcome this major limit, frequencies allocated to mobile networks are reused in a regular areas, i.e. cells, each covered by a single base station: this is the principle of frequency reuse for cellular networks (Rappaport, 2009).

OFDMA-based systems suffer more from inter-cell interference than CDMA-based cellular systems or others, hence FFR is one of the frequency planning techniques proposed for LTE systems to mitigate the inter-cell interference. This scheme is mainly based on the partition of a cell into several regions and the application of a different frequency reuse factors in each one.

There are two major frequency reuse patterns for mitigating inter-cell interference: FFR and soft frequency reuse (SFR). In FFR, the spectrum is divided into two parts. One half is allocated to the inner region of every cell of the system. The second half is divided into three distinct subparts (or a number of subparts equal to the reuse factor) and allocated to the edge ring of contiguous cells as depicted in Figure 1.5.

In SFR, the overall bandwidth is shared by all base stations (i.e. a reuse factor of one is applied), while cell-edge users transmit at lower levels than cell-center users in order to reduce interference with neighbouring cells as depicted in Figure 1.6

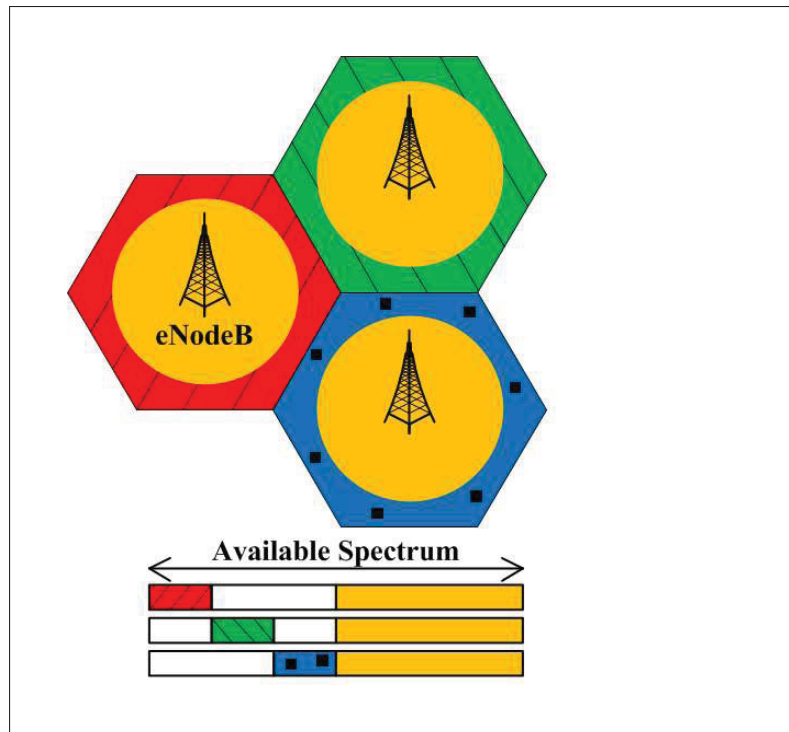


Figure 1.5 Fractional frequency reuse scheme
Taken from AboulHassan *et al.* (2015)

In frequency reuse schemes, the location of the users within a cell is essential with regard to decide on which part of the spectrum is dedicated to it. One practical method to determine the location of users is to use the average SINR of the users in a cell, which gives us an indicator of the user's distance from their base station. The base station defines a threshold: if the SINR is less than the threshold the user is classified as cell-edge user, and if the SINR is greater than the threshold the user is classified as cell-center user.

Owing to FFR, macrocells and overlaying femtocells do not operate in the same frequencies, therefore avoid cross-tier interferences. In (Lee *et al.*, 2010b), under the macrocell allocating frequency band by the FFR, the femtocell chooses sub-bands which are not used in the macrocell sub-area to avoid interference.

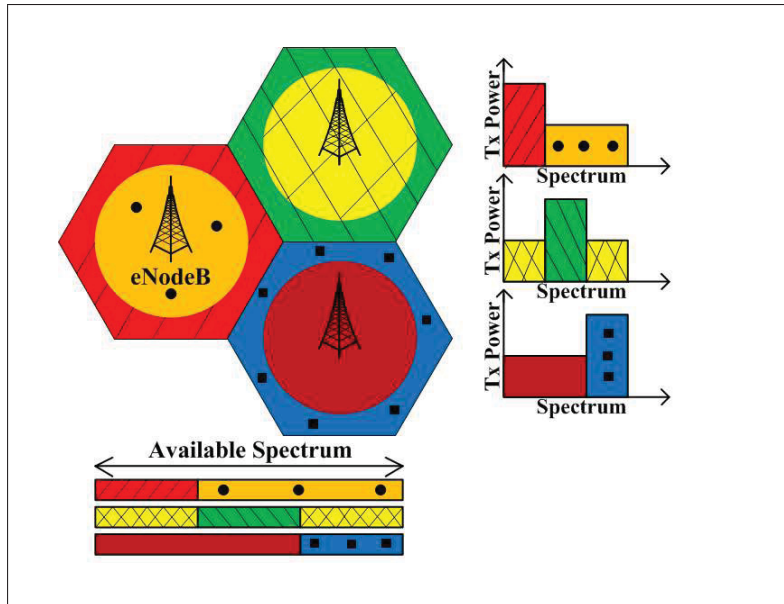


Figure 1.6 Soft frequency reuse scheme
Taken from AboulHassan *et al.* (2015)

1.3.2 Interference and resource management approaches for OFDMA-based HetNets : a literature review

1.3.2.1 Resource Allocation Optimization Problems

Since OFDMA has been adopted as the radio technology access of the current and next generation of wireless networks (WiMAX, LTE, 5G), resource allocation for OFDMA HetNets has become an essential topic of research. Before the emergence of dense deployments of small-cells, research has focused on the resource allocation under fairness criteria and minimum rate constraints, such as cross-layer optimization problems in OFDMA single-cell systems (Wong *et al.*, 1999; Jang & Lee, 2003; Kivanc *et al.*, 2003; Shen *et al.*, 2005; Song & Li, 2005a,b). In the more recent literature, research has considered multi-tier networks and proposed resource allocation algorithms for co-channel deployments (Li & Liu, 2006; Venturino *et al.*, 2009; Wang & Vandendorpe, 2011).

Since most of the resource allocation optimization problem are integer programs, namely mixed linear programs with a utility function bounded by linear constraints and restrictions

on some components, they are generally NP-hard (Luo & Zhang, 2008). Hence, various works have decomposed the sub-channel and power allocation into sub-problems to reduce the complexity and find the sub-optimal but efficient solutions under QoS and fairness constraints.

The key requirements for the design and optimization of multiple access in wireless networks are as follows (Gummalla & Limb, 2000):

- Maximize network throughput: throughput referring to the amount of data successfully transmitted by the nodes over a time period;
- Minimize delay : delay referring to the time required for an amount of data to be transmitted successfully;
- Maximize fairness: fairness referring to a measure of whether the nodes are receiving a fair share of radio resources;
- Improve power efficiency: power efficiency being an important performance metric for battery-powered wireless devices and stations.

A resource allocation optimization problems aims to solve a problem that requires to determine the joint sub-channel and power allocation for all users of the system in the different existing cells, in order to optimize an objective function subject to spectrum, power and QoS constraints. There are several optimization problem algorithms proposed in the recent literature.

In (Venturino *et al.*, 2009) a dual-based low complexity algorithm is proposed, and its convergence and local optimality proved. In (Ha & Le, 2014) a max-min radio resource allocation for two-tier resource allocation framework for OFDMA HetNets is proposed. A distributed low complexity algorithm is proposed to find the optimal solution for the problem, its convergence is proved and its complexity analysed by the authors. In (Lee *et al.*, 2011), a dedicated signalling channel is established in order to allow information exchange among HeNBs. These exchanged informations include in particular the interference gain between HeNBs and the

traffic load of HeNBs, hence allowing to formulate an optimization problem that maximizes the sum of the logarithmic rate of all FUEs. A new iterative water-filling algorithm to approximate the solution of such an optimization problem is proposed. In Lopez-Perez *et al.* (2009), the authors develop two new resource allocations algorithms in OFDMA femtocells. One where macrocells can use the entire spectrum and each femtocell uses a random fragment. And an other method called Centralized-Dynamic Frequency planning where femtocells send their request to a centralized node to find the optimal allocation for each femtocells and this last scheme converges easily to the optimum.

1.3.2.2 Power Control under Co-channel Assignment

Despite the orthogonality within a cell in OFDMA systems, users still suffer from interferences. Indeed, when neighbouring cells allocate the same time-frequency resource blocks, they cause interferences among users. The most affected are the cell-edge users in the down-link transmission since they are almost equidistant from two base stations and suffer from low desired power and high interference power (Ghosh *et al.*, 2010). We have studied above interference-aware allocation approaches to mitigate the interferences, we will now discuss the power control approach as a solution to the interference issues.

In a two-tier network, the traditional power control schemes are not sufficiently efficient and robust. For instance, the channel inversion employed by users causes considerable deterioration of small-cell SINR. This is due to the high power of transmission of cell edge users that causes cross-tier interference to the surrounding small-cells. Instead of allocating a fixed HeNBs power recent papers focus on the dynamic power control, although is not straightforward in OFDMA systems since it requires accurate measurements of all gains in all radio links. A number of research works focuses on power control algorithms for OFDMA small-cells networks.

In the uplink, power control schemes for FUEs have been proposed in (Jo *et al.*, 2009), in order to adjust the maximum uplink transmit power P_{max} as a function of the cross-tier interference

level in an open-loop and closed-loop technique. In the open-loop, the femtocell estimates the additional cross-tier interference to the MBS due to the FUEs and adjusts the maximum transmit power in the way that it does not reach the maximum acceptable interference level. In the closed-loop control a femtocell adjusts the maximum transmit power P_{max} as a function of the additional cross-tier interference to the MBS due to the femtocell user and as a function of the level of noise and uplink interference at the MBS.

In the downlink, various interference mitigation strategies for OFDMA-based small-cell networks, based on hybrid co-channel assignment and power control have been recently developed. Hybrid interference management schemes which combine power control with resource partitioning are promising. Power control schemes are important in that MBSs and SBSs can use the entire bandwidth with interference coordination. For this purpose, the HeNB should be capable of identifying the users to which it causes degradations. However, this scheme is not efficient when a MUE is located very close to a FBS since the user will suffer from strong interferences. With split spectrum approaches, interference between MeNB and HeNB can be eliminated, nonetheless, multiple frequency bands are required. Both approaches can be then exploited in a hybrid scheme, to make a complete design responding to various problems encountered in HetNet. In the hybrid approach, the entire bandwidth is split into 2 sets: one set of subchannels dedicated to the MUEs and one set of subchannels shared by MUEs and FUEs. Inside the set of shared subchannels, the subcarriers of one subset are allocated with upper power, and the subcarriers in the other subset are allocated with power by water-filling. Pao *et al.* (2013) have considered the method of water filling power allocation for cross-tier interferences mitigation. The upper power limit is defined as transmit power limit for a FBS in a subcarrier to ensure a the QoS requirements of its neighbouring MUEs. The aim is then to find the users to which the dedicated part of the sub-carriers is allocated and the users using the same frequencies with power control.

An algorithm for joint power control in both tier and channel assignment guaranteeing a given transmission has been developed in (Sun *et al.*, 2012). The downlink interference problem has been addressed in (Sun *et al.*, 2012) by considering the QoS requirement for both MUE and

FUE in term of SINR. A more advanced approach, is the design of power adaptation algorithms with the ability of adapting the transmission power of MBSs and FBSs dynamically according to the interference induced by their transmissions while reducing the energy consumption depending on the traffic of the network.

In (Moon & Cho, 2009), in order to guarantee the SINR of MUEs, the amount of power allocated to each subcarrier should be less than some the upper power limit. When a pair of victim/aggressor are identified, for instance when a MUE suffer interferences from a neighbouring FBS, the FBS is allocated subchannels from a dedicated set where the power is limited to the upper power limit.

1.3.3 Resource management in self-organizing small-cells networks

The sub-section above has addressed the case where the MBS manages the informations gathered from the HeNBs, and manages the coordination with the other SUEs in its covered zone. Since the number of BSs increases considerably in HetNets, optimization of network parameters with such a high number of nodes becomes complex and costly. Therefore, the need for self-optimization becomes inevitable. In this section, we describe the variation where the HeNBs are able to get informations as well, so they can be self-configurable and self-optimized units. To reach this objective, the SBSs are able to sense the activity of neighbouring SUEs and MUEs. Three approaches can be used: HeNBs sense and identify the subchannels used in its area, then make the best spectrum allocation decision , the second approach where the HeNBs exchange informations about their spectrum usage and needs, and the third one where the measurement reports (user's location, active sub-channels...) periodically sent by the UEs to their HeNBs are used to mitigate interferences.

1.3.3.1 Distributed and Cognitive approaches for Self-Organizing Small-cells HetNets

When co-channel deployment is applied, the most widely used technique to mitigate cross-layer and co-layer interference is the centralized approach where a central entity is in charge

of allocating channels to the cells after collecting information from the cell's users. However, high computational complexity and severe time overheads lead to look for new methods as the distributed approach where the cells manage their own sub-channels and in which two cases are to consider.

On the one hand, the non-cooperative approach in which small-cells manage its resources without regard to the performances of the others users (opportunistic access). In this case, each base station is unaware of the spectrum use in other cells, and no cooperation among neighbouring base stations is possible. The subcarrier and power allocations follow the theory of non cooperative games (Chen *et al.*, 2008).

On the other hand, the cooperative approach in which the SBSs access the spectrum according to the spectrum use of the neighbouring small-cells, will permit to obtain better performances than the non-cooperative approach. The throughput and the global performance of the system are optimized simultaneously. This is achieved by exchanging information among neighbouring base stations to ensure a better fairness and overall throughput in the system.

The spectral capacity of the network operators is currently submerged by the growing demand of the new electronic devices and applications. To meet this demand and increase the capacity of the networks, the operators are interested by the deployment of a dynamic spectrum access through cognitive radios. The UEs are equipped with sensing features which allow them to sense the environment , analyse the informations and adapt their behaviour according to these values. This type of deployment can be applied to a two-tier small-cells networks.

The authors in (Zhang *et al.*, 2010), show how the HeNBs can estimate the cross tier interferences based on the path loss informations and access strategically to the spectrum, avoiding the co-tier interferences. An HeNB tries first to select the component carriers (CCs) not used by any of its neighbours, then tries to select the CCs used by the farthest neighbours, and finally the CCs used by the less neighbours. As depicted in Figure 1.7, HeNBs 1 and 3 are far distant but both close to HeNB2. Thus, HeNB 1 and 3 can both choose CC1 and CC2 for

their downlink transmission while HeNB2 will have to select different CCs to avoid inter-cell interferences.

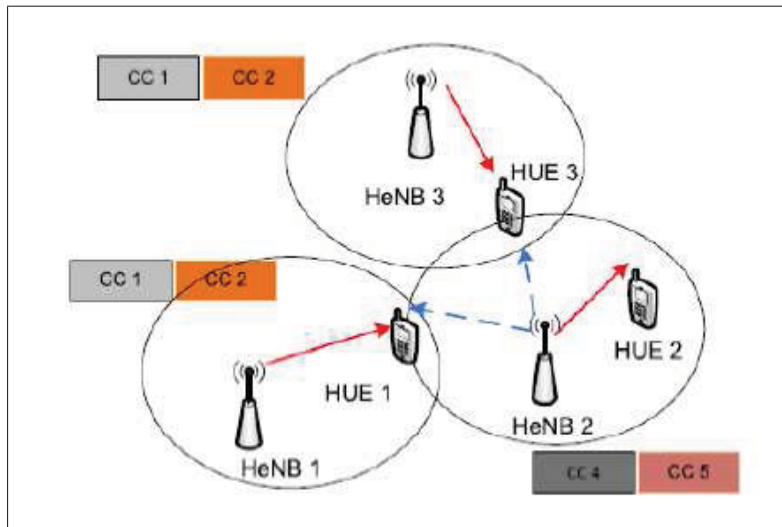


Figure 1.7 An example of co-tier interference management in cognitive radios
Taken from Zhang *et al.* (2010)

In (Naranjo *et al.*, 2012), the authors propose a dynamic spectrum access scheme for LTE technologies based on cognitive radio where a central entity called the Spectrum Policy Server (SPS) is responsible for the spectrum management of the entire HetNets network. This allows interactions between receivers and transmitters for a better use of spectrum resources. The second advantage, is that this type of access enables the radio access to the spectrum portions initially reserved to a primary user if the secondary user does not disrupt the primary usage. In this scheme, two mobile network operators (MNOs) exploit separately a macrocell network and a femtocell network. The spectrum allocation for the MBS is static while the spectrum for the HeNBs is shared and allocated dynamically by the two different operators. This sharing is orchestrated by the SPS which define policies and rules for the HeNBs spectrum access. The SPS collect informations from the base stations and key performance indicators (geographic position of the base stations, coverage area, cells load, frequency band) in order to make decisions regarding the spectrum management. The analysis of this data permits to estimate the

bandwidth required by each base station and to control the low frequency and high frequency of each one for a better spectrum efficiency and higher data rates in the networks.

1.3.3.2 Cluster based resource management in OFDMA Small-Cells Networks

The aim of the cluster based model, is to mitigate interferences between femtocells and macro-cells in order to maximize the global network throughput. (Li *et al.*, 2010) investigates the best way to share the allocated bandwidth in order to maximize the QoS requirement satisfaction. This is achieved through first, measure the distance between two different HeNBs, if the result is below a predefined threshold, the two HeNBs are assigned to different clusters, otherwise, they are assigned to the same clusters. The members of the same cluster are allocated different subcarriers, thus, strongly mitigating the co-tier interferences. The femtocell system controller (FSC) of the MBS is responsible for gathering informations from the HeNBs and aggregate the HeNBs according to their locations. Regarding the resource sharing, the spectrum is divided into two portions, one dedicated to the MUEs and the second shared by the MUEs and the HeNBs. The dedicated portion of the spectrum help avoiding deadzone problems in the downlink transmissions.

A clustering algorithm CFCA (Combination of Frequency bandwidth dynamic division and Clustering Algorithm) based on the graph method, is proposed in (Hatoum *et al.*, 2011) to find the optimal clustering of femtocells in the system. In this paper, the authors introduce a new metric called the throughput satisfaction rate per femtocell which is the ratio of the received number of allocated RBs to the total femtocell demand. They propose an algorithm called FCRA (femto-cell cluster-based Resource Allocation) to maximize this metric, involving three phases: cluster formation, cluster-head resource allocation and resource contention resolution. First, the algorithm form different clusters in the network, then, a cluster-heads allocate the resources to the femtocells on each cluster by resolving a min-max femtocells resource allocation problem. And finally, given that two femtocells associated with two different cluster-head may have been assigned the same resource blocks each user contending for a resource will

send a report to its HeNBs. Finally, the HeNBs resolve the contention by sampling a Bernoulli distribution.

In (Rose *et al.*, 2012), the authors develop an algorithm of trial and error (TE) capable to auto-configure the transmission parameters (power and channels) in clustered based networks by using only one feedback bit. This feedback contains an evaluation of the transmission link quality. Two types of feedback strategies have been developed: one based on the SINR measured at the reception and one based on the cyclic redundancy check insuring the integrity of the packet. In a crowded network when several clusters try to share the same limited resource the TE algorithm can find a parameter configuration in order to satisfy the QoS requirements of most clusters and by using a low amount of power. The clusters not able to satisfy their QoS requirement will be turned off automatically to avoid unnecessary power consumption and limit additional interferences in the network. When the clusters change rapidly, the network topology changes, hence the algorithm has to react fast to satisfy the UEs requirement in the changing environment. This is achieved by increasing for a short time the power level or by reorganizing the channel allocations.

1.3.4 Call admission control in small-cells HetNets

To provide integrated services such as voice data multimedia with the level of QoS required, Call Admission Control (CAC) is used for admission or rejection of an incoming request from a user based on the capability of the network to satisfy its level of requirement. CAC allows to limit the number of calls into the system in order to reduce the congestion and the number of calls dropped or blocked. It is necessary to have an adequate CAC to balance the call blocking and call dropping and provide the QoS required (Lau & Maric, 1998).

In two-tier networks, an adequate CAC is required to coordinate spectrum sharing and admission control for both types of users (MUEs and SUEs) and to balance the traffic loads among the small-cells and macrocells of the network. When different types of access modes co-exist in a small-cells based network (open access, closed access, and hybrid access modes), CAC

manages the access of different types of users and cells, and is essential to protect the QoS of the CSG users in a hybrid access mode. Due to mobility, the CAC becomes more complicated and the problem has been widely investigated in the last few years. Indeed, a call not being completed in one cell might have to be handled by a neighbouring cell without being dropped.

Moreover, during a call process if there are not enough resources to maintain the same QoS level in the new cell, the handoff call might be dropped (Fang & Zhang, 2002). Thus, the handoff calls are assigned a higher priority over the new calls, and various handoff priority-based CAC schemes have been proposed:

- Bounding scheme: limit the number of new calls in the cell to be at most $K \leq C$ (C being the number of channels in a cell) while handoff calls can be accepted as long as there is available channels;
- Cutoff priority scheme: a new call can be accepted if the total number of busy channels is at most $K \leq C$ while handoff calls are accepted as long as there is available channels;
- Guard channel/thinning scheme: a new call is accepted with probability α_i if there are i new calls in the cell.

The new call bounding scheme is the most commonly used, and the transition diagram of this scheme is depicted in Figure 1.8. A number C of subchannels are available in a cell on call require one channel to be processed. New calls and handoff calls arrive according to a Poisson process with arrival rates λ and λ_h respectively. The holding time of new and handoff calls are exponential with the average value $1/\mu$ and $1/\mu_h$, thus the service rates are μ and μ_h . The system state is defined as $S = \{(n_1, n_2) | 0 \leq n_1 \leq K, n_1 + n_2 \leq C\}$

$q(n_1, n_2; \bar{n}_1, \bar{n}_2)$ denote the probability transition rate from state (n_1, n_2) to state (\bar{n}_1, \bar{n}_2) , hence the following set of equations is obtained:

- $q(n_1, n_2; n_1 - 1, n_2) = n_1 \mu (0 < n_1 \leq K, 0 \leq n_2 \leq C);$

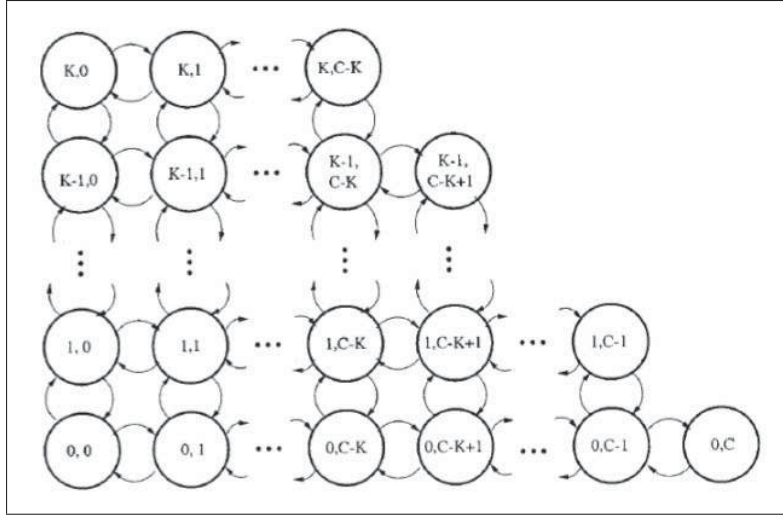


Figure 1.8 Transition diagram for the new call bounding scheme
Taken from Fang & Zhang (2002)

- $q(n_1, n_2; n_1 + 1, n_2) = \lambda (0 \leq n_1 < K, 0 \leq n_2 \leq C)$;
- $q(n_1, n_2; n_1, n_2 - 1) = n_2 \mu_h (0 \leq n_1 \leq K, 0 \leq n_2 \leq C)$;
- $q(n_1, n_2; n_1, n_2 + 1) = \lambda_h (0 \leq n_1 \leq K, 0 \leq n_2 \leq C)$.

Considering $\rho = \lambda / \mu$ and $\rho_h = \lambda_h / \mu_h$, the following equation is obtained:

$$p(n_1, n_2) = \frac{\rho^{n_1}}{n_1!} \cdot \frac{\rho_h^{n_2}}{n_2!} \cdot p(0, 0), \quad 0 \leq n_1 \leq K, n_1 + n_2 \leq C, n_2 \geq 0 \quad (1.3)$$

From the normalization equation, the steady state probability $p(0, 0)$ is obtained allowing to determine the probability of blockage of a call in the system: $p(0, 0) = \left[\sum_{0 \leq n_1 \leq K, n_1 + n_2 \leq C} \frac{\rho^{n_1}}{n_1!} \cdot \frac{\rho_h^{n_2}}{n_2!} \right]^{-1}$

Both the blocking probability of new calls and dropping probability of handoff calls, may be obtained through the same process.

An analytical model for teletraffic performance analysis of hierarchically overlaid systems is developed in (Rappaport Stephen & Hu, 1994), with an approach based on multidimensional

birth-death processes. The performances curves show the effects of various allocations of resources among the microcells and overlaying macrocells.

The authors in (Le *et al.*, 2013a), consider the mobility and QoS-aware admission control problem for OFDMA femtocell networks. An admission control algorithm that efficiently associates low-speed and high-speed users with FBS and MBS to avoid large handoff overhead.

1.4 Game theoretic approaches for resource management in HetNets

Game theory is a very useful mathematical tool to model and analyse decision-making problems in wireless networks where agents or players have conflictual interests. These tools have been widely used in economy to model the competition in markets and have recently brought interest to model these problems in wireless networks (Han *et al.*, 2012; Akkarajitsakul *et al.*, 2011).

A general definition of a game has been given in (Anpalagan *et al.*, 2015): *A game is a process in which the agents select certain strategies from their own strategy sets and obtain payoffs according to the strategies of all agents.* A game consists of a set of players, a set of strategies available to those players, and a specification of payoffs for each combination of strategies. In this section , we discuss the applications of game theory for resource allocation and interference management in dense small-cells networks.

1.4.1 Applications of game theory in wireless communications and networking

We will first identify the motivations of using game theory for self-organizing small-cells Het-Nets. First of all, in ultra dense networks, centralized algorithms might be inefficient due to the high complexity induced by the large amount of information shared among the dense population of nodes. Accordingly, distributed decision-making for self-organizing networks is achieved through game theoretic models allowing local interactions in a group of competing entities. These local gathering and processing reduce significantly the complexity of the resource management algorithms and allow the networks to be more scalable and robust.

Secondly, as stated above, the nodes in heterogeneous networks may be deployed by either the operators or the users. When the same resources are shared, the operation of one network tier may affect the others and game theory is an efficient tool for modelling interactive behaviour among different entities. Unlike optimization models we have studied in 1.3.2, the mutual impact among the nodes during the decision-making process can be accurately taken into account with game theory mathematical frameworks. Moreover, the payoff function in game theory allows to take into account several performances metrics of nodes like capacity, delay, throughput, SINR etc. and to model the different levels of QoS the system nodes have to meet.

Two major game-theoretic approaches can be used, namely the cooperative and noncooperative approaches. In noncooperative games, each player chooses its strategy independently for improving its own performances or reducing its losses independently of other players choices (Saad *et al.*, 2009b). The most well-known solution concept for noncooperative games is the Nash equilibrium (Başar & Olsder, 1998). Several papers have investigated the modelization of resource allocation, power control, and admission control with noncooperative games (Han & Liu, 2008; Alpcan & Basar, 2005b; Alpcan *et al.*, 2002b).

On the other hand, cooperative games provide mathematical tools to model the behavior of rational players when they form coalitions and make agreements to maximize their profit. The main branch of cooperative games describes the formation of groups of players, named coalitions. With the need for self-organizing, decentralized and autonomous networks, cooperative approaches have emerged as a key solution for the success of dense heterogeneous networks.

Some papers in the recent literature have considered the application of game theory to model and analyze the resource management problems in two-tier small-cells networks. Power control and subchannel allocation problem has been tackled with a game theoretic approach through a non-cooperative game modelling the interferences among MUEs and FUEs in (Chandrasekhar *et al.*, 2009). The Nash equilibrium of the transmission power is obtained in this work. Another game has been proposed in (Huang & Krishnamurthy, 2011), for subchannel allocation in two-tier femtocell networks, considering the correlated equilibrium as solution of the game.

In (Ko & Wei, 2011), a dominant-strategy equilibrium is proposed to analyze the MUEs and FUEs resource request strategies.

Most of the papers consider the traditional achievable rate as the payoff function. But other papers have proposed original payoff functions to find the optimal resource allocation strategy. For instance, in Hong *et al.* (2009), the traditional utility function is replaced by the logarithmic function of the achievable rate minus the cost of the transmission power of the FUEs. This work is extended in (c. Hong & Tsai, 2010), to take into account both MUEs and FUEs averages utilities. A hierarchical game has been proposed in (Guruacharya *et al.*, 2010), namely a Stackelberg game where the macrocells are the leader in the systems and the small-cells the followers and where the objective of both types of stations is to maximize its capacity under power constraints.

All of those papers have considered mainly noncooperative approaches. We will see in the next subsection how the cooperative games can be applied to the resource management problem in two-tier networks and present the motivations of this application.

1.4.2 Coalitional and canonical games and their applications

As stated earlier, a coalitional game is a branch of cooperative game to model cooperative behavior of players. A coalitional game is defined by the pair (\mathcal{N}, v) , \mathcal{N} denotes a set of players $\mathcal{N} = \{1, \dots, N\}$ who seek to form coalitions to strengthen their positions in the game. When a coalition S is formed, its member act as a single entity in the game. The coalition value denoted by v is a utility function quantifying the worth of a coalition in a game. Two types of coalitional games are to distinguish : canonical coalitional games and coalition formation games.

When the coalition value depends solely on the members of the coalition S with no regards to the players of the set $\mathcal{N} \setminus S$, we say that the game is in characteristic form with transferable utility (TU). The TU implies that the total utility of the coalition is allocated to the coalition as

a whole and then can be distributed among its members. Hence, irrespective to the division of the coalitional payoff, the members of the coalition enjoy the same total utility.

Two conditions apply to classify a coalitional game as canonical:

- The coalitional game must be in characteristic form;
- The coalitional game must be superadditive. For a TU game, the superadditivity implies that the formation of a large coalition out of disjoint coalitions, guarantees at least the value that is obtained by the disjoint coalitions separately and is defined as (Myerson, 1997)

$$v(S_1 \cup S_2) \geq v(S_1) + v(S_2) \forall S_1 \subset \mathcal{N}, S_2 \subset \mathcal{N}, S_1 \cap S_2 = \emptyset. \quad (1.4)$$

Since the canonical coalitional game satisfies the superadditivity property, the aim is to divide and allocate the value among players in a grand coalition. For this purpose, we need to apply an imputation value, which is a payoff vector $x \in \mathbb{R}$ that ensures the stability of the grand coalition. The most renowned solution concept for canonical games is the core. The core of a canonical game is the set of payoff allocations that guarantees that no player or group of players has an incentive to leave the grand coalition \mathcal{N} and to form another coalition $S \subset \mathcal{N}$ (Myerson, 1997). It is defined as:

$$\mathcal{C} = \left\{ x : \sum_{i \in \mathcal{N}} x_i = v(\mathcal{N}) \text{ and } \sum_{i \in S} x_i \geq v(S) \forall S \subseteq \mathcal{N} \right\} \quad (1.5)$$

Hence, for all the canonical games applied to wireless communications problems, researchers seek for imputations values that lies in the core to justify the stability of the grand coalition and the optimality of the solution for the coalitional game.

Recently, there has been an increasing interest in canonical coalitional games and some papers have investigated ways to use this type of games for solving wireless communications problems. In (La & Anantharam, 2003), the authors propose a cooperative game model to tackle the problem of fairly allocating the transmission rates between multiple users accessing a wireless

Gaussian MAC channel. To maintain the characteristic form of the utility function, it is considered that the players in $\mathcal{N} \setminus S$ are jammers. The utility of a coalition $v(S)$, achieved by the coalition $S \subseteq \mathcal{N}$, represent the capacity of S when the players $\mathcal{N} \setminus S$ are intentionally jamming the communications of the players in S .

In (Mathur *et al.*, 2008), the rate achieved by the users is considered for the utility function and the stability of the grand coalition is studied for the cooperation between single antenna receivers and transmitters in an interference channel. The game is modelled with the links being the players, the receivers cooperate by jointly decoding while the transmitters are not cooperating. The value $v(S)$ being the maximum sum-rate achieved by the receivers belonging to S , it is proven that a proportional fair rate allocation lie in the core, and hence constitute a suitable allocation as it ensures the stability of the grand coalition.

In (Han & Poor, 2009), a canonical coalitional game is proposed to solve the problem known as the curse of the boundary nodes in packet forwarding ad hoc networks.

However, regarding two-tier HetNets, few papers have considered canonical games to solve in inherent problem of resource management in ultra-dense small-cells networks. Moreover, very few papers have investigated the collaboration between the harmed MUEs and neighbouring SBSs for instance when the first fails to connect to the SBSs. Yet another problem not fully investigated is when the cooperative games involve hybrid or open-access small-cells.

1.5 Recent opportunities: small-cells deployment in the mmWave spectrum

The exponential growth of data traffic in mobile networks and the bandwidth shortage facing wireless carriers have motivated the exploration of higher frequency bands for the 5G mobile networks. To keep up with this rapid increase of mobile data growth, another key is the spectrum. Indeed, as data rate requirements increase, proportionally larger channel bandwidths are required to support the increased throughput capacity. Wireless systems have restricted their operation to a short range of microwave frequencies that extend from 700 MHz to a 2.6 GHz. The global spectrum bandwidth allocation does not exceed 700 MHz while only 200 MHz in

average are available per wireless provider. This bandwidth is currently fully occupied in peak times and urban areas where an explosive number of wireless devices are operating in this short range of frequencies.

Although new technologies such as massive MIMO and small-cells as well as research advances in spectrum sharing help addressing the efficient use of spectrum, they will not be sufficient to support the future mobile data traffic explosion. There is no other way to add bandwidth than using higher frequencies and with the huge available bandwidth in these frequencies, mmWave systems can provide multiple gigabit rates. Figure 2.2 in (Wells, 2009), illustrates this trend where commercially available wireless systems where the carrier frequency versus the transmission speed are plotted.

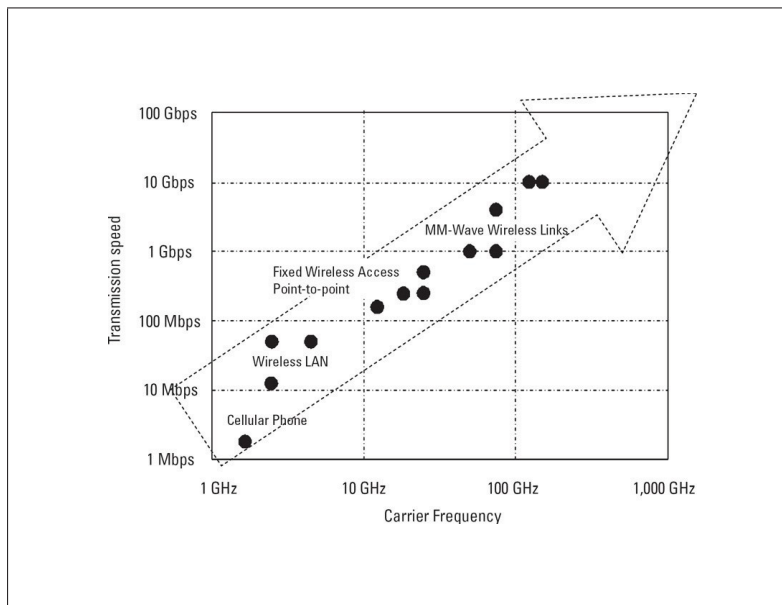


Figure 1.9 Trend of commercially available wireless systems: increasing carrier frequency and bandwidth enable increasing data rates

The main reasons why the millimeterwave spectrum has stayed idle in the past is that for high-frequency radio systems, the huge propagation loss compared to microwave communications are a significant factor in limiting wireless performance. The high potential of millimeter-wave

communication systems has generated the need to carry out many studies in view of rain on radio propagation at these frequencies. Measures on rain specific attenuation with simultaneous measurement of rain rate distribution have been conducted in (Qingling & Li, 2006) and have been plotted in Figure 1.10. Similar measurement have been conducted by Rappaport *et al.* (2011) for atmospheric absorption and the results are depicted in Figure 1.11.

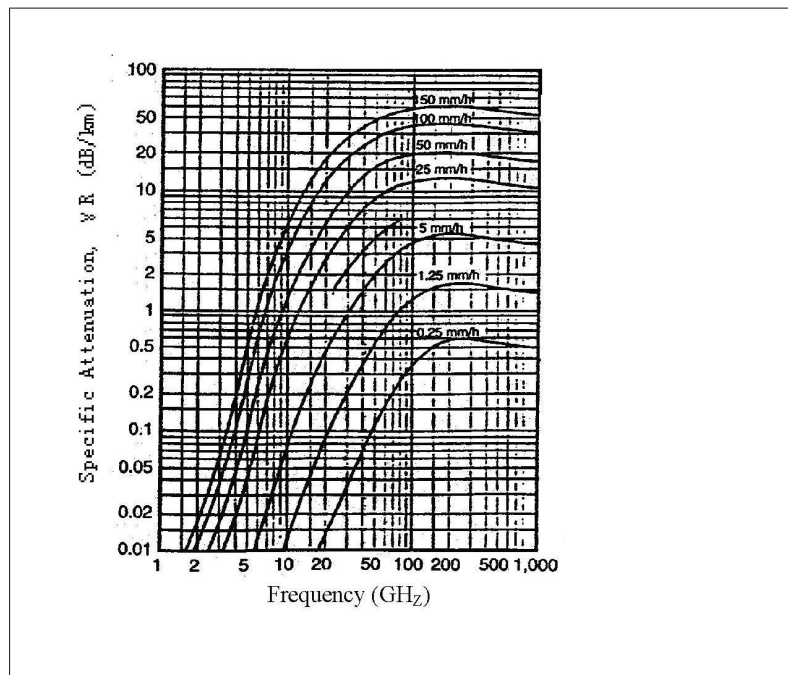


Figure 1.10 Rain attenuation in mmWave frequencies
Taken from Qingling & Li (2006)

The five available mmWave frequency bands for wireless communications systems and the corresponding available bandwidth explored in (Ghosh & Tal., 2014) and presented in the following:

- 28 GHz band: The 27.5 – 28.35 GHz (850 MHz) and 29.1 – 29.25 GHz (150 MHz) are licensed. This is the lower band of the mmWave spectrum and unlike at 60 GHz, atmospheric absorption does not significantly contribute to additional path loss, making it suitable for outdoor mobile communications;

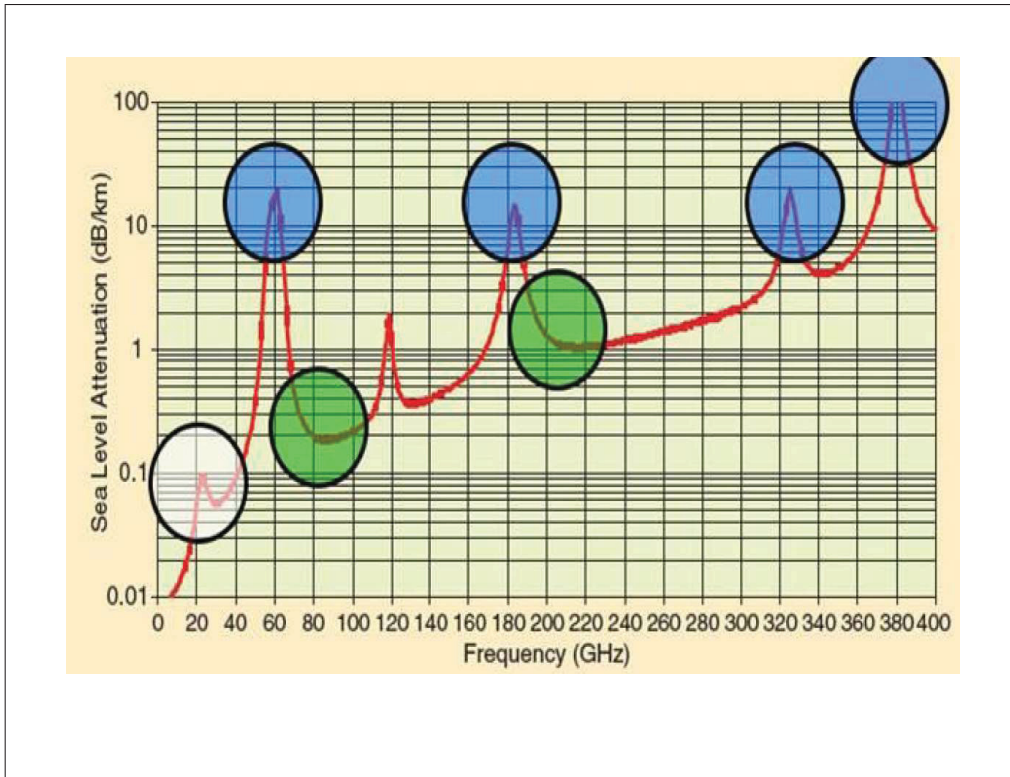


Figure 1.11 Atmospheric absorption across mm-wave frequencies in dB/km
Taken from Rappaport *et al.* (2011)

- 38 GHz band: The 38.6 – 40 GHz band is licensed. Similar to the 28 GHz band, the outdoor cellular propagation measurements in NYC show that this band is suitable for outdoor mobile communications when coupled with the use of large antenna arrays and with the help of beamforming when directional antennas are used;
- E-band or the 70 GHz and 80 GHz bands: 71 – 76 GHz and 81 – 86 GHz respectively are lightly licensed and can be aggregated up to a total of 2×5 GHz. These bands can suffer from high rain attenuations at long distances but are suitable candidates for indoor communications and small-cell areas;
- 60 GHz band : The mobile communications standards for 5G do not consider the unlicensed 57 – 64 GHz band (V-band) which may not be the first choice for a cellular mmWave system since it has a large amount of oxygen absorption and rain attenuation. Moreover, 802.11ad

also known as WiGig (or 60GHz Wi-Fi), is designed to be used in this frequency range (Nitsche & al., 2014).

Two recent research advances have encouraged the use of millimeterwave frequency for mobile communications. First, the mmWave chips suitable for commercial mobile devices have been recently developed as well as highly directional antenna designs. Furthermore, as progress has been made in power amplifiers and due to the small wavelengths, large arrays can be now fabricated in very small areas (less than 1 cm^2). Therefore, a mobile device may be composed of several arrays to provide path diversity from blockage, like human obstruction. The second trend encouraging the use of mmWave frequencies, is the densification of networks explained earlier, allowing smaller radius of cells suitable for high frequency communications.

Recent channel measurement of mmWave signal in urban environment have been conducted in the bands 28 GHz, 38 GHz and 70-80 GHz (Rappaport & al., 2013; Azar *et al.*, 2013a; Zhao *et al.*, 2013; Nie *et al.*, 2013; Samimi *et al.*, 2013; Rappaport *et al.*, 2013; MacCartney & Rappaport, 2014) To combat severe propagation loss, directional antennas are employed at both transmitter and receiver to achieve a high antenna gain.

In (Azar *et al.*, 2013a), outage study has been performed in Manhattan. It has been shown that in highly obstructed environment, when the combined TX-RX antenna gain is 49 dBi, the maximum coverage is 200m in average. Furthermore, 57% of locations were outage but mostly when the RX was located at a distance greater than 200 m from the TX.

In (Akdeniz & al., 2014), detailed spatial statistical models of channels at 28 GHz and 73 GHz in NYC and channel parameters such as path loss, number of spatial clusters, outage and angular dispersion have been derived. The main result obtained was that spatial multiplexing and diversity can be supported at many location up to 200 m and that multiple path clusters are received in highly NLOS environment.

The performances of mmWave cellular networks were simulated in prior works (Akdeniz & al., 2014; Akdeniz *et al.*, 2013; Rappaport & al., 2013) using insights from propagation channel

measurements. In (Bai *et al.*, 2014), it is shown that mmWave cellular networks can provide a high coverage and capacity when small-cells are densely deployed. Based on the real-world measurements at 28 GHz and 38 GHz in New York City and Austin, Texas, respectively, Rapaport & al. (2013) has demonstrated the potential of these two mmWave bands for outdoor mobile communications. Again based on these two measurements campaigns, Sulyman *et al.* (2014a) presents empirically-based large-scale propagation path loss models for cellular network planning in mmWave spectrum. In this paper, simple modifications of current path loss models used in today microwave bands have been applied to fit the propagation data measured in the two mmWave bands. Networks simulations for 5G have then been performed, showing that with random beamforming, 5G networks would require three times more deployed base stations in the same coverage area compared to microwave systems. It has also been that the capacity of mmWave systems is 20 times the capacity of today's cell networks, while this results can be increased when using the best single best pointing beams and multi-beam combining.

We can observe from the measurements that the 28 GHz and 38 GHz bands suffer from low rain attenuation and oxygen absorption while they are significant in the 60 GHz and 70-80 GHz bands. This can motivate the use of the 28 GHz and 38 GHz bands for outdoor communications while the E-bands may be dedicated to indoor communications. In Ghosh & Tal. (2014), a case is made for using mmWave bands for a 5G systems. An enhanced local area (eLA) is presented in the paper for 5G networks, where the proposed system exploits large bandwidths in mmWave spectrum with a proper small-cells densification to achieve peak data rates up to 10 Gbps and edge rates over 100 Mbps. The proposed eLA is based on overlapping deployment strategies and simultaneous connexions of users to both the LTE overlay and to one or several mmWave access points.

Although the amount of bandwidth available in mmWave is very large, the propagation properties in these frequencies are challenging and vary greatly from lower to higher bands. Hence, these bands need to be allocated properly in order to exploit both the advantages and the limits of the four main mmWave frequency bands presented below.

1.6 Conclusion of chapter I and proposed research plan

We have presented in this chapter three sections presenting the context, the challenges and the state of the art related to the topic of research of this thesis. In the first place, we have presented the small-cell technology in general, the concept of access modes, the motivations of their dense deployment and how they will play a major role in 5G. In the second section, we have presented the technical challenges of the dense deployment of small-cells and their co-existence with the traditional macro-tier. In the third section, we have investigated the major contributions in terms of interference management and resource allocation in the past years and highlighted the missing parts and what could be improved in future studies. Finally the three following sections have focused in the literature review related to the three topics investigated more deeply in the following chapters of this thesis, i.e. call admission control in two-tier HetNets, game theory for cooperative resource allocation in small-cells based networks and mmWave communications for short-ranges communications in next generations of wireless communications systems. We have summarized in Figure 1.12 all the existing subchannels allocation techniques for two-tier HetNets and have highlighted in green the parts that have been investigated in this thesis and the specific chapters covering these techniques.

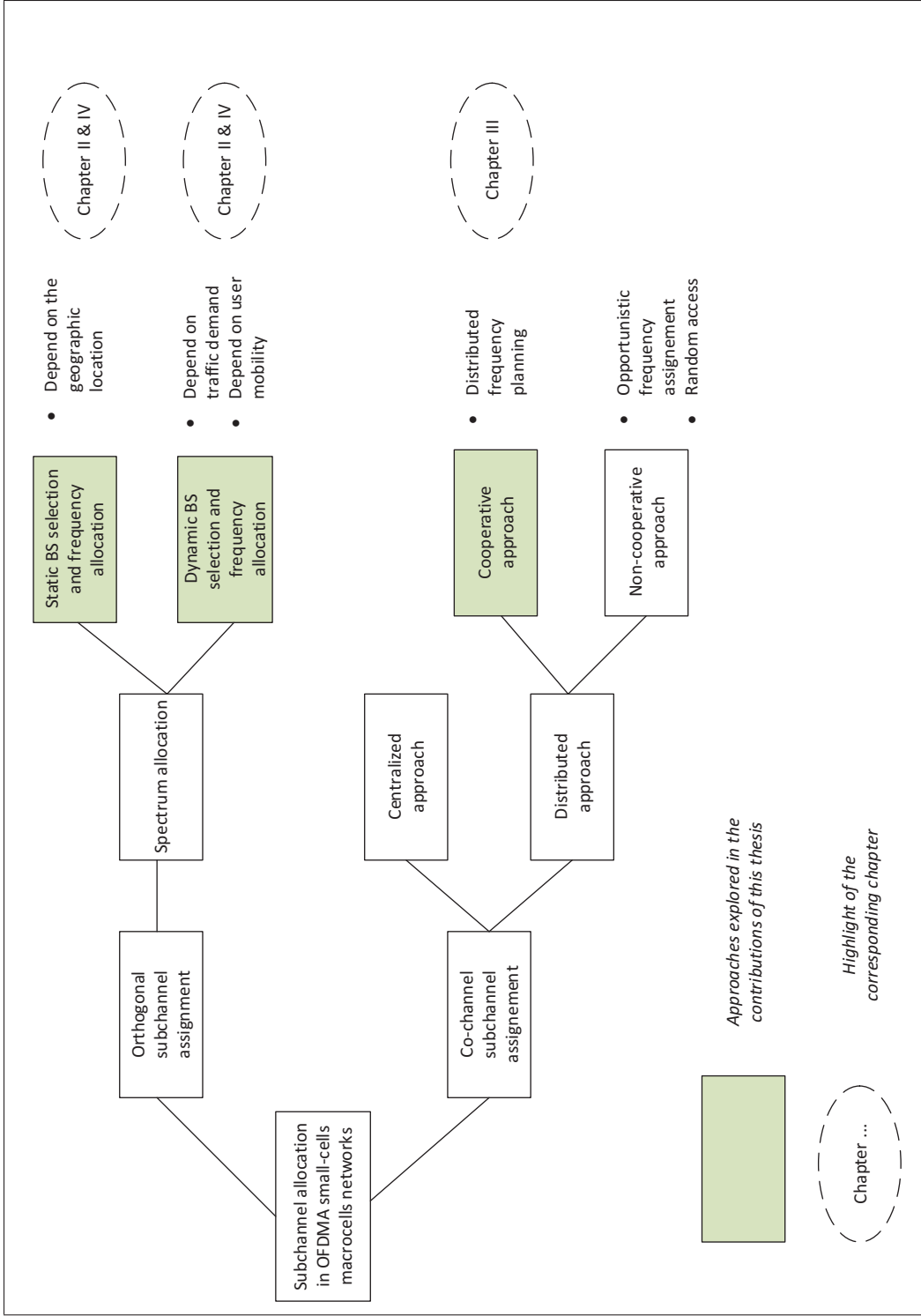


Figure 1.12 Flow chart illustrating the existing resource allocation techniques and situating the contributions of this thesis

CHAPTER 2

QOS-AWARE ADMISSION CONTROL FOR OFDMA FEMTOCELL NETWORKS UNDER FRACTIONAL FREQUENCY-BASED ALLOCATION

Fractional Frequency Reuse (FFR) is considered to provide enhancement in total throughput and an important reduction of the outage probability in two-tier macrocell-femto cell networks. However the allocation in FFR can create high cross-tier interferences to users located in the boundaries of the various zones. We propose a FFR scheme to alleviate the downlink cross-tier interference for users in these particular zones, joint with a QoS-aware analytical model to derive the blocking probabilities for different cell zones. The optimal parameters for cell channel partitioning in the proposed FFR-scheme are integrated to enhance the proposed system. Numerical results demonstrate the performance enhancement of the proposed joint FFR allocation and admission control scheme. Compared to current FFR and admission control strategies, our scheme permits to increase overall traffic by up to 40 % at cell center and 30 % at cell edge, for any given blocking probability. The main results of this paper have been published in a conference paper (Hajir & Gagnon, 2015).

2.1 Introduction

2.1.1 Motivation and prior related work

The proliferation of mobile devices and mobile Internet usage in past years has led to an increase in the demand for higher capacity and data rates. To address this demand in growth, one solution is to enhance the network coverage and capacity by placing transmitters and receivers closer together and through aggressive reuse of the cellular spectrum. In recent years, the heterogeneous based deployment model is being explored by mobile operators and the research community. This strategy allows for a higher data rate and increased reliability for users, as well as a reduced amount of traffic on an expensive macrocell network for the operator (Lopez-Perez *et al.*, 2009).

Resource allocation based interference management in OFDMA-based two-tier networks is a significant research topic and comes in various forms. Closely related to radio resource allocation, call admission control (CAC) is responsible for admitting or rejecting a call request from a user based on the current network load and QoS requirement of users. An efficient CAC scheme is required in multi-tier networks to achieve a higher spectrum efficiency and QoS requirements satisfaction in each tier of the system. When these two elements of radio resource management are joint, interferences are significantly mitigated and a high spectrum utilization and capacity are achieved.

There have been some works in the recent literature that address interference management or admission control for two tier networks, but very few are addressing jointly the frequency allocation and CAC efficiently. In Lee *et al.* (2010b), femtocells have access to the entire sub-bands unused by the macrocell sub-area. However it creates a high level of interference to the macrocell user equipments (MUEs) located in the edge of the neighboring cells as the users from two different tiers use the same subchannels. Indeed, the received signal power of the sub-bands allocated to the neighbouring macrocells is relatively strong compared to the femtocells located in the boundary of the macrocell. In (Maheshwari & Kumar, 2000), blocked microcell calls are allowed to overflow to the macrolayer while the macrocell calls have no alternate route if the available subchannels are not sufficient, which leads to higher blocking probabilities in the macrocell areas. Also this scheme can not be applied to macrocell-femtocell networks since it does not take into consideration cross-tier interferences. In Guvenc *et al.* (2008), a FFR based allocation scheme was proposed considering the handoff and coverage of femtocells but MUEs in edge zones suffer from high interferences induced by nearby FBS.

In (Farbod & Liang, 2007), the CAC problem is formulated as a Semi-Markov decision problem but does not consider the QoS constraints. In Le *et al.* (2013a), a QoS-aware admission control scheme is proposed but FUEs and MUEs compete for the same subchannels in the edge zone which leads to high cross-tier interferences when a MUEs in the vicinity of a FUEs fail to connect to the nearby femtocell base stations (FBS). Moreover, closed access mode is applied in the center zone resulting in high blocking probabilities for MUEs compared to FUEs. In

Zhang *et al.* (2014), femto QoS-aware joint subchannel and power allocation is investigated but the performances of MUEs have not been considered.

2.1.2 Main contribution and organization

In this chapter, an interference management and call admission control scheme for OFDMA macrocell-femtocell network is proposed. A sector-based FFR scheme is developed to protect users in the boundaries of center zones and edge zones from cross-tier interferences and allowing MUEs to achieve higher rates. This scheme is associated with a QoS-aware admission control strategy that efficiently associates users with femtocell and macrocell base stations (MBS) as well as allowing an alternative route to any user blocked from accessing subchannels in its original layer. FUE calls can overflow to the MBS when they fail to connect with the nearby FBS and MUEs can borrow the unused subchannels from other zones. An analytical model is developed to conduct a performance evaluation of the proposed admission control scheme. Finally the numerical results proving the efficiency of the proposed framework are presented.

2.2 System model of the proposed FFR

We consider the downlink of a macrocell-femtocell network employing Frequency-Division Duplex (FDD) and OFDMA. The subchannel allocation for sector-based FFR is illustrated in Figure 2.1. The scheme avoids downlink cross-tier interference by assigning sub-bands from the entire allocated frequency band to the FBS that are being used neither in the macrocell sub-area nor the neighbouring macrocell areas. The macrocell is divided into center zone and edge zone including three sectors per region. The center zone has a reuse factor of one while the edge zone a reuse factor of three. The entire spectrum is divided into two parts, one is allocated to the center and the other one is divided by three, each portion is assigned to an edge zone of the three-cell sectors (Lee *et al.*, 2010b).

In the following, we refer to a center zone and an edge zone of a given macrocell sector as a center macro-area and edge macro-area. We refer to a femtocell overlaying the center macro-area and edge macro-area as center femto-area and edge femto-area. Moreover, we refer to the portion of bandwidth allocated to the center and edge macro-area as center and edge macrolayer, and the portion of bandwidth allocated to the center and edge femto-area as center and edge femtolayer.

The sub-bands are denoted by A,B,C,D. The sub-band A is used in the center macro-area and the sub-bands B,C,D are applied to edge regions as depicted in the figure. A femtocell in the center zone chooses sub-bands that are not used in the macrocell sub-area. It additionally excludes the sub-band used by the edge macrolayer of the current sector given the high received signal power of this sub-band for the femtocell. For example in the zone C1, a femtocell uses the sub-bands C and D. A femtocell in the edge area excludes the sub-bands of the center macrolayer. Additionally the edge of the sector is divided into two zones and the femtocell excludes the sub-band used by the neighbouring edge macrolayer according to its location. For example in E1 of macrocell 1, a femtocell excludes the sub-band A used by the center macrocell, the sub-band B used by the edge macrocell of the current sector and the sub-band C used by the neighboring edge of macrocell number 2. In E2, a femtocell excludes the sub-bands A and B similarly to E1 but will exclude this time the sub-band D used by the sector edge of the neighbouring macrocell number 3.

2.2.1 QoS constraints

We define in this section the QoS constraints in the considered two-tier network. The downlink signal-to-interference-plus-noise ratio (SINR) achieved by a FUE y_f associated with femtocell f on a particular subchannel k can be written as Saquib *et al.* (2013):

$$\gamma_{y_f,f}^k = \frac{P_f^k G_{y_f,f}^k}{\sum_{m \in M} P_m^k h_{y_f,m}^k G_{y_f,m}^k + \sum_{f' \in F'} P_{f'}^k G_{y_f,f'}^k + N} \quad (2.1)$$

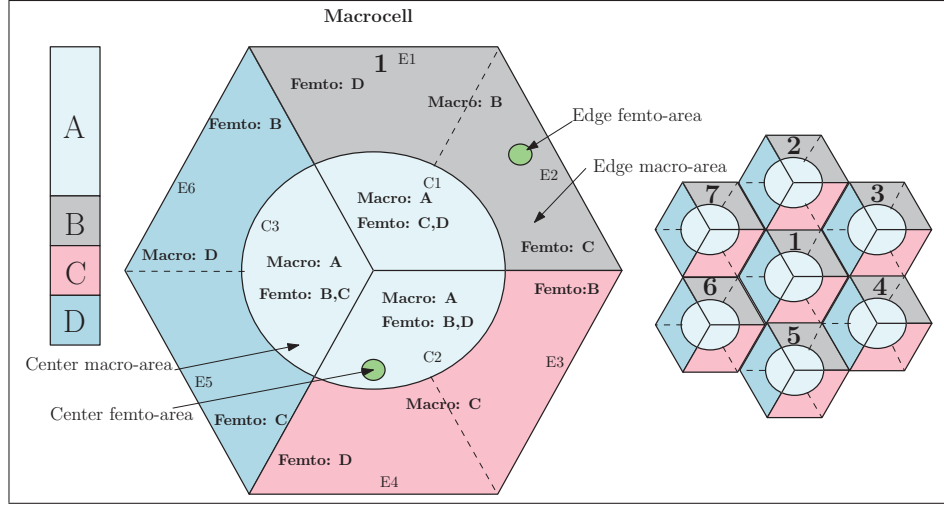


Figure 2.1 Interference management scheme using an adjusted FFR3 model

where N denotes the Gaussian noise power, $G_{y_f,f}^k$ and $G_{y_f,m}^k$ represent the channel gains from FBS f and MBS m to FUE y_f respectively in femtocell f on subchannel k . Their models are explained in section 2.6. The signal-to-interference-plus-noise ratio (SINR) achieved by a MUE x_m associated with macrocell m on a particular subchannel k can be written as:

$$\gamma_{x_m,m}^k = \frac{P_m^k G_{x_m,m}^k h_{x_m,m}^k}{\sum_{m' \in M'} P_{m'}^k h_{x_m,m'}^k G_{x_m,m'}^k + \sum_{f \in F} P_f^k G_{x_m,f}^k + N} \quad (2.2)$$

where P_m^k is the transmit power from MBS m on subchannel k , $h_{x_m,m}^k$ is the exponentially distributed channel fading power gain associated with subchannel k . $G_{x_m,m}^k$ and $G_{x_m,f}^k$ represent the path loss associated with k from a MBS m and FBS f to a MUE x_m respectively in macrocell m .

From 2.1, we can determine $r_{x_f,f}^k$ denoting the minimum rate achieved by a FUE y_f on k . The minimum achieved rate is obtained by the worst case where the user is located at the boundary of its corresponding zone Le *et al.* (2013b):

$r_{x_f,f}^k = W \int_0^\infty \log(1+x) f_{\gamma_{y_f,f}^k}(x) dx$ where W denotes the bandwidth of one subchannel and $f_{\gamma_{y_f,f}^k}$ the probability density function (PDF) of $\gamma_{y_f,f}^k$. In the same way, we can determine the minimum rate achieved by a MUE x_m on a subchannel k : $r_{x_m,m}^k = W \int_0^\infty \log(1+x) f_{\gamma_{m,m}^k}(x) dx$.

Let $s_f^{y_f}$ and $s_f^{x_m}$ be the number of subchannels allocated for a FUE in femtocell f and for a MUE in macrocell m respectively. To guarantee the QoS requirement the number of subchannels that must be allocated for a FUE and for a MUE respectively, should satisfy these constraints:

$$s_f^{y_f} \geq \frac{R_{min}^f}{r_{x_f,f}^k}, s_f^{x_m} \geq \frac{R_{min}^m}{r_{x_m,m}^k}, \quad (2.3)$$

where R_{min}^f, R_{min}^m denote the target minimum rates for FUEs and MUEs respectively. These constraints will be used for admission control design.

2.3 LTE resource blocks specifications

In this section, we resume the specifications of 3GPP for LTE and LTE-A, as well as the technologies used in the 3GPP standards for mobile communications that will be taken into account in this thesis. In LTE/LTE-A multi-tier networks, OFDM is used for downlink and single-carrier FDM waveform is used for uplink over 20 MHz bandwidth. The subcarrier spacing is 15 kHz and therefore the OFDM symbol duration is 66.67 kHz. For full-duplex FDD, uplink and downlink frames are separated by frequency and are transmitted continuously and synchronously. In TDD mode, the uplink and downlink subframes are transmitted on the same frequency and are multiplexed in the time domain.

One subchannel during one time slot constitutes a resource block (RB). The terms resource blocks and subchannels will be used interchangeably and are used multiple times in this thesis. We define the physical characteristic of this element. It refers to the minimum scheduling unit in DL and UL. An LTE RB consists of 12 sub-carriers in the frequency domain (180 kHz) and one time slot in the time domain (0.5 ms). One subframe is composed of two-time slots. UE

is dynamically allocated multiples of RB pairs, each of which is two RBs side to side with duration 1 ms. In one time slot, there are 7 OFDM symbols. The bandwidth defined by the standards are 1.4, 3, 5, 10, 15 and 20 MHz.

Table 2.1 Frequency measures and number of elements

Bandwidth	Number or resource blocks	Number of subcarriers
1.4 MHz	6	72
3 MHz	15	180
5 MHz	25	300
10 MHz	50	600
15 MHz	75	900
20 MHz	100	1200

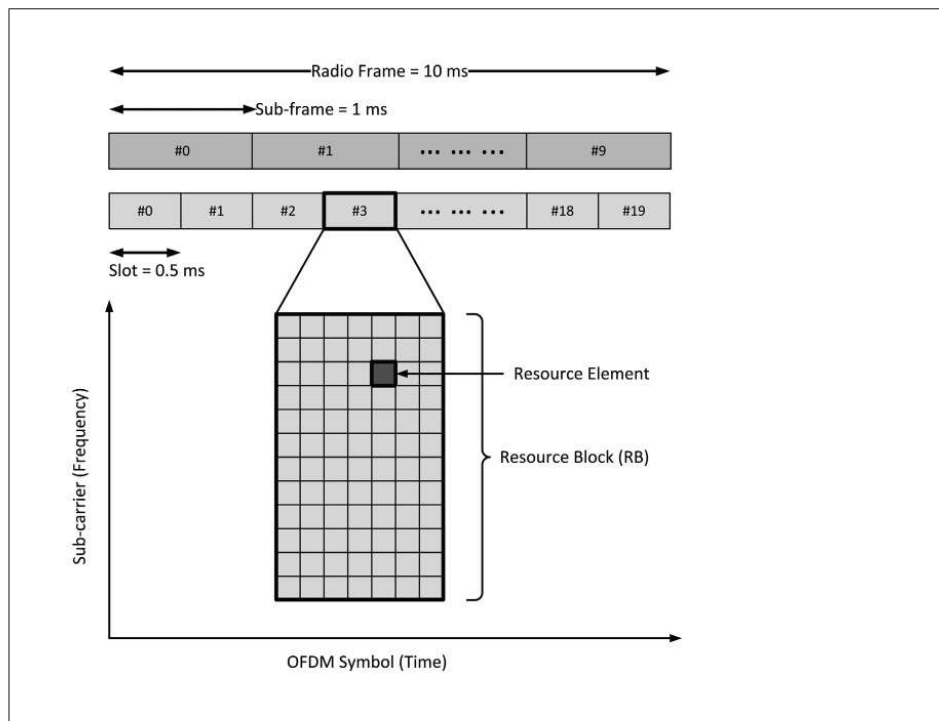


Figure 2.2 LTE Physical Layer Structure

2.4 Admission control policy

We propose a Qos-aware call admission control scheme for macrocell-femtocell networks with the detailed rules described in the following. Given the proposed FFR scheme, each macrocell area is divided into cell-center and cell-edge zones, which are separated by a circular boundary and then separated into three distinct sectors. We apply an open access mode for femtocells, where all the users located in the coverage area of a FBS are allowed to connect to the corresponding FBS.

We assume that a new call or a handoff call arriving at the femtocell area will always first attempt to connect with the corresponding FBS. Users located in a femtocell area can also connect to the nearby MBS. Any call outside any femtocell area is directed to the MBS. The bandwidth requirements are determined in the above section from the average rate requirements and the the worst-case average rate achieved by users in each area. The corresponding values are presented in Table I. For simplicity ,we develop the admission control rules for center users only. However the analysis described in the paragraphs below applies identically to the edge analysis by denoting c_{F1} and c_{M1} , c_{F2} and c_{M2} respectively.

A new call generated in a center femto-area is directed to the corresponding FBS. If the number of available subchannels offered is less than c_{F1} the call is directed to the MBS and try to use center macrolayer subchannels. If the number of available center macrolayer subchannels is less than c_{F1} the call is dropped. If subchannels become available later the call is repacked to the FBS.

A new call generated in a center macro-area will try to occupy center macrolayer subchannels. If the number of center macrolayer subchannels is less than c_{M1} it will attempt to use edge macrolayer subchannels. If there are not sufficient edge macrolayer subchannels the call is dropped. If center macrolayer subchannels become available later the cell-center calls occupying the edge macrolayer subchannels will be shifted back to the center macrolayer.

2.5 Performance analysis

As previously established, in the proposed FFR3 based network each macrocell is divided into three distinct sectors indexed by $i \in \{1, 2, 3\}$. Sector i has $m_1^{(i)}$ femtocells in the center zone and $m_2^{(i)}$ femtocells in the edge zone. We propose an isolated sector analytical framework for performance analysis of the proposed admission control scheme (Rappaport Stephen & Hu, 1994). For simplicity we omit the sector index i in all notations. All new call and handoff call arrival processes among regions are assumed to follow Poisson processes. Cell region sojourn times and call conversation times are exponentially distributed.

We analyze three separate Markov Chains (MCs): two one-dimensional MCs $\Gamma_{F1}(t)$ and $\Gamma_{F2}(t)$ describing the dynamics for calls at time t connecting to a FBS located in the center area and to a FBS located in the edge area respectively, and one 6-dimensional MC $\Delta(t)$ describing the dynamics for calls connecting to the MBS. Let $\Delta = \{X_{M1}(t), Z_{M1}(t), W_{M1}(t), Y_{M2}(t), Z_{M2}(t), W_{M2}(t)\}$, $\Gamma_{F1} = \{U_{F1}(t)\}$ and $\Gamma_{F2} = \{U_{F2}(t)\}$. To simplify the 6-dimensional MC we analyse the center macrolayer and edge macrolayer separately. All the values are described in table I.

Let $\Delta_{M1}(t) = \{X_{M1}(t), Z_{M1}(t), W_{M1}(t)\}$ the MC that captures the number of calls connecting to the MBS and using center macrolayer subchannels and $\Delta_{M2}(t) = \{X_{M2}(t), Z_{M2}(t), W_{M2}(t)\}$ the MC that captures the number of calls connecting to the MBS and using edge macrolayer subchannels. Interactions between the MCs are captured through the corresponding handoff rates obtained from the stationary analysis of the MCs detailed in the next section. The stationary analysis gives us the average values of the corresponding quantities in the defined MCs, denoted by \bar{X}_{M1} , \bar{Z}_{M1} , \bar{W}_{M1} , \bar{X}_{M2} , \bar{Z}_{M2} , \bar{W}_{M2} . To obtain the handoff rates we first initialize their values to zero, then we perform the stationary analysis of the MCs before updating the handoff rates and repeating these 2 last steps of the procedure until convergence.

2.5.1 Mobility and handover in out of the two-tier network

2.5.1.1 Teletraffic flow coefficients

We will define in this subsection the teletraffic flow coefficients corresponding to the fraction of calls handed over from one given zone to another.

Let $\alpha_{M2,M2}$; $\alpha_{M1,M1}$; $\alpha_{M2,M1}$; $\alpha_{M1,M2}$; $\alpha_{M2,F2}$; $\alpha_{M1,F1}$ be the fractions of calls that are handed over from an edge macro-area to a neighbouring edge macro-area, from the cell center sector to the neighbouring cell center sectors, from an edge macro-area to a center macro-area, from a center macro-area to an edge macro-area, from an edge macro-area to an overlaying femto-area and finally from a center macro-area to an overlaying femto-area.

Let R be the largest distance from the macrocell center to the macrocell edge, r the radius of the inner circular region and r_f the radius of the femtocell area. The teletraffic flow coefficients can be calculated as:

$$\begin{aligned}\alpha_{M2,M2} &= \frac{3R}{3R + \frac{2\pi r}{3} + 2m_2\pi r_f}; & \alpha_{M1,M1} &= \frac{2r}{2r + \frac{2\pi r}{3} + 2m_1\pi r_f} \\ \alpha_{M2,M1} &= \frac{\frac{2\pi r}{3}}{3R + \frac{2\pi r}{3} + 2m_2\pi r_f}; & \alpha_{M1,M2} &= \frac{\frac{2\pi r}{3}}{2r + \frac{2\pi r}{3} + 2m_1\pi r_f} \\ \alpha_{M2,F2} &= \frac{2m_2\pi r_f}{3R + \frac{2\pi r}{3} + 2m_2\pi r_f}; & \alpha_{M1,F1} &= \frac{2m_1\pi r_f}{2r + \frac{2\pi r}{3} + 2m_1\pi r_f}\end{aligned}$$

Table 2.2 Key parameters and variables

$X_{M1}(t)$ ($X_{M2}(t)$)	Number of calls located in center (edge) macro-area using subchannels from center (edge) macrolayer
$Z_{M1}(t)$ ($Z_{M2}(t)$)	Number of calls located in center (edge) femto-area overflowed to the MBS using subchannels from center (edge) macrolayer
$W_{M1}(t)$ ($W_{M2}(t)$)	Number of calls located in edge (center) macro-area using subchannels from center (edge) macrolayer
$U_{F1}(t), U_{F2}(t)$	Number of calls which connects to a FBS in a center femto-area and edge femto-area
$k_{F1}(t), k_{F2}(t)$	Number of subchannels allocated to center femto-area and edge femto-area respectively
$k_{M1}(t), k_{M2}(t)$	Number of subchannels allocated to center macro-area and edge macro-area respectively
$c_{F1}(t), c_{F2}(t)$	Number of subchannels required by a call in a center femto-area and edge femto-area
$c_{M1}(t), c_{M2}(t)$	Number of subchannels required by a call in a center macro-area and edge macro-area
$\lambda_{M1}^n, \lambda_{M2}^n, \lambda_{F1}^n, \lambda_{F2}^n$	New call arrival rate of a call to a center macro-area, edge macro-area, center femto-area and edge femto-area
$\lambda_{M1 \rightarrow M1}^h$	Handoff rate for calls to the center macro-area from center macro-area of neighbouring sectors in a given macrocell
$\lambda_{M2 \rightarrow M1}^h$	Handoff rate for calls to the center macro-area from edge macro-area
$\lambda_{M1 \rightarrow M2}^h, \lambda_{M2 \rightarrow M2}^h$	Handoff rate for calls to the edge macro-area from center macro-area and from neighbouring edge macro-area
$\lambda_{M1 \rightarrow F1}^h, \lambda_{M2 \rightarrow F2}^h$	Handoff rate for calls to the femtocell area from the underlying center macro-area and edge macro-area
$\lambda_{F1 \rightarrow M1}^h, \lambda_{F2 \rightarrow M2}^h$	Handoff rate for calls to the center macro-area and edge macro-area from the overlaying femtocell area
μ^{-1}	Mean duration time of a call in the system
$\theta_{M1}^{-1}, \theta_{M2}^{-1}, \theta_{F1}^{-1}, \theta_{F2}^{-1}$	Mean sojourn time of a call in the center macro-area, edge macro-area, center femto-area and edge femto-area

2.5.1.2 Calculation of handoff arrival rates

We express the handoff rates values described in Table I as:

$$\begin{aligned}
\lambda_{M2 \rightarrow M2}^h &= \alpha_{M2,M2} \cdot \theta_{M2} \cdot (\bar{X}_{M2} + \bar{W}_{M1}); \\
\lambda_{M1 \rightarrow M1}^h &= \alpha_{M1,M1} \cdot \theta_{M1} \cdot (\bar{X}_{M1} + \bar{W}_{M2}); \\
\lambda_{M2 \rightarrow M1}^h &= \alpha_{M2,M1} \cdot \theta_{M2} \cdot (\bar{X}_{M2} + \bar{W}_{M1}); \\
\lambda_{M1 \rightarrow M2}^h &= \alpha_{M1,M2} \cdot \theta_{M1} \cdot (\bar{X}_{M1} + \bar{W}_{M2}); \\
\lambda_{M2 \rightarrow F2}^h &= \alpha_{M2,F2} \cdot \theta_{M2} \cdot \frac{\bar{X}_{M2}}{m_2}; \quad \lambda_{M1 \rightarrow F1}^h = \alpha_{M1,F1} \cdot \theta_{M1} \cdot \frac{\bar{X}_{M1}}{m_1}; \\
\lambda_{F1 \rightarrow M1}^h &= \theta_{F1} \cdot (\bar{Z}_{M1} + m_1 \bar{U}_{F1}); \quad \lambda_{F2 \rightarrow M2}^h = \theta_{F2} \cdot (\bar{Z}_{M2} + m_2 \bar{U}_{F2})
\end{aligned}$$

We can then express the total handoff rates to each of the areas under consideration:

$$\begin{aligned}
\lambda_{M1} &= \lambda_{M1}^n + \lambda_{M1 \rightarrow M1}^h + \lambda_{M2 \rightarrow M1}^h + \lambda_{F1 \rightarrow M1}^h + m_1 \lambda_{F1} B_{F1}; \\
\lambda_{M2} &= \lambda_{M2}^n + \lambda_{M1 \rightarrow M2}^h + \lambda_{F2 \rightarrow M2}^h + m_2 \lambda_{F2} B_{F2}; \\
\lambda_{F1} &= \lambda_{M1 \rightarrow F1}^h + \lambda_{F1}^n; \quad \lambda_{F2} = \lambda_{M2 \rightarrow F2}^h + \lambda_{F2}^n
\end{aligned} \tag{2.4}$$

2.5.2 Stationary analysis of Markov chains $\Delta_{M1}(t)$ and $\Delta_{M2}(t)$

The analysis for center and edge macro-area are similar as the same admission control policies are adopted for both. We present the detailed analysis and show how to calculate the blocking probabilities for MC $\Delta_{M1}(t)$ only. We define s as a general state for the MC Δ_{M1} with $\vec{g}(s) = \{g_1(s), g_2(s), g_3(s)\}$; $g_1(s), g_2(s), g_3(s)$ representing the values of $X_{M1}(t), Z_{M1}(t), W_{M1}(t)$ in state s , respectively. Let $\vec{v}_i, i = 1, 2, 3$ be a three-dimensional vector whose i -th element is one and other elements zero and $k(s) = (g_1(s) + g_2(s)) c_{M1} + g_3(s) c_{M2}$.

2.5.2.1 Calculation of transition rates

The transition rates $q(i, s)$ from predecessor state i into state s where $i \neq s$ can be written as follows.

The transition rate due to a center macro-area call arrival $\vec{g}(s) = \vec{g}(i) + \vec{v}_1$:

$$q(i, s) = \lambda_{M1}; \text{ if } k(s) \leq k_{M1}$$

The transition rate due to the departure of a call occupying the center macro-area subchannels $\vec{g}(s) = \vec{g}(i) - \vec{v}_1$:

$$q(i, s) = (\mu + \theta_{M1})g_1(i); \text{ if } k(i) \leq k_{M1}$$

The transition rate due to a center femto-area arrival call which tries to occupy the center macro-area subchannels: according to our admission control policies center femto-area calls only try to occupy center macro-layer subchannels if center femto-layer subchannels are all used. When $g_2(s) = 0$, if a call arrives to a center femto-area it will try to occupy center macro-layer subchannels when blocked from the FBS with the conditional probability calculated in the next section B_{F1} . When $g_2(s) > 0$, all center macro-layer subchannels are occupied, therefore a new call arriving to the center femto-area will always try to occupy center macro-layer subchannels $\vec{g}(s) = \vec{g}(i) + \vec{v}_2$:

$$q(i, s) = \begin{cases} B_{F1}\lambda_{F1} & \text{if } g_2(s) = 0, k(s) \leq k_{M1} \\ \lambda_{F1} & \text{if } g_2(s) > 0, k(s) \leq k_{M1} \end{cases}$$

The transition rate due to a departure of a call in a center femto-area occupying center macro-layer subchannels. We also take into consideration the repacking rule when a call is shifted back to center femto-layer subchannels. Let $N_{max}^{F1} = \frac{k_{F1}}{c_{F1}}$ be the maximum number of calls

occupying center femtolayer subchannels $\vec{g}(s) = \vec{g}(i) - \vec{v}_2$;

$$q(i, s) = (\mu + \theta_{F1})g_2(i) + N_{max}^{F1}(\mu + \theta_{F1}); k(i) \leq k_{M1}$$

The transition rate due to an edge macro-area call arrival which tries to occupy center macro-layer subchannels. According to our admission control policies, edge macro-area calls only try to occupy center macrolayer subchannels if the edge macrolayer subchannels are all occupied. When $g_3(s) = 0$, if a call arrives to the edge macro-area it will try to occupy the center macro-area subchannels if it is blocked from accessing edge macrolayer subchannels with the conditionnal probability B_{M2} . In the case where $g_3(s) > 0$, all the edge macrolayer subchannels are occupied, therefore a new call arriving to edge macro-area will always try to occupy center macrolayer subchannels $\vec{g}(s) = \vec{g}(i) + \vec{v}_3$:

$$q(i, s) = \begin{cases} B_{M2}\lambda_{M2} & \text{if } g_3(s) = 0, k(s) \leq k_{M1} \\ \lambda_{M2} & \text{if } g_3(s) > 0, k(s) \leq k_{M1} \end{cases}$$

The transition rate due to a departure of a call in edge macro-area which is occupying center macrolayer subchannels. The departure can be due to a call completion or a shifting back to edge macrolayer subchannels. Let $N_{max}^{M2} = \frac{k_{M2}}{c_{M2}}$ be the maximum number of calls occupying edge macrolayer subchannels $\vec{g}(s) = \vec{g}(i) - \vec{v}_3$:

$$q(i, s) = (\mu + \theta_{M2})g_3(i) + N_{max}^{M2}(\mu + \theta_{M2}); k(i) \leq k_{M1}$$

2.5.2.2 Calculation of the blocking probabilities

We first write the flow balance equations for all possible states. There are a set of $s_{max} + 1$ simultaneous equations for the unknown state probabilities $\pi(i)$ of the form :

$$\sum_{j=0}^{s_{max}} q(i, j) \pi(i) = 0; \sum_{j=0}^{s_{max}} \pi(i) = 1; i = 0, 1, 2, \dots, s_{max} \quad (2.5)$$

Where $q(i, j)$ represents the net transition flow into state j from state i and $\pi(i)$ the total transition flow out of state i . The equations express that in a steady state the net probability flow into any state is zero and the sum of the probabilities is unity. We can find the stationary distribution of MC $\Delta_{M1}(t)$ then we can calculate the blocking probabilities of calls in the center macrolayer. We now derive the blocking probabilities of calls in cell center area. Recall that a center macro-area call will be blocked if it cannot find sufficient subchannels, which are pre-allocated to cell center macro-area. The blocking probability of center macro-area or center femto-area calls trying to use center macrolayer subchannels can be calculated as:

$$B_{M1} = \sum_{S \in S_0} \pi(s); S_0 = \{s : k(s) > k_{M1} - c_{M1}\} \quad (2.6)$$

The blocking probability of edge macro-area calls trying to use center macrolayer subchannels can be calculated as:

$$B_{M12} = \sum_{S \in S_1} \pi(s); S_1 = \{s : k(s) > k_{M1} - c_{M2}\} \quad (2.7)$$

Using Little's theorem, we can compute the average number of calls in the center macrolayer.

$$\begin{cases} \bar{X}_{M1} &= \frac{\lambda_{M1}}{\mu + \theta_{M1}}(1 - B_{M1}) \\ \bar{Z}_{M1} &= \frac{\lambda_{F1}}{\mu + \theta_{F1}}(1 - B_{M1}) \\ \bar{W}_{M1} &= \frac{\lambda_{M2}}{\mu + \theta_{M2}}(1 - B_{M12}) \end{cases} \quad (2.8)$$

2.5.3 Stationary analysis of Markov chains Γ_{F1} and Γ_{F2}

As we defined previously, MC $\Gamma_{F1}(t) = \{U_{F1}(t)\}$ captures the number of calls of a particular center femto-area and $\Gamma_{F2}(t) = \{U_{F2}(t)\}$ captures the number of calls of a particular edge femto-area. The center femto-area and edge femto-area analysis are similar. We will present the detailed analysis of the center femto-area only. We remind here that $N_{max}^{F1} = \frac{k_{F1}}{c_{F1}}$ is the maximum number of calls occupying center femtolayer subchannels. When $U_{F1} = N_{max}^{F1}$, the center macrolayer holds at least one call that belongs to the femtocell with probability $P(Z_{M1} > 0/U_{F1} = N_{max}^{F1})$. Hence owing to repacking, the transition rate from the state $U_{F1} = N_{max}^{F1}$ to $U_{F1} = N_{max}^{F1} - 1$ is:

$$P(Z_{M1} = 0/U_{F1} = N_{max}^{F1})N_{max}^{F1}(\mu + \theta_{F1}) \quad (2.9)$$

The remaining transition rates are unaffected by repacking. In order to calculate the blocking probability, we need the following probability $P(Z_{M1} = N_{max}^{F1} | U_{F1} = 0)$.

Owing to the fact that calls are always offered to femtocell first, and owing to repacking, when we have $Z_{M1} > 0$ then $U_{F1} = N_{max}^{F1}$. Furthermore the set of states with $Z_{M1} > 0$ is entered only from the set of states when $U_{F1} = N_{max}^{F1}$. We can admit that the process Γ_{F1} conditioned on $U_{F1} = 0$ is just the Erlang-B process with offered load $\beta_{F1} = \lambda_{F1}/(\mu + \theta_{F1})$ and number of servers N_{max}^{F1} (Maheshwari & Kumar, 2000).

$$\begin{aligned} B_{F1} &= P(Z_{M1} = N_{max}^{F1} | U_{F1} = 0) = Erlang_B(\beta_{F1}, N_{max}^{F1}) \\ \bar{U}_{F1} &= \beta_{F1}(1 - B_{F1}) \end{aligned} \quad (2.10)$$

2.6 Numerical results

We present the numerical results to illustrate the performances of the proposed joint frequency partitioning and call admission control scheme. We consider 25 femtocells located in the center and 30 femtocells in the edge of each given sector of the central macrocell in a cluster of 7 macrocells. The distance between two neighbouring femtocells is set to $100m$ and the radius of a femtocell is set to $30m$. The radius of the macrocell is set to $R = 500m$ and the radius of the center macro-area is set to $r = 280m$. The total number of available subchannels in one macrocell is $N = 100$, shared among the sub-bands A,B,C and D as depicted in Figure 2.1. 40% of total bandwidth is allocated to sub-band A and the remaining is shared equally among B,C and D.

2.6.1 Results on the best parameters for resource partitioning

In figures 2.3 and 2.4, we illustrate the blocking probabilities of calls connecting to MBS and FBS in different areas versus the percentage of bandwidth allocated to center macro-area (sub-band A). These results are shown for two different values of traffic density $TD = 20, 25 \text{ calls}/\text{min}/\text{km}^2$. The blocking probability of center macro-area decreases quickly as the percentage of subchannels allocated to sub-band A increases, up to a minima reached between 40% and 45%. After that, the blocking probability increases quickly. This can be explained as follows. When sub-band A size increases, the number of subchannels shared equally by B,C and D decreases, which leads to higher blocking probabilities in the corresponding zones as well as an increase of number of calls being overflowed from the center femto-area and from edge macro-area trying to borrow center macro-area subchannels. The figures suggest that a good value for the percentage of the bandwidth allocated to a macrocell center is about 40%.

2.6.2 Performance results in terms of blocking probability

To calculate the required number of subchannels, we consider the worst case where FUEs and MUEs are located on the boundary of the corresponding region. The path-loss in dB is calcu-

lated as Le *et al.* (2013b): $G_{i,j}^k(d) = [44.9 - 6.55 \log_{10}(h_{BS}) \log_{10}(d) + 34.46 + 5.83 \log_{10}(h_{BS}) + 23 \log_{10}(f_c/5) + n_{ij}W_{i,j}]$, d being the distance between a user i and a base station of either type j , h_{BS} the height of the base station chosen as $25m$ for MBSs and $10m$ for FBSs. f_c is the carrier frequency which is set to 2 GHz. n_{ij} denotes the number of walls and $W_{i,j} = 5dB$ denotes the wall loss. For the path-loss from a FBS to an indoor FUE connected with an other FBS $n_{ij} = 2$, for all other cases $n_{ij} = 1$. The minimum required rates for MUEs and FUEs are $R_{min}^m/W = 6$ b/s/Hz and $R_{min}^f/W = 10$ b/s/Hz respectively. Other system parameters are set as follows: noise power $N = 10^{-15}$, MUEs' and FUEs' average service time $\mu = 1min$, sojourn times $\theta_{M1} = \theta_{M2} = 0.5$ and $\theta_{F1} = \theta_{F2} = 0.15$. We assume that indoor traffic density in a femtocell is 20 times of the outdoor traffic. The transmission power of FBSs and MBSs are $40mW$ and $15W$ respectively.

In the proposed FFR-3 model, the MUEs in the center macro-area are protected from the interferences caused by nearby femtocells as the spectrum is orthogonally partitioned among FUEs and MUEs in a given macrocell. MUEs in edge macro-area are also protected from the cross-tier interferences caused by the overlaying femtocells of their zone and by femtocells in the sectors of neighbouring cells. The required number of subchannels for calls in center macro-area increases from $c_{M1} = 1$ with the proposed frequency partitioning scheme to $c_{M1} = 2$ in the traditional FFR-3. Similarly in the edge macro area the required number of subchannels increases from $c_{M2} = 2$ to $c_{M2} = 3$. This results in much lower blocking probabilities when the proposed FFR-3 is applied compared to a traditional FFR-3 scheme, as we can see in Figure 2.5 and Figure 2.6 illustrating the blocking probabilities of MUEs in center and edge zone versus the traffic density. The results are also compared with a model permitting no sharing of subchannels between center macro-area and edge macro-area layers, to demonstrate the efficiency of the joint frequency and CAC model. Femtocells suffer from less cross-tiers interferences in the adjusted FFR-3 but higher co-tier interferences as they are allocated less subchannels in each zone. We obtain the same required number of subchannels $c_{F1} = 3$ and $c_{F2} = 4$ in both schemes and we can see in figures 2.5 and 2.6 that the blocking probability of femtocells are kept low for any given traffic density.

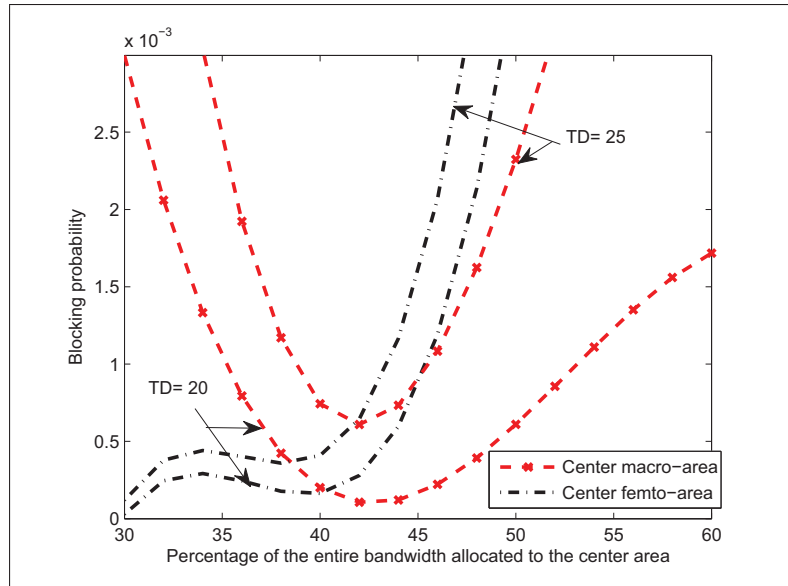


Figure 2.3 Blocking probability of calls connecting to a MBS and FBS in center area versus the percentage of bandwidth allocated to the center macro-area

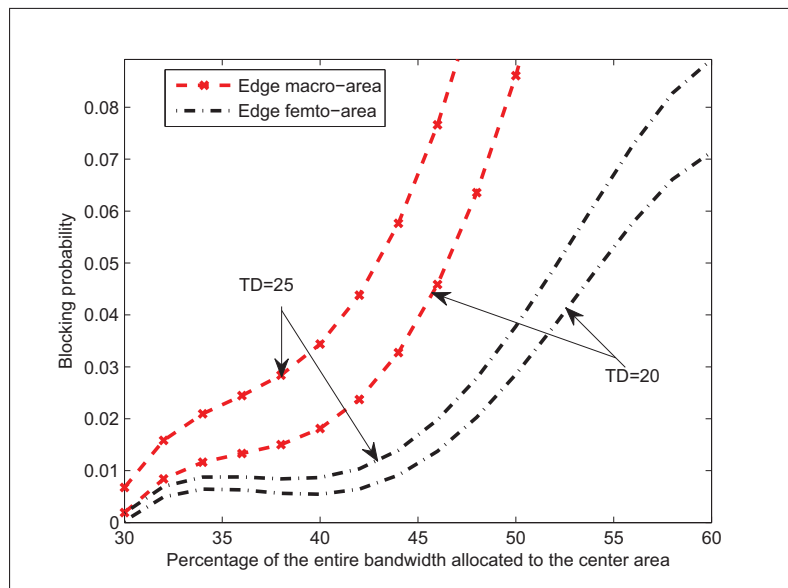


Figure 2.4 Blocking probability of calls connecting to a MBS and FBS in edge area versus the percentage of bandwidth allocated to the center macro-area

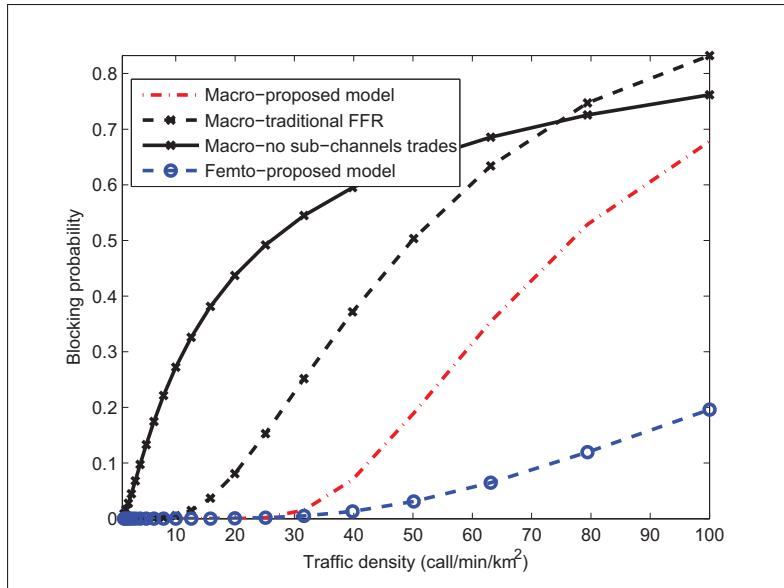


Figure 2.5 Blocking probability of calls connecting with MBS and FBS in center area versus the outdoor traffic density

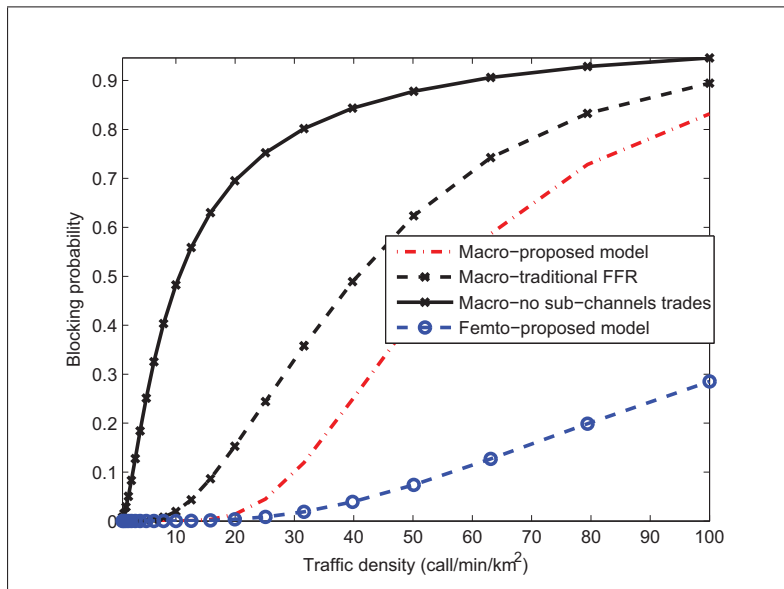


Figure 2.6 Blocking probability of calls connecting with MBS and FBS in edge area versus the outdoor traffic density

2.7 Conclusion

We have proposed an FFR scheme for sector-based two-tier macrocell-femtocell networks joint with a QoS-aware admission control strategy. The optimal parameters for cell channel partitioning in the proposed FFR scheme and an analytical model for performance evaluation of the proposed system have been developed. Finally, numerical results are presented to demonstrate the performance enhancement in term of blocking probabilities of the proposed framework.

CHAPTER 3

COALITIONAL GAMES FOR JOINT CO-TIER AND CROSS-TIER COOPERATIVE SPECTRUM SHARING IN DENSE HETEROGENEOUS NETWORKS

With the dense deployment of small-cells in the next generation of mobile networks, users from different tiers suffer from high downlink interferences. In this chapter, we propose a game theoretic approach for joint co-tier and cross-tier collaboration in heterogeneous networks and analyze the relevance of the proposed scheme. First, we propose a coalition structure game (CS game) with a Weighted Owen value as imputation, where the Small-cell Base Stations (SBSs) and their connecting Macrocell User Equipments (MUEs) form a priori union. We prove that the proposed framework optimizes the users profit. As an additional global benefit, the SBSs are encouraged to host the harmed public users in their vicinity. Secondly, we propose a canonical game with a Weighted Solidarity value as imputation to allow cooperation among SBSs and MUEs when they fail to connect to nearby SBSs. We prove that the weak players are protected in this scheme and that a high degree of fairness is provided in the game. We compare through extensive simulations the proposed frameworks with state-of-the-art resource allocation solutions, access modes and legacy game-theoretic approaches. We show that the proposed framework obtains the best performances for the MUEs and Small-cells User Equipments (SUEs) in terms of throughput and fairness. Throughput gain is in order of 40% even reaching 50% for both types of users. The main results of this chapter have been published in a conference paper (Hajir *et al.*, 2016c) and journal paper (Hajir *et al.*, 2016a).

3.1 Introduction

3.1.1 Motivations and prior related works

One of the main challenges of the fifth generation mobile networks is responding to the exponentially increasing demand for higher data capacity and data rates. This involves a greater spectrum in low and high bands and more antennas, as well as the deployment of more small-cells overlaying the existing macrocells. Indeed, operators are looking to offload traffic from

their Macrocell Base Stations (MBSs) as they anticipate data traffic to grow by 1000 times by 2018. Accordingly, the dense deployment of small-cells is a crucial part of addressing this growth. These small-cells are connected to the backhaul network via optical fibre or DSL and allow not only higher spectrum efficiency but also greater overall network capacity. There are several additional advantages, such as improved indoor coverage, reduced costs and power consumption along with a higher Quality of Service (QoS) satisfaction (Lee *et al.*, 2014a). However, the coexistence of users and base stations from both tiers comes with several challenges.

In order for capacity to increase in tandem with the addition of small-cells, a rigorous interference and resource management has to be planned. An approach that eliminates cross-tier interference is the split-spectrum policy in which the small-cell tier uses a dedicated bandwidth distinct from the macro-tier (Hajir & Gagnon, 2015; Guvenc *et al.*, 2010; Wu *et al.*, 2009). The drawback of this approach is inefficiency in terms of spectrum reuse.

On the other hand, the co-channel deployment approach allows both macrocells and small-cells to access to the entire spectrum resource, though cooperation among the different tiers is required. Two types of interference induced by the co-channel deployment can seriously degrade the performances of the network, e.g., the cross-tier interference (from the MBS to the SBSs) and co-tier interference (from SBSs to SBSs).

In order to mitigate these interferences several decentralized solutions have been proposed (Guvenc *et al.*, 2008; Lee *et al.*, 2010a; Mustika *et al.*, 2011; Zhang *et al.*, 2014). On one hand, non-cooperative approaches have been widely studied and are characterized by the independent decisions of the players who aim to improve their own performances. To solve non-cooperative games, the most widely-used concept is the well-known Nash equilibrium (Başar & Olsder, 1998). Non-cooperative game theory has been considered for resource allocation (Chandrasekhar *et al.*, 2009; Barbarossa *et al.*, 2010; Semasinghe *et al.*, 2015; Alpcan & Basar, 2005a) and power control (Alpcan *et al.*, 2002b; Kang *et al.*, 2012). A non-cooperative evolutionary game based on stochastic geometry analysis for small-cells resource

allocation is presented in (Semasinghe *et al.*, 2015). On the other hand, with the need for self-organizing, decentralized and autonomous networks, cooperative approaches have emerged as a key solution for the success of dense heterogeneous networks.

According to the cooperative approach, game theory is an essential tool in helping the various entities make decisions in two-tier networks (Saad *et al.*, 2009a). A cooperative game can occur in a group (i.e., a coalition) in which the players share information and try to attempt to negotiate the attainment of common objectives. Coalitional games can be classified into two categories (Saad *et al.*, 2009a): canonical games and coalition structure games, both will be studied in this chapter. In a canonical game, all players aim to form and stabilize a grand coalition. The value of the coalition is then divided among the players such that none of the players has any incentive to leave the grand coalition. In coalition structure games, players are rational in forming coalitions or a priori unions in order to maximize profit.

In (Langar *et al.*, 2015) and (Pantisano *et al.*, 2013), the authors proposed a canonical and a coalitional game model, respectively, as a technique for co-tier interferences mitigation among cooperative small-cells. In (Hoteit *et al.*, 2012), the authors propose a bankruptcy game approach for resource allocation in cooperative networks. However, according to these three frameworks, a split-spectrum approach is adopted, and hence the cross-tier cooperation is not investigated.

A theoretical game-based cognitive radio resource management approach is proposed in (Lien *et al.*, 2011) and (Ma *et al.*, 2015). In these studies, a coalition game is developed for use in subchannel allocation in situations where cognitive small-cells act as secondary users and have a higher priority than MUEs but the collaboration between the two tiers is not investigated; in these cases, the priority applied can result in a deterioration of the macro-tier performances. In (Pantisano *et al.*, 2012), the authors consider the cross-tier cooperation among SUEs and MUEs in order to alleviate the downlink interference. It allows the MUEs to explore nearby small-cells by cooperating with the SUEs, which act as relays; however, in these cases the

closed-access mode is adopted which prevents the MBS from offloading its high data traffic to the small-cell tier.

A hybrid access mode is a promising solution as it allows a public user suffering from downlink interferences from a nearby SBS to connect to this small-cell in order to process its demands. However, only a limited amount of the small-cell resources is available to all users, while the rest is operated within a closed subscribed group (CSG) manner (de la Roche *et al.*, 2010).

Very few papers have investigated the collaboration between the harmed MUEs and neighbouring SBSs in instances when the first fails to connect to the small-cell. Yet another problem not fully investigated is when the cooperative games involve hybrid or open-access small-cells. Several questions arise: How can the cooperation between users and base stations from different tiers be modelled? How can the small-cell tier properly process the MUEs demands, while managing the cooperative resource allocation in a fair and strategic manner? How can the SBSs be encouraged to serve public users without degrading their own performances? How can the different bargaining power levels be managed in a game?

Such questions are essential to the successful dense deployment of small-cells; our proposed cooperative model attempts to provide solutions to these issues.

3.1.2 Main contributions and organization

The main contribution of this chapter is to propose a new cooperative-game framework for co-tier and cross-tier interference mitigation and resource management under an open-access mode of small-cells, which allows the MBS to offload its data traffic to the dense small-cell tier. When MUEs are served by a nearby SBS, we propose forming a union of the related SBS and MUEs in a given game in order to attribute a reasonable profit to the hosted MUEs while rewarding the SBS for actively participating in the interference mitigation process. Accordingly, when the union SBS-MUEs is formed, its members commit themselves to bargaining with the others as a unit. Any gain obtained by the players of the unions are then shared according to a coalition structure solution (i.e. Weighted Owen). When the harmed MUE fails to connect

with a nearby SBS, it participates in a cooperative game with its interferers in order to split the available resources following a solidarity-based imputation scheme (see Fig.3.1 and Fig. 3.2).

Our key contributions are summarized in the following:

- a. We create a new collaborative framework based on two different game theoretic approaches in which the end user benefit is quantified in terms of throughput and fairness for both MUEs and SUEs of the system;
- b. We address the resource allocation problem when MUEs and SUEs coexist in a small-cell coverage area using a CS game based on the formation of unions when SBSs host public users in their neighbourhood;
 - We prove that the proposed CS game under a Weighted Owen imputation value optimizes the profit of the MUEs and SBSs which participate in the unions. A direct consequence is that the SBSs are encouraged to host the harmed public users in their coverage area as the users joining forces get a better profit than bargaining individually;
- c. We address the co-tier and cross-tier resource allocation problem when MUEs are not hosted but interfered by neighbouring SBSs using a canonical game approach;
 - We propose a new algorithm for the computation of the canonical game imputation (i.e. a Weighted Solidarity value). We prove that it protects the weak players when their power of bargaining is low and provides a higher degree of fairness. Additionally, it does not allow any user to obtain more than its claim and discourages players from asking for higher demands.

In section 3.2, we present the problem formulation and motivations, followed by the SBSs and MUEs interference set formation process in section 3.3. In section 3.4 we present the cooperative game framework and the identified imputation values. Finally, to validate the effectiveness of our proposed cooperative game approach, we present the simulation results in Section 3.5.

3.2 Problem formulation and motivations

In cooperative games, users are given the opportunity to collaborate in order to split the available resources. With the development of self-organizing and decentralized small-cells, the latter should be capable of managing not only the interferences they induce to each other but also the interferences induced to the neighbouring MUEs. To do so, it is essential to incorporate a cross-tier interference collaborative mitigation scheme into the existing co-tier models. The SUEs can be easily represented by their SBSs that participate in the game and redistribute the payoff among their CSG users. However, as we want our model to be distributed, we need to incorporate the MUEs into the game as players. Indeed, when MUEs are interfered with one or several SBSs, they compete with the latter for the same resources in a co-channel deployment. Hence, they can form a coalition and bargain their resources with the interfering SBSs. A second plausible scenario might involve the MUE connecting with a nearby hybrid or open-access SBS: if the SBS represents the MUE in the game, it might unfairly split the resources among its own CSG and public users. The concept that players have a right to talk in a game, has been introduced in (Vidal-Puga, 2005) and it is one that we also wish to be extended to MUEs of the system. Indeed, in a resource allocation game, the SBSs express their demands in terms of a number of tiles (i.e. resources) and participate in a game with the other agents in order to split the available resources. When the nearby MUEs are attached to a given SBS, their demands are "absorbed" by the paired SBS (added to the initial demand of the SBS CGS users). However, the reward might be unfairly redistributed by the hosting SBS among the users of both types (subscribers or public users).

The coalition structure will give us an essential model in which players need to organize themselves into groups for the purpose of sharing the network's resources. This is a great opportunity for heterogeneous networks in which the neighbourhood small-cells concept described earlier in which the small-cells are encouraged to allow the access to public users in their neighbourhood. It is no longer appropriate to consider the SBSs as single players. Indeed, the SBS plays the game for the purpose of reallocating its payoff to its own users but the MUEs must have the chance to participate in the negotiation process too, in order to not be cheated by the

SBSs who might prioritize their own subscriber users. This is facilitated by the introduction of a coalition structure into the game which consists of a partition of players into a union. This can be considered analogous to a family that has to take into account all its members before making decisions that impact them. Such an approach also creates a better bargaining situation, as the other party has to convince jointly all the members. Some imputation values, like the Owen value (Aumann & Dreze, 1974) ignore the power of the unions and attribute the same weight to the unions as to single players. The imputation value of our model is therefore superior because it gives a greater weight to the unions while allowing entities from both tiers to participate in the spectrum sharing. In this way, a single game allows us to fairly manage inter-union collaboration as well as intra-union resource bargaining. In turn, this also facilitates the achievement of an overall consensus, in which each user has a right to talk in the game.

3.3 System model

We consider the downlink of an Orthogonal Frequency Division Multiple Access (OFDMA) macrocell network overlaid by N SBSs and K MUEs. The SBSs reuse the entire bandwidth allocated to the underlying macrocell. Let $\mathcal{F} = \{F_1, \dots, F_n, \dots, F_N\}$ be the set of SBSs and $\mathcal{M} = \{M_1, \dots, M_n, \dots, M_K\}$, the set of MUEs in a given macrocell. For their downlink transmission, SBSs might cause co-tier interference to the neighbouring SBSs and cross-tier interference to the surrounding MUEs as we consider a spectrum-sharing approach. In non-cooperative networks, the users of both tiers consider the downlink interferences of all surrounding SBSs. Here, under the cooperative approach, SBSs and MUEs of the system collaborate in order to share the available resources and mitigate the co-tier and cross-tier interferences. Each SBS and MUE of the system determines its interfering set in the downlink in order to form cooperative sets as depicted in Figure 3.1 and Figure 3.2.

3.3.1 Interference set detection

Each user SUE within a given small-cell F_n boundary, calculates the ratio of the received signal from F_n to the signal received from all surrounding macrocells and from the surrounding

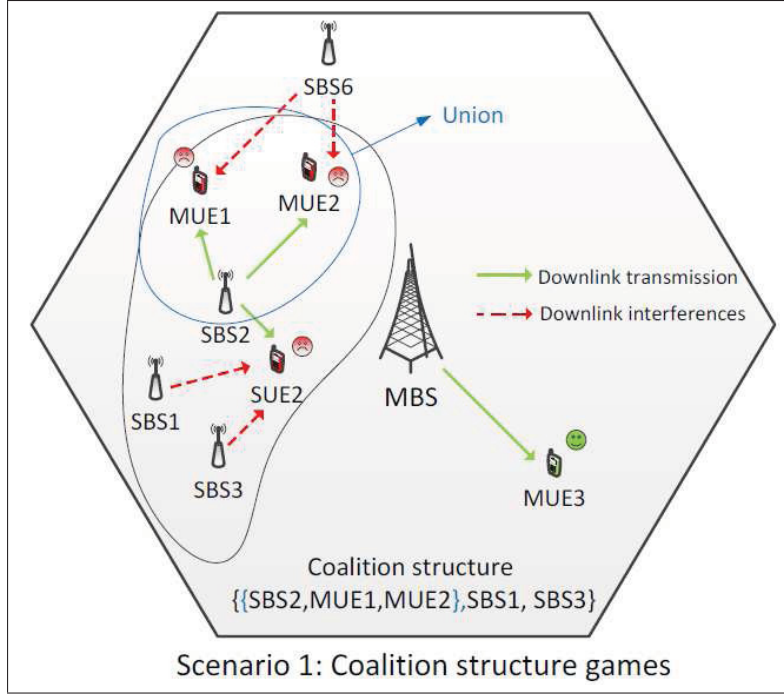


Figure 3.1 An illustration of a scenario leading to the proposed coalition formation and coalition structure game

SBSs (Langar *et al.*, 2015). To determine the interference set of the small-cell of interest, we need to consider only the interference induced by one SBS at a time. The downlink signal-to-interference-plus-noise ratio (SINR) achieved by a SUE y_n associated with small-cell F_n on a particular tile k when interfered by small-cell $F_{n'}$ is given by (Langar *et al.*, 2015):

$$\gamma_{y_n, F_n}^k = \frac{P_{F_n}^k G_{y_n, F_n}^k}{\sum_{m \in M} P_m^k G_{y_n, m}^k + P_{F_{n'}}^k G_{y_n, F_{n'}}^k + \sigma^2} \quad (3.1)$$

where G_{y_n, F_n}^k and $G_{y_n, m}^k$ represent the long term channel gain including the path-loss and shadowing from SBS F_n and MBS m to SUE y_n , respectively, in small-cell F_n on tile k , σ^2 the noise power and M the set of surrounding MBSs. Let I_n^f be the interference set of F_n composed of F_n and SBSs causing interferences to its users. If the SINR γ_{y_n, F_n}^k achieved by FUE F_n is inferior to a certain SINR threshold δ_f , then the SBS $F_{n'}$ is considered to be an interferer of F_n and joins its interference set I_n^f . We proceed this way for each SBS in the network until all SBSs have

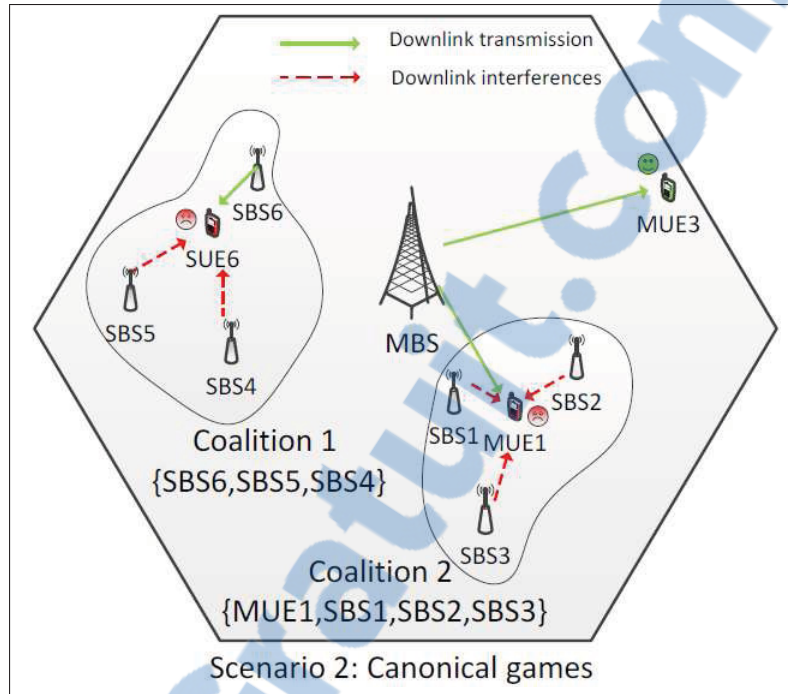


Figure 3.2 An illustration of a scenario leading to the proposed coalition formation and canonical game

formed their interference set or remained alone if they are not interfered by any neighbouring SBSs.

In the same manner, each MUE calculates the ratio of the received signal from its corresponding MBS to the signal received from all surrounding small-cells and macrocells. Similarly, we take into account only the interference induced by one SBS at a time to determine if it is an interferer of the MUE M_n . The SINR achieved by a MUE M_n associated with macrocell m on a particular tile k when interfered by the small-cell F_n can be written as:

$$\gamma_{M_n,m}^k = \frac{P_m^k G_{M_n,m}^k}{\sum_{m' \in M'} P_{m'}^k G_{M_n,m'}^k + P_{F_n}^k G_{M_n,F_n}^k + \sigma^2} \quad (3.2)$$

$G_{M_n,m}^k$ and G_{M_n,F_n}^k represent the long term channel gain including path loss and shadowing, associated with k from a MBS m and SBS F_n to a MUE M_n , respectively, in macrocell m .

Let I_n^m be the interference set of M_n composed of M_n and SBSs interfering with M_n . Here, if the SINR $\gamma_{M_n,m}^k$ achieved by MUE M_n is under to a certain SINR threshold δ_m , the SBS F_n is considered to be an interferer of M_n and joins the interference set I_n^m .

Within the interference set I_n^m , if the MUE M_n is located in the coverage area of a SBS F_n , and if the MUE receives a better SINR from this SBS than from its serving MBS it always tries to connect to the corresponding SBS. If the MUE succeeds in connecting to a nearby SBS, the two are assumed to be paired in the sequel. These pairs will be used in the next section to build the CS games. Once we have determined the interference set for each SBS and MUE of the system, we sort these interference sets in descending order, firstly according to their cardinality and secondly according to the overall demand of the interference set.

3.4 Cross-tier macrocell-smallcells cooperation as coalitional games

3.4.1 Proposed game theory approach

In the presence of dense small-cell deployment within urban environments, the overall demand in the shared spectrum often exceeds the number of available tiles $|Z|$ (Hoteit *et al.*, 2012). Assuming that in the same interference set, the SBSs and MUEs can share information about their demands, we formulate the problem of co-tier and cross-tier interference mitigation and resource allocation as a cooperative game. To solve the problem mentioned above, we propose the following approach. When a MUE connects to a SBS, the latter does not absorb the demand of the connecting public user. Instead, the MUE is considered as a player, even if the demand of the MUE will be processed by the paired SBS. The MUE will join the SBS in a union, known as a priori union. If the MUE fails to connect to the nearby SBS, the MUE acts as a single player and participates in a resource allocation game with the nearby SBSs. In such a case, the demand of the MUE will be processed by the MBS. Such a game is also played when only SBSs are involved in an interference set (co-tier model).

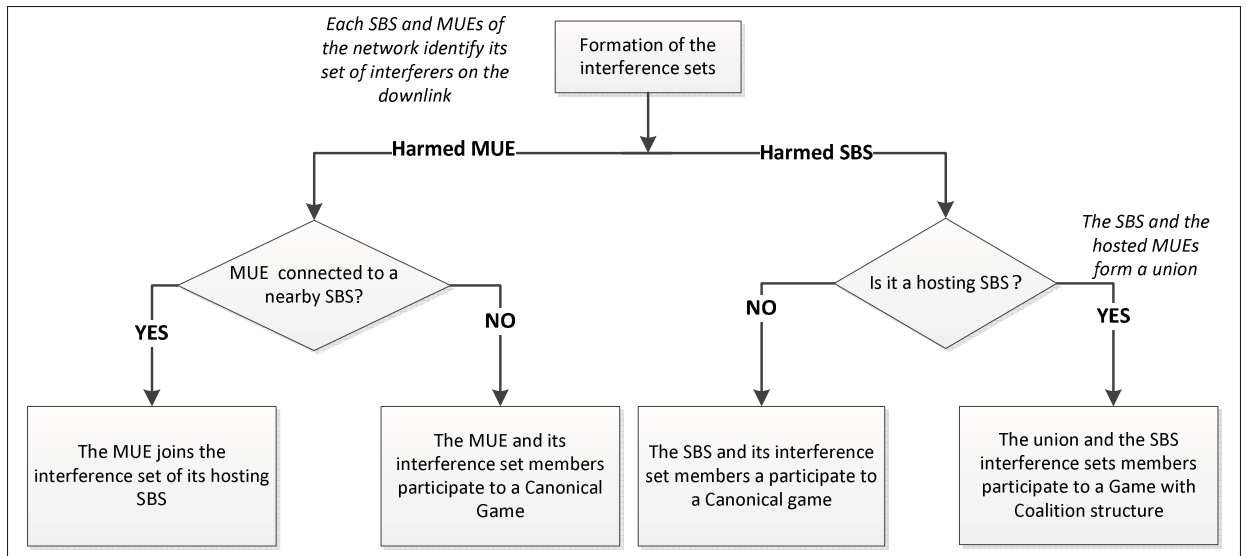


Figure 3.3 General flow chart describing the formation of the coalition structures and the classification of the two game

Cooperative games involve a set of players in a system, who seek to form cooperative groups (i.e interference sets) in order to improve their performances. The aim of the proposed cooperative approach is: 1) to form an interference set in order to reduce co-tier and cross-tier downlink interferences, 2) to find a binding agreement among the agents of the same set to split the available resources.

We follow the steps described in Figure 3.3. The first step is the interference set detection developed in section 3.3.1. The next step is a game iteration following the order in the sorted list of detected interference sets. The type of the game depends upon the type of the harmed agent in the formed interference set (MUE or SBS). If a SBS is not hosting any MUE or if a harmed MUE fails to connect to a nearby SBS, it participates in a canonical game with its interference set members. However, if the SBS is hosting a MUE, they form a union and a CS game is played between this union and the interference set of the paired SBS. Both type of games are defined in the sequel.

3.4.2 Definition and formulation of the game

As mentioned before, in the presence of dense small-cell deployment within urban environments, the overall demand in the shared spectrum often exceeds the number of available tiles $|Z|$ (Hoteit *et al.*, 2012). Assuming that the SBSs and MUEs belonging to the same interference set I_n can share informations about their respective demands and allocations, the resource allocation problem can be formulated as a cooperative game with transferable utility. Let I_n denotes the interference set of the current game iteration. It corresponds either to I_n^f or I_n^m but we omit this differentiation for simplicity.

Definition 1. A cooperative game with transferable utility (TU-game) is a pair (\mathcal{N}, v) where \mathcal{N} is a non-empty set and $v : 2^{\mathcal{N}} \rightarrow \mathbb{R}$ a characteristic function defined on the power set of \mathcal{N} satisfying $v(\emptyset) = 0$

We consider $\mathcal{N} \equiv \mathcal{I}_n$ and we define the worth $v(S)$ associated to each coalition $S \subseteq \mathcal{N}$ the amount of available resources not claimed by its complement nor already allocated to players of \mathcal{N} in a precedent iteration of the game.

$$v(S) = \max\{0, |Z| - \sum_{j \in \mathcal{N} \setminus S} d(j) - \sum_{j' \in \mathcal{C}} p(j')\}, \forall S \subseteq \mathcal{N} \setminus \{\emptyset\} \quad (3.3)$$

with $\mathcal{C} \subseteq \mathcal{N}$ being the set of players of \mathcal{I}_n that have already participated to the game in a previous iteration, $p(j')$ being the number of resources allocated obtained by the users of \mathcal{C} and $d(j)$ the number of tiles claimed by the complement of the coalition S . Indeed, a SBS or MUE can be part of several interference sets, and following the order of the interference sets described above (i.e the largest and most demanding sets first), one agent might have already played and received its payoff in a previous interference set.

3.4.3 Non-emptiness of the core and stability of the grand coalition

We assume that the grand coalition \mathcal{N} will be formed, it is then necessary to explain why it is stable. Hence, as the core of a canonical game is directly related to the grand coalition's stability we need first to prove that the core is non-empty for the considered game in 3.3. It has been proven in (Shapley) that convex games have non-empty core, hence ensuring the stability of the grand coalition.

A TU game is convex if and only if:

$$v(S \cup T) \geq v(S) + v(T) \forall S, T \subseteq \mathcal{N} \quad (3.4)$$

Yet, as the characteristic function in 3.3 corresponds to the function of a bankruptcy game, the proof of the convexity of a bankruptcy games as the one considered here in 3.3 can be found in (Curiel *et al.*). This convexity property also implies that the game is superadditive and supermodular (Shapley, 1952), hence satisfying the following inequality: $v(S \cup \{i\}) - v(S) \leq v(T \cup \{i\}) - v(T) \forall S \subset T \subset \mathcal{N} \setminus \{i\}$. This inequality implies that the marginal contribution of a player to a coalition is larger than its marginal contribution to another smaller coalition, hence ensuring the stability of the grand coalition.

For the CS game proposed in the subsection D, we consider the same characteristic function defined in 3.3. The union formed and the coalition structure incorporated into the game act only as an additional element which influences how the worth of the grand coalition is split among its members.

Once we assumed that the players of a game form the so-called grand coalition; the problem then is to agree on how to share the received profit $v(\mathcal{N})$ among the players in an interference set. The output of this decision is called the imputation of the game $x = (x_1, x_2, \dots, x_n)$ which is a payoff vector where player i receives x_i .

In the next section, we discuss the possible imputation values satisfying efficiency ($\sum_{i \in \mathcal{N}} x_i = v(\mathcal{N})$) that we can use for the proposed games. We will explain which imputation values are

the most appropriate for these games if fairness and stability are the most desired properties of the payoff.

3.4.4 The proposed canonical game

As depicted in Figure 3.3, upon each significant change in demands or network topology, the SBSs and the MUEs of the system determine their set of interferences following the method detailed in Section 3.3. If the MUE fails to connect to a nearby SBS, it participates in a canonical game with the members of its interference set. Similarly, if a SBS is not hosting any MUE, it participates in a canonical game with the other agents of its coalition. As aforementioned, we assumed that the SBSs and MUEs of each interference set agree to form the grand coalition. We will develop here how the payoff of the grand coalition $v(\mathcal{N})$ will be split among these players.

3.4.4.1 Imputation value for the canonical game

Let us first define the most well-known solution, the Shapley value $Sh(\mathcal{N}, v)$ as (Shapley, 1952):

$$Sh_i(\mathcal{N}, v) = \sum_{S \subseteq \mathcal{N}: i \in S} \frac{(|\mathcal{N}| - |S|)! (|S| - 1)!}{|\mathcal{N}|!} \Delta^i(v, S) \quad \forall i \in \mathcal{N} \quad (3.5)$$

$\Delta^i(v, S)$ is the marginal contribution of a player i in coalition S defined as $\Delta^i(v, S) = v(S \cup i) - v(S)$.

The drawback of this solution is that it essentially considers the productivity of the players. In other words, the stronger a player is, the higher its payoff in the game. Yet, the strength of a player in the proposed game is determined by its demand, and therefore low-demand users might be affected by this imputation value. With both types of players in the game, the SBSs generally have more bargaining power in the game as they collect the demands of their several SUEs, while the MUE acts as a single player weighing only its own demand. In any case, it is

important to avoid rewarding the players who have higher demands so that those who would claim more resources in order to gain a stronger position within the game are prevented from doing so.

Solidarity Value

We want to apply a solution concept that incorporates some degree of solidarity so as to protect the MUEs from powerful SBSs and also to protect other weak SBSs within a given interference set. An appealing solution is the Solidarity value $Sl(\mathcal{N}, v)$ which takes into account the principles of productivity and redistribution, expressed as (Nowak & Radzik, 1994):

$$Sl_i(\mathcal{N}, v) = \sum_{S \subseteq \mathcal{N}: i \in S} \frac{(|\mathcal{N}| - |S|)! (|S| - 1)!}{|\mathcal{N}|!} \Delta^{av}(v, S) \quad \forall i \in \mathcal{N} \quad (3.6)$$

with $\Delta^{av}(v, S) = \frac{1}{S} \sum_{i \in S} \Delta^i(v, S)$. Productivity is taken into account as the marginal contribution $\Delta^i(v, S)$ appears in the calculation. This value also shows some redistribution; not only is the player's marginal contribution considered, but so too is that of the players in a given coalition. In this way, the weak players of the game are protected.

Let $E[\delta_{\gamma_i}(\mathcal{N}, v)]$ be the average gain of player i . This value refers to the expected variation in the payoff of player i assuming that each player of \mathcal{N} has the same opportunity to leave the game .

Axiom 1. *An imputation value satisfies the equal average gains if $\forall (\mathcal{N}, v)$ and $\forall \{i, j\} \subseteq \mathcal{N}$, $E[\delta_{\gamma_i}(\mathcal{N}, v)] = E[\delta_{\gamma_j}(\mathcal{N}, v)]$.*

It has been proven in Theorem 3 (CALVO & GUTIRREZ, 2013) that the solidarity value satisfies the equal average gains axiom. This provides two important assets for wireless communications systems. First, it incorporates a major sense of fairness into the game due to the equal average gain described above. Secondly, the agents of the network are not motivated by claiming more than what they really need to process their calls, thereby avoiding the cheating

behaviour of some players who might ask for more resources in order to increase their bargaining power. However, this solution has an important limit, which is expressed in the remark below.

Remark 1. *A player might receive more than their claim when the solidarity value is used as imputation, thereby violating the satiation axiom defined below.*

Axiom 2. *After applying an imputation value to a game (\mathcal{N}, v) , no player of a bankruptcy game should receive more than their claim. Therefore, if $\sum_{i \in \mathcal{N}} d_i \geq Z; x_i \leq d_i, \forall i \in \mathcal{N}$*

Note that the game under study, defined in 3.3, is a bankruptcy game, since the amount of resources available for each interference set is below the total demand of the members of the set. However, when the solidarity imputation value is applied in order to share the amount of available resources, some claimants may receive more than they claim, which violates the above satiation axiom. This is based on the fact that the solidarity value contributes to the expected average marginal contribution of a player. Here, productive players cede some parts of their marginal contributions to the weaker members, which reflects a sort of social sympathy and is a desired property of the solidarity value. Thus, the variance of the payoff distribution has been reduced. When a user with a low demand is part of an interference set containing several powerful users, the satiation axiom is difficult to satisfy as several of them will contribute to the marginal contribution of the weak members.

Proposed Weighted Solidarity value

When the problem specified in Remark 1 is encountered, we need to apply a solution with the same degree of social empathy but that protects the system from attributing a profit exceeding the claim of the users. Indeed, in this case the solidarity value outperforms its initial role of protecting weak users and actually allocates a bigger payoff to them than it should. We propose a weighted solidarity value when the payoff obtained by the solidarity value is higher than a player's claim. The weights of the weighted solidarity value allow us to decrease the power of some users who receive an excessive amount of resources in order to limit the maximum

of their profit to their demands. We propose to compute the appropriate weights in order to satisfy the satiation axiom for every player of the game. To do so, we need first to identify the users for whom the payoff obtained by the solidarity value is greater than the demand. If there is only one user of the interference set violating the satiation axiom, the weight applied to this user is the ratio of the demand by the payoff obtained from the solidarity value. This is explained by the fact that the non-weighted form of the Solidarity value simply uses a weight vector equal to one.

Otherwise, if there are more than two users in a given interference set violating the satiation axiom, we need to compute the optimal weight vector to remedy this violation. To do so, we solve an equation in which the number of variables is equal to the number of users violating the satiation rule. Let $\mathcal{J} \subseteq \mathcal{N}$ be the partition of users for whom the payoff obtained by the solidarity value exceeds their demands, and let $d = (d_1, \dots, d_n)$ be the vector of demands where d_i stands for the demand of user $i \forall i \in \mathcal{N}$. Let $w = (w_1, \dots, w_n)$ be the vector of weights where w_i is the weight of the player $i \in \mathcal{N}$ and $\sum_{i \in \mathcal{N}} \frac{w_i}{|\mathcal{N}|} = 1$.

We need to solve the linear system for all $i \in \mathcal{J}$ of the form:

$$w_i = \frac{\frac{d_i}{|\mathcal{J}|} * \left(|\mathcal{N}| + \sum_{k \in \mathcal{J} - \{i\}} w_k - |\mathcal{J}| \right)}{Sl_i(\mathcal{N}, v)} \quad \forall i \in \mathcal{J} \quad (3.7)$$

We can then update the vector of weights with the set of solutions obtained from the resolution of the above set of equations $(w_i)_{i \in \mathcal{J}}^*$. We express the final weight vector to be used for the weighted solidarity value as:

$$w_i = \begin{cases} 1 & \text{if } i \in \mathcal{N} \setminus \{\mathcal{J}\} \\ (w_i)^* & \text{otherwise} \end{cases} \quad (3.8)$$

Algorithm 3.1 summarizes the different steps to compute the proposed weighted solidarity value.

Axiom 3. *The weighted solidarity value with the computed weights satisfies the satiation rule.*

This is explained simply by the fact that the weight vector that has been applied does not allow any user to obtain more than its claim.

Algorithm 3.1 Calculate the imputation $(x_i)_{i \in \mathcal{N}}$ of (\mathcal{N}, v)

```

1: Initialize  $(w_i) = 1 \forall i \in \mathcal{N}$  {The weight vector elements are all set to one}
2: Initialize  $\mathcal{J} = \{\emptyset\}$ 
3:  $x_i \leftarrow Sl_i(\mathcal{N}, v) \forall i \in \mathcal{N}$  {We compute the imputation value with the Solidarity Value}
4: for all  $i \in \mathcal{N}$  do
5:   if  $x_i > d_i$  then
6:      $\mathcal{J} := \mathcal{J} \cup i$  {If the payoff obtained by the solidarity value exceeds user's  $i$ 
       demand,  $i$  joins the subset  $\mathcal{J}$  of satiation axiom violating users}
7:   end if
8: end for
9: if  $\mathcal{J} \neq \{\emptyset\}$  then
10:  Go to procedure {We need to compute the weighted solidarity value  $\forall i \in \mathcal{N}$ }
11: else
Ensure:  $x_i$  {The satiation axiom has not been violated by any user of  $\mathcal{N}$ }
12: end if
13: Procedure:  $Sl_i^{w_i}$ 
    {Procedure to compute the weighted solidarity value of users  $i \in \mathcal{J}$ }
Require:  $(Sl_i(\mathcal{N}, v), d_i) \forall i \in \mathcal{J}$ 
14: Find the solutions of the set of linear equations (7)
15:  $w_i = (w_i)^* \forall i \in \mathcal{J}$  and  $w_i = 1 \forall i \in \mathcal{N} \setminus \{\mathcal{J}\}$ 
    {We update the vector of weights with the weights resulting from the resolution of the
    linear equations as in (8)}
16:  $x_i^* \leftarrow Sl_i^{w_i} \forall i \in \mathcal{N}$  {We compute the imputation value with the weighted Solidarity
    Value}
Ensure:  $x_i \leftarrow x_i^* \forall i \in \mathcal{N}$ 

```

3.4.5 The proposed coalition structure game

We recall first the motivations behind the CS game. After the MUEs have identified their set of interferers, a harmed MUE leaves its interference set and joins that of a hosting SBS, if it can connect to it. Note that two types of SBSs have been identified: the hosting SBS which corresponds to the small-cell permitting access to one or more MUEs; and the non-hosting SBSs that do not have any connected MUE. In the latter case, the non-hosting SBS participates in a canonical game with its interference set members, as discussed in the previous section. On the other hand, when a SBS type is hosting, it participates with its interference set members in a cooperative resource allocation game in which the SBS and its hosted MUEs (one or several) form a priori union. The resulting coalition structure is incorporated into the game.

Definition 2. *If $P = \{P_1, P_2, \dots, P_m\}$ is a partition of \mathcal{S}_n that satisfies $\cup_{1 \leq j \leq m} P_j = \mathcal{N}$ and $P_i \cap P_j = \emptyset$ if $i \neq j$ then P is a coalition structure over \mathcal{N} . The sets $P_j \in P$ are the unions of the coalition structure.*

Let $P(\mathcal{N})$ be the set of all coalition structures over $\mathcal{N} \equiv I_n$. We will denote the game (\mathcal{N}, v) with the coalition structure $P \in P(\mathcal{N})$ as (P, \mathcal{N}, v) . In the proposed game, a MUE always tries first to connect to the closest SBS of the formed interference set.

If connected, the hosting SBS F_1 and its n' connecting MUEs form a union $\{F_1, M_1, \dots, M_{n'}\}$. The coalition structure obtained from the incorporation of this union can be expressed as: $P = \{\{F_1, M_1, \dots, M_{n'}\}, \{F_2\}, \{F_3\}, \dots, \{F_n\}\}$, where $\{F_1, M_1, \dots, M_{n'}\}$ is a partition of \mathcal{S}_n^f formed by the related SBS-MUEs; every other player is a singleton.

Hence, we need to find an appropriate coalitional value to split the resources among and within the unions. Specifically, we propose that in a coalitional structure game the hosting SBS and its interference set members first play a quotient game (i.e game among the unions) in which the union acts as a single player. Next, they play an internal game (a game within a union among the members of the union) to split what the SBS-MUE union has obtained. Let (M, v_P) be the quotient game induced by the CS game (P, \mathcal{N}, v) , considering the unions of P as play-

ers. Furthermore, let (P_k, v_k) be the internal game taking place among the players within each union. Earlier, we defined a value as a function that assigns to each game (\mathcal{N}, v) a vector $(x)_{i \in \mathcal{N}}$ representing the amount that each player i in \mathcal{N} expects to get in the game. Similarly here, a coalitional value is a function that assigns a vector of worth to each game with coalition structure (P, \mathcal{N}, v) . One of the most important coalitional values is the Owen value (Aumann & Dreze). The Owen value applies the Shapley value at both levels, among the unions and within the unions.

3.4.5.1 The weighted Owen value as the imputation value of the CS game

We restrict our attention here to coalitional values satisfying the efficiency property; yet, the grand coalition is formed and the coalition structure described above is incorporated in the game, hence influencing the way the amount obtained by the grand coalition is shared among its members. Note that the agents of a CS game play first a quotient game (i.e, a game among the unions) where the union acts as a unit, followed by an internal game (a game within a union among the players of the union) to split what the union has obtained. We will separately define the values applied to compute the payoff of the player in the quotient game from those applied in the internal game. The coalitional value applied to this type of game is the weighted Owen value (Kalai & Samet, 1987). The weighted Owen value takes the size of each union into account. Indeed, the use of a symmetric imputation value would be unjustified as the players are groups of agents in the proposed model. The size of the unions depends on the number of MUEs hosted by the SBSs in the system. An obvious candidate for the quotient game is the weighted Shapley value by which users are weighted by the size of the unions they stand for. The inter-coalitions and intra-coalitions bargaining processes and the corresponding imputation values are now described.

The quotient game

When a SBS and its connecting MUEs form a partition and compete with the other members of the harmed SBS interference set as a unit, a situation in which coalitions have different sizes

develops. It seems reasonable to assign a size-aware weight to each coalition. Let's define the reduced game (M, v_P) corresponding to the quotient game induced by the CS game (P, \mathcal{N}, v) , considering the unions of P as players. Here, $M = (1, 2, \dots, m)$, with m representing the number of unions in the game and $v_P(K) := v(\cup_{i \in K} P_i)$ for all $K \subseteq M$. In the quotient game, the profits are divided among unions following the weighted Shapley value. The weighted Owen value computes the weights from the given coalition structure, the weights being proportional to the size of the coalition. Hence $w_u = \frac{|P_u|}{|\mathcal{N}|} \forall P_u \in P$, having $\sum_{u \in M} w_u = 1$. The unanimity games will allow us to define the weighted Shapley value, which describes how a coalition splits one unit between its members: for all $K \subseteq \mathcal{N}$, the unanimity game of the coalition K , (\mathcal{N}, u_K) , is defined by:

$$u_K(S) = \begin{cases} 1 & \text{if } S \supseteq K \\ 0 & \text{otherwise} \end{cases} \quad (3.9)$$

Recall that the unanimity game is only used to help us define the used values.

We can then define the weighted Shapley value for each unanimity game (\mathcal{N}, u_K) as (Kalai & Samet, 1987):

$$Sh_i^w(\mathcal{N}, u_K) = \begin{cases} \frac{w_i}{\sum_{j \in K} w_j} & \text{for } i \in K \\ 0 & \text{otherwise} \end{cases} \quad (3.10)$$

where $w = (w_i)_{i \in \mathcal{N}}$ is a vector of positive weights. The coalition splits the payoff among its members proportionally according to their weight.

As the SBS and MUE form a union and the other players are singletons in an interference set, the union has more weight in the game, and therefore gets a larger profit than if the MUE and SBS were acting as singletons. Hence, we protect the MUE and we reward the collaborating SBS by allowing the harmed public users to connect.

Remark 2. *As the weighted Shapley value satisfies efficiency in the internal game (P, v) , it follows that the weighted Owen value satisfies the quotient game property. We can then state that the profit of each coalition corresponds to its weighted Shapley value in the game among*

coalitions, with weights given by its size. Then

$$\forall P_u \in P, \sum_{i \in P_u} \mathcal{U}_i^{\mathcal{N}} = Sh_i^{wM}(v/P) \quad (3.11)$$

Proposition 1. *When the estate is shared with the weighted Owen value \mathcal{U} , a player of both types (e.g., MUE or SBS) gets a better profit by joining forces than they do bargaining themselves.*

Proof. Let P_u and P_v represent two coalitions belonging to P , and let $P^{u+v} = (P \setminus \{P_u, P_v\}) \cup \{P_u \cup P_v\}$. We will say that a coalitional value \mathcal{U} is joint monotonic if (Vidal-Puga, 2005):

$$\sum_{i \in P_u \cup P_v} \mathcal{U}_i^N(P) \leq \sum_{i \in P_u \cup P_v} \mathcal{U}_i^N(P^{u+v}) \quad (3.12)$$

This means that if P_u and P_v join forces, they win a better profit than they would acting as singletons. The proof of the joint-monotonicity of the weighted Owen value in convex games is presented in Annex 1. Our game under study in 3.3 corresponds to a bankruptcy game, it has been proven it is convex in (Curiel *et al.*). The proof of the joint monotonicity of the weighted Owen value in convex games concludes the proof of Proposition 1. \square

The internal game

Regarding the internal game, the weighted Owen value attributes the final payoff to the users of each union by splitting the worth gained by the quotient game with the Shapley value. The solution value for the internal game (P_k, v_k) is the Shapley value with $v_k(S) = Sh_k^w(M, v_{P|S})$. That is, $\varphi_i(P, \mathcal{N}, v) = Sh_i(P, v_k)$. We remind here that the internal game will take place among the hosting SBS and its hosted MUEs. We note that we use the Shapley value in the internal game to avoid penalizing the hosting SBS. Indeed, if a solidarity-based value is applied in the internal game, the unique SBS if its demand is high, will have to participate to the marginal contribution of the several MUEs in its union. This will result in lower SBS performance. On the other hand, as a weighted Owen value has been applied in the quotient game, a substantial

amount of resources have been obtained by the union, and as there is only one SBS per union, the MUEs will still have a significant payoff. As it is important to reward the hosting SBSs while attributing a reasonable amount of resource to the hosted MUEs in each union, the Shapley value is the most appropriate in this case.

Algorithm 3.2 Proposed algorithm for cooperative downlink cross-tier interferences mitigation and resource management

- 1: **Initial State:** Deployment of the SBSs and MUEs in the system and each agent expresses its demand in term of number of tiles.
- 2: *Phase I: Interference set detection*
- 3: a) Based on the minimum required SINR the SBSs and MUEs of the system determine their set of interferences I_n^f and $I_n^m \forall f \in F$ and $\forall m \in K$. If the SINR received by a harmed MUE from a nearby SBS is higher than the one received by the MBS, the MUE tries to connect to the corresponding SBS.
- 4: b) The interference sets are sorted according first to cardinality, then to the overall demand in a descending order.
- 5: *Phase II: The game iteration*
- 6: **repeat** For each interference set I_n^m following the settled order
- 7: **if** the harmed MUE succeeded in connecting to a nearby SBS **then**
- 8: a) The MUE leaves its respective interference set and joins the one of its hosting SBS.
- 9: b) The agents of the interference set who have not participated to a game in a precedent iteration form a coalition structure \mathcal{N} with the formed a priori union and all the other SBS as singletons.
- 10: c) A CS game (P, n, v) is played (i.e a quotient game and an internal game)
- 11: d) Every player $i \in \mathcal{N}$ receives the payoff x_i from the Weighted Owen value
- 12: **else**
- 13: a) The MUEs and their interfering SBS who have not played to a game in a previous iteration form the grand coalition and participate in a canonical game
- 14: b) The players receive their payoff from the Solidarity value or the weighted Solidarity value.
- 15: **end if**
- 16: **until** all players of the system have played
- 17: *Phase III: Resource allocation*
- 18: The MUEs and SUEs receive from their serving base station (MBS or SBS) the resources obtained from the game.

3.5 Simulation results and analysis

Table 3.1 Numerical values

Macrocell dimensions	400 m * 400 m
Small-cell coverage area	40 m
SINR threshold for MUEs (δ_m) (SUEs (δ_f))	15dB(20 dB)
Thermal noise density	-174 dBm/Hz
Carrier frequency	2 GHz
Maximum transmitted power at the MBS (SBS)	40 W(40 mW)
Number of MUEs per macrocell	50
Bandwidth reservation of prioritized SBSs	$\delta = 80\%$
Height of the MBS (SBS)	25 m(10 m)
Number of tiles allocated per cell (both tiers)	100 tiles
Demand in term of tiles per user (SUE or MUE)	1 – 25 tiles
Number of users per small-cell	4
Number of users per macrocell	100

In this section, we present the simulation results of our proposed cooperative game approach. We assume that a macrocell is overlaid by 200 small-cells in a spectrum-sharing network. We simulated several scenarios of varying user demand and location within the network. The simulation parameters are summarized in Table I. Based on the SINR, the agents determine their interfering sets. We consider the pathloss model of Winner II calculated in dB as: $G_{i,j}^k(d) = 44.9 - 6.55 \log_{10}(h_{BS}) \log_{10}(d) + 34.46 + 5.83 \log_{10}(h_{BS}) + 23 \log_{10}(f_c/5) + n_{ij}W_{i,j}$, d being the distance between a user i and a base station of either type j , h_{BS} the height of the base station, f_c the carrier frequency. Also, n_{ij} denotes the number of walls and $W_{i,j} = 5dB$ denotes the wall loss. Note that for communications from a SBS to an indoor SUE attached to another SBS, $n_{ij} = 2$, for all other cases $n_{ij} = 1$. The SBSs collect the demands of their users and the MUEs of the system express their demands in terms of number of tiles. We assume that the users of the system have equal priority; the proposed framework can be easily adapted to different degrees of priority in a future study. We ran 500 simulations, allowing us to reach a confidence level of 99.8%.

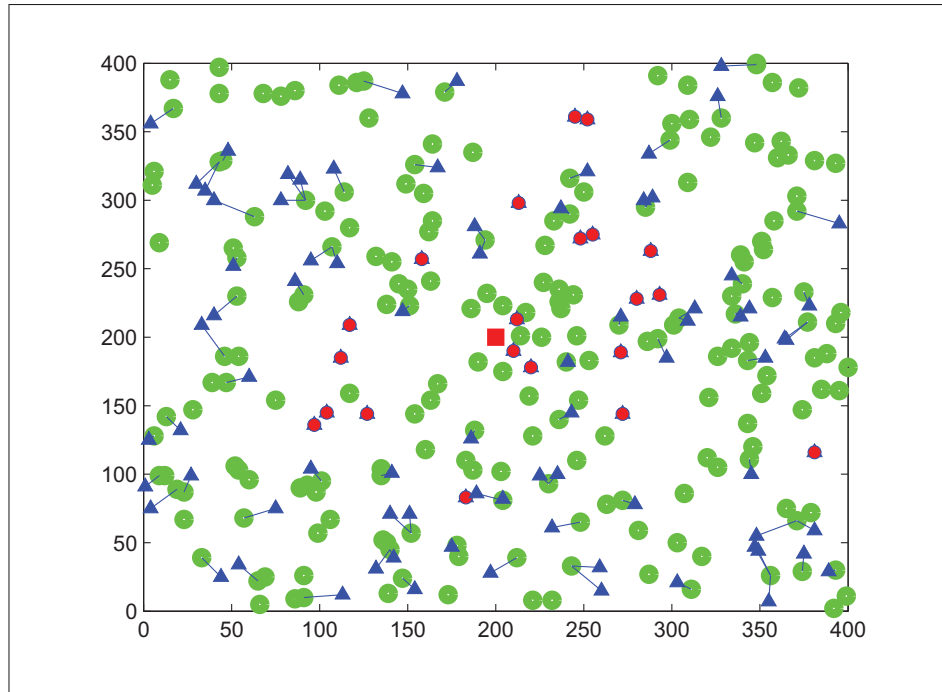


Figure 3.4 A snapshot of a dense small-cell networks. The SBSs are modelled by a Poisson process represented by green points. The center red square represents the MBS, the blue triangles represent the MUES: those with a red point in the centre are served by the MBS; those with a blue point are served by the SBS offering the best SINR. The blue lines represent the link between a SBS and its hosted MUE

3.5.1 Computational complexity

First, we will discuss the computational complexity of the proposed framework. The complexity of the different coalitional values can be compared for the canonical game. Recalling that the Shapley value is obtained with $O(2^n)$ operations with n the number of players in an interference set (maximum 12 in our simulations) (Deng & Papadimitriou, 1994). For the CS game, the computational complexity of the Owen and weighted Owen value are similar. These values are the average of all marginal contributions of i in all orderings of the players that preserve the grouping of the players into unions. Hence, they need $O(A * 2^k + 2^A)$ operations to be computed, with A the number of unions and k the maximum number of agents in a union. In Equation (3.5), we can see that the computational complexity of the solidarity value is similar

to the Shapley value, which is $O(2^n)$. However the computation time of the Solidarity value is slightly higher but the difference is negligible. This is explained in Equation (3.5), as to compute the Solidarity value we do not only need to compute the marginal contribution of a player but also the marginal contribution of the other players in a given coalition. In terms of average computation time, the solidarity values needs 0.23 seconds to be computed in the symmetric version and 0.27 seconds for the weighted version. For the coalition structure values, 0.028 seconds are needed for the Owen value and 0.032 seconds for the Weighted Owen value. These lower computational time of the CS game are justified by the partnership in this type of games that allows us to treat a union of partners as an individual, hence reducing the size of the game. At the same time, the size of the game is essential to the computational complexity in game theory which permits a lower computational time. The computational complexity of the solidarity value is marginally higher. The empirical tests performed on the executing times of each method show that the variances are very small (executing times are nearly similar). However, the computational complexity of the centralized approach is much higher and has an average computation time of dozens of seconds. Note that the centralized approach simulated in this chapter refers to the Centralized-Dynamic Frequency Planning (Lopez-Perez *et al.*, 2009).

3.5.2 Comparison with other schemes of the art

In Figure 3.4, we presented a snapshot of a dense heterogeneous network in which 200 small-cells overlay a macrocell with 100 MUEs. This shows that the MUEs located in the center area of the cell are better served by the MBS as the required SINR is reached. However, in the cell edge most of the MUEs fail to reach their required SINR when connected to the MBS, and therefore need to be served by the SBS offering the best signal. We notice from the density of the network that in both cases cooperative spectrum access is needed as the users from both tiers compete for the same resources under the co-channel deployment. In Figure 3.5, we compare the F-ALOHA (Chandrasekhar & Andrews, 2009) and the centralized approach (Lopez-Perez *et al.*, 2009) to the proposed game theory model. Our proposed model shows

better performances in all cases for dense (100 SBSs) and very dense (200 SBSs) network configurations. In high-density cases, with our model we have 50% of users obtain a throughput of more than 90% compared to only 30% with the centralized approach.

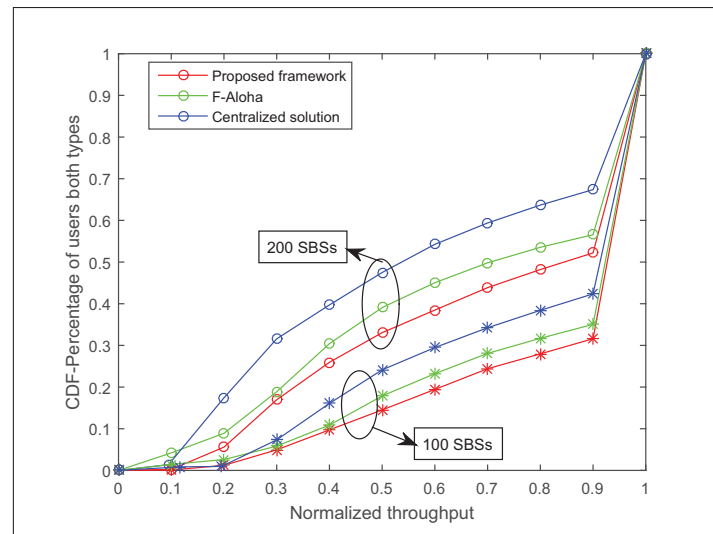


Figure 3.5 Throughput Cumulative Distribution Function for users of both types: Comparison of the centralized approach, the F-Aloha method and the proposed framework

3.5.3 Comparison with other types of access

In Figure 3.6, we compare our model to a traditional open-access mode and hybrid prioritized access. In the former case, the SBSs of the system collect the demands of the connected users of both types (CSG users and public users) and participate to a resource allocation game with the neighbouring SBSs. The MUEs that are served by a SBS do not participate in the canonical game. The SBSs redistributes the obtained payoff proportionally among their users of both types. Under the hybrid-access model, the SBSs similarly collect the demand of both type of users but prioritize their CSG users during the redistribution stage; in fact, 80% of resources are reserved for the CSG users. We can observe that the median throughput is always higher for our framework and specially for the high density case as it is equal to 0.9, meaning that

50% of the users have a throughput of 0.9 or more while the median throughput is only equal to 0.45 for the other access modes. Our framework outperforms these two access modes for the following reason: it incorporates the coalition structure, and so the number of users in the resulting union impacts the payoff distribution. This proves that it is not only sufficient to have more bargaining power (a larger demand), but also numerical superiority in order to reap a better reward, which our model achieves. Moreover, the hybrid access heavily penalizes the MUEs in the system, as the hybrid SBSs will take advantage of the connection of the MUEs to obtain more bargaining power in the game and then unfairly redistribute the resources.

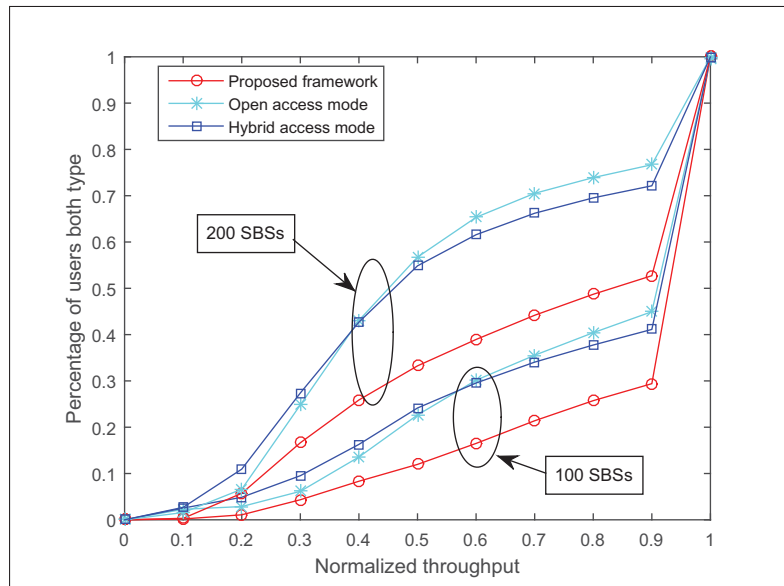


Figure 3.6 Throughput Cumulative Distribution Function for users of both types: Comparison of the proposed framework with the open-access mode and the traditional hybrid-access mode $\delta = 0.8$

3.5.4 Comparison with other cooperative game solutions

We want to show the superiority of our two-level models. Therefore, it is necessary to compare them with several other game-theoretic models. First, we compare our framework to a coalitional game without a coalition structure, which means the unions are not taken into con-

sideration and the payoff is distributed as if every player of a given interference set is a singleton. We divide the estate using the most common value, the Shapley value. The second model of comparison used the proposed coalitional structure game model while applying the Owen value. Therefore, the size of the unions are not taken into account and have the same weight equal to that of the single players in the interference set. It is essential to compare our model to these two approaches, as it shows that the incorporated formation of the union is necessary, as is the application of the imputation value. In Figure 3.7, we present these performances for both types of users in the system. We can observe that our framework outperforms the two other approaches: the median throughput is always higher for our framework and specially for the high density case as it is equal to 0.9, meaning that 50% of the users have a throughput of 0.9 or more while the median throughput is only equal to 0.5 for the other cooperative game models. In Figures 3.8 and 3.9, we analyze separately the performances of the MUEs and the SUEs in the system to show that we have not penalized one type of player for the benefit of another. Clearly, all the MUEs and the SUEs have consistently achieved better performances in the system. In Figure 3.8, we can observe that our model allows 88% of the MUEs with a throughput higher than 0.9 compared to 58% with the centralized approach 62% with the Shapley value and 65% with the Owen value. In Figure 3.9, we can observe that the median throughput is always higher for our framework :in the high density case the median throughput is equal to 0.55 while it is only equal to 0.45 for the other models, in the low density case the median throughput is equal to 0.85 for our model and approximatively 0.75 for the three other frameworks. We also want to demonstrate that the users participating in a cooperative game that are part of a union have an advantage bargaining as a union than they do acting as singletons. Therefore, in Figures 3.10 and 3.11, we isolate the users within unions and analyze their performance in contrast to that which would be achieved if the same users participated in the game independently. It is essential to show again that the proposed framework allows us to protect the harmed MUEs while rewarding the hosting SBSs who participate actively in the interference mitigation. As depicted in these figures, both types of players show better performances at all levels, although SUEs show a slightly lower performances in high throughput. This is explained by the fact that the other models strongly penalize the MUEs in the higher

throughput as they have more bargaining power, and can therefore allow SBSs to negotiate a larger profit.

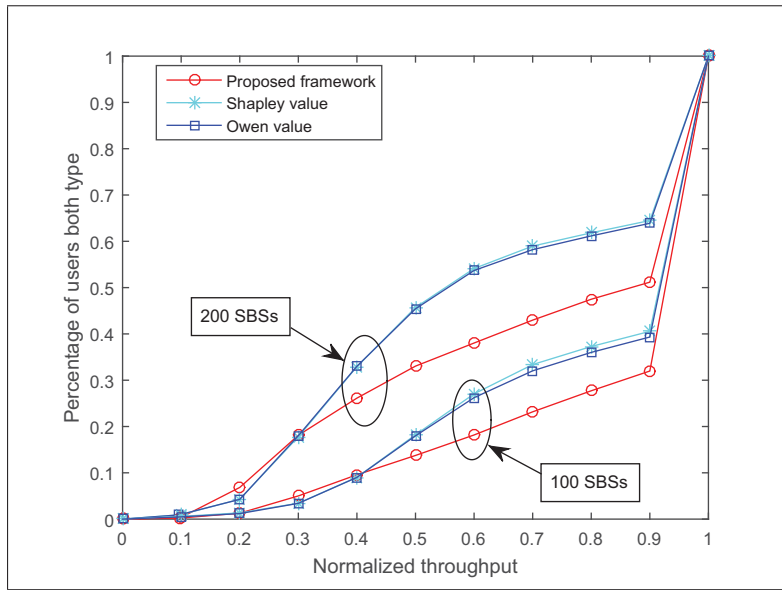


Figure 3.7 Throughput Cumulative Distribution Function for users of both types: Comparison of the proposed framework with other coalitional games

3.5.5 Impact of interference degree and user demands

Here, we assess how the allocated resources are affected by demand volume and the interference degree of the network. Figure 3.12 investigates the impact of the interference degree on the performances of the proposed model. The interference degree corresponds to the cardinality of the interference set. In this case, we are evaluating the gain of payoff using the traditional hybrid access model as a basis. We can see that the proposed model consistently outperforms the other frameworks, reaching up to 300% of gain in very high interference levels. This improvement is justified by the use of the unions because in very dense interference sets the cardinality of the unions is taken into account and the user can obtain an adequate reward. This is added to the solidarity value applied in the canonical games, which protects the

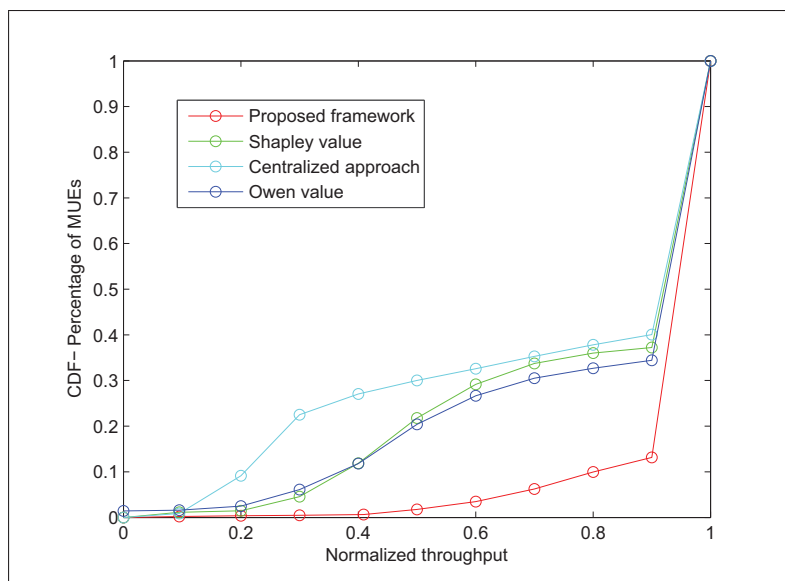


Figure 3.8 Throughput Cumulative Distribution Function for all MUEs of the system: Comparison of the centralized approach, the shapley value, the owen value and the proposed framework

weak players that generally suffer from unfair payoff distribution in high interference degrees in the other models.

Figure 3.13 shows the performances in terms of user demand. Clearly, our model performs better at all levels of demand, although the gain is less important at high user demand. Note that the centralized approach achieves slightly better performances in the highest level of demand. This can be interpreted as an opportunity, since from a network-management standpoint, the users should be discouraged from requesting high demands. In Figure 3.14, we summarize the two types of games that can occur under the proposed cooperative model. We compute the number of games that take place at each iteration. Note that an iteration occurs whenever the topology of the network or the demand expressed by the users change significantly, and results on the participation in the resource allocation game of every player in the network. We have run the simulations for two levels of interference (required SINR) and noticed that the number of canonical games is not affected by the level of interference. In fact, as the deployment of small-cells is very dense, the number of canonical games that occur is slightly affected by the

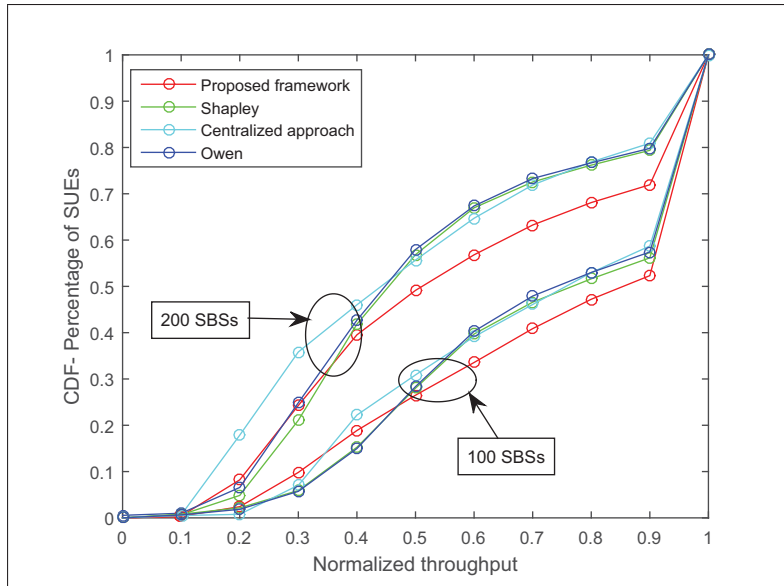


Figure 3.9 Throughput Cumulative Distribution Function for all SUEs of the system: Comparison of the centralized approach, the shapley value, the owen value and the proposed framework

interference level. We notice that this number decreases with the growth of MUEs population. Naturally, as the number of MUEs in the system increases, they are more likely to connect to nearby SBSs and to participate in CS games instead.

3.5.6 Performance analysis of the proposed Weighted Solidarity value

In Figure 3.15, we present the results of the proposed weighted solidarity value. Recall that this value has been proposed in order to alleviate the problem of satiation violation of the solidarity value. For the sake of analysis, we isolated for each interference set \mathcal{I}_n the users belonging to the subset \mathcal{J} (players obtaining more than what they claimed with the solidarity value) from the other players of the same interference set. We isolate the games in which the satiation rule has been violated and compare the performance of our model with the traditional solidarity value. The expected result is that no player obtains more than it claims, accordingly the normalized throughput should not exceed 1. In Figure 15-c, we notice that the satiation violation for the solidarity value as the average normalized throughput reaches up to 270 %.

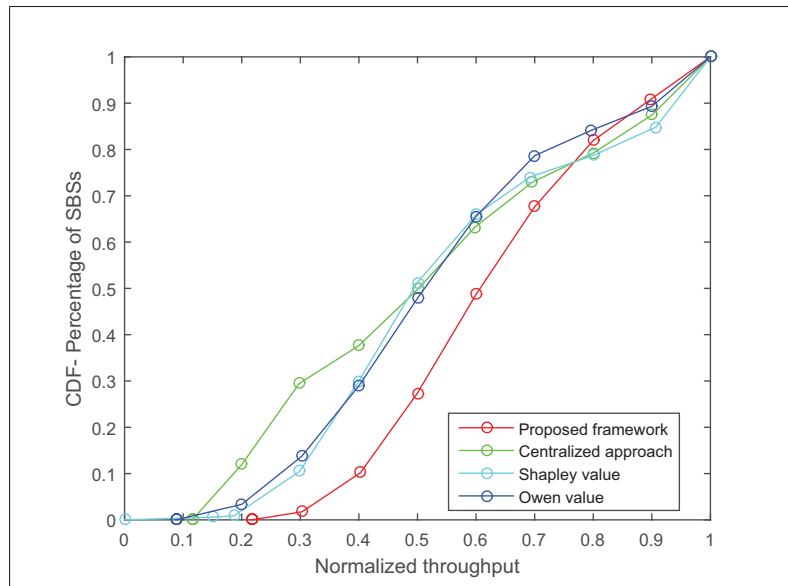


Figure 3.10 Throughput Cumulative Distribution Function for SBSs inside a union only: Comparison of the centralized approach, the Shapley value, the Owen value and the proposed framework

This naturally affects the others players of the game because this excess of resources is not redistributed among players. We also notice from this figure, that in our proposed model all the users with excess of payoff in the solidarity value have now obtained the maximum of their demands and the excess is redistributed to the other members of the system. This is further shown in Figures 15-a and 15-b, where the players belonging to $\mathcal{N} \setminus \mathcal{J}$ benefit from this scheme since they reach a higher throughput on the different degrees of interference and demand.

3.5.7 Performance evaluation in terms of fairness

Finally, in Table II, we present the results of the fairness evaluation for each scheme presented in the previous results. The Jain's fairness index is defined as (Jain *et al.*, 1984):

$$Fairness = \frac{\sum_{i=1}^N (x_i/(d_i))^2}{(N \sum_{i=1}^N (x_i/(d_i))^2)} \quad (3.13)$$

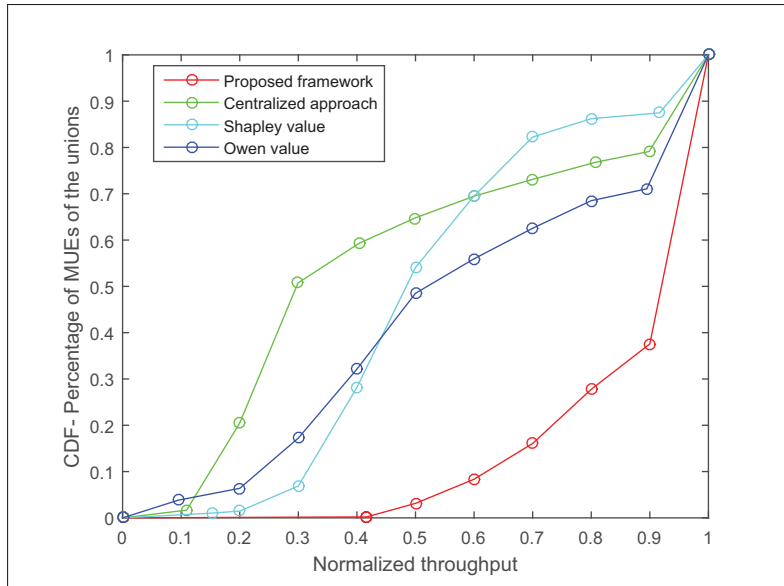


Figure 3.11 Throughput Cumulative Distribution Function for MUEs inside a union only: Comparison of the centralized approach, the Shapley value, the Owen value and the proposed framework

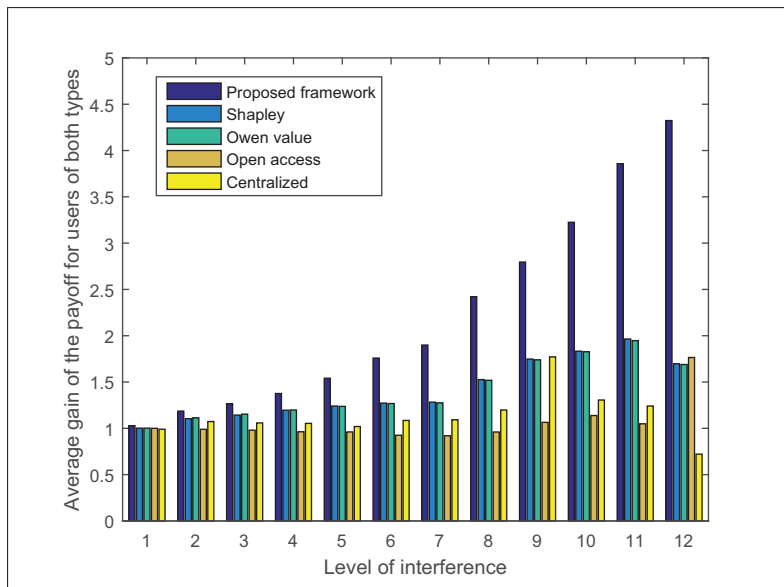


Figure 3.12 Average gain of the payoff as a function of the interference degree with the hybrid access as basis of comparison ($\delta = 0.8$)

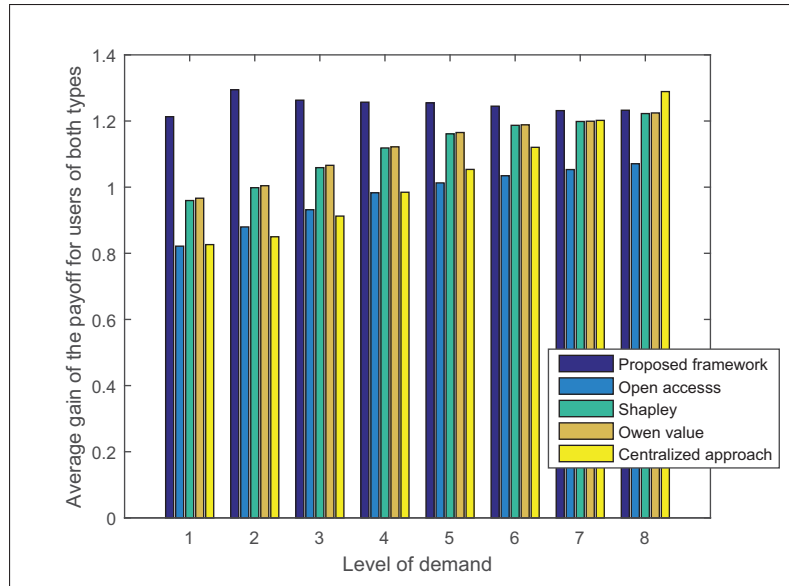


Figure 3.13 Average gain of the payoff as a function of the level of demand with the hybrid access as basis of comparison ($\delta = 0.8$)

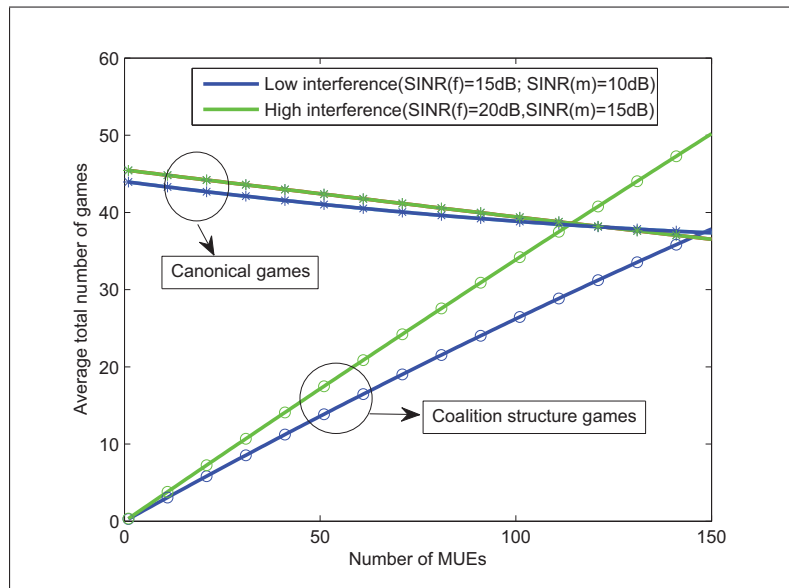


Figure 3.14 Number of canonical games and CS games played at each iteration of the system for two levels of interferences

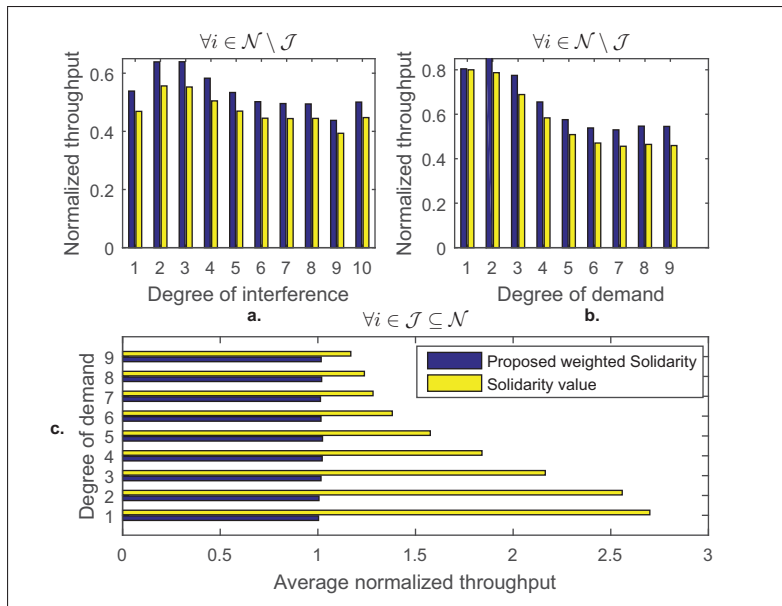


Figure 3.15 Throughput Cumulative Distribution Function for the users of a system participating to a canonical game when the satiation axiom is violated: Comparison of the proposed weighted solidarity value (with the computed weights in algorithm 3.1) and the Solidarity value

where x_i indicates the allocated resources to user i . We can notice that our proposed model gives the highest fairness, thanks to the combination of two game-theoretic approaches adapted to each situation. First, the proposed framework gives the right to play to every user of the network such that no user is penalized by a representing entity in the game (i.e a prioritized SBS). It also allows to protect the weak players according to the equal average gains in the proposed Weighted Solidarity value. Finally, the priority given to unions ensures that bigger profits are allocated to groups composed of multiple users instead of being monopolized by singletons, hence achieving a higher fairness among users. When the coalition utility is divided among the its members, each player receives a payoff denote by x_i .

Table 3.2 Mean Fairness Index

Proposed model	Shapley value	Owen value	Open access	Hybrid prioritized access
0.8256	0.7973	0.7967	0.7680	0.7591

3.6 Conclusion

In this chapter, we have proposed a novel framework of cross-tier cooperation among SBSs and MUEs that offers a significant improvement in performance for users from both tiers. This framework also provides more fairness to the game through an adaptive and solid game theoretic model. It allows the public users to connect to nearby SBSs and thereby offload the traffic of the macrocells, while rewarding this desired cross-tier collaboration. Weak players in the system whose demand is lesser are protected under this model. It also permits every single public user to participate in the resource allocation game and to not be penalized when SBSs are prioritized. Compared to several alternative solutions and access modes, we showed that our proposed approach achieves better performance in terms of throughput and fairness for both types of users (MUEs and SUEs). Future work will extend the proposed model to a QoS and mobility-aware framework. The model could also be enhanced by adding an admission control policy allowing to block users who fail to obtain the minimum requirements in the proposed framework, and redistribute the retrieved resources among the accepted users. Different levels of power transmission, as well as various traffic classes and priorities could also be investigated.

CHAPTER 4

TOWARDS 1GBPS IN ULTRA-DENSE SYSTEMS : A SPATIAL FREQUENCY REUSE MODEL FOR SMALL-CELLS BASED MMWAVE NETWORKS

4.1 Introduction

With the exponential growth of demand in terms of traffic and data rates, one of the most promising potential for the the fifth generation mobile networks is the use of the millimeter-wave (mmWave) frequency bands. Although the available bandwidth in the mmWave frequency is significantly large, high frequencies pose several challenges in term of propagation loss, hence effective utilization of the spectrum is important. Due to significant pathloss, the higher mmWave bands are better suited to the operation of short ranged small cells, while the lower frequency bands are appropriate for outdoors users.

We propose in this chapter, a spatial frequency reuse model for two-tier ultra-dense networks, where a dedicated band is allocated to inner and outer regions of macrocells and small-cells in order to properly exploit the advantages and limits of the mmWave frequencies. Based upon the analytical framework provided in this work, the downlink coverage and single user throughput are characterized. The performances of this scheme are also evaluated in terms of achieved throughput, through system-simulations using recent mmWaves large-scale path loss models. All the results are compared to traditional microwave systems and mmWave models with no reuse. We reach an average of 20% of coverage gain with more than 70% of the users having a throughput greater than 500 Mbps and nearly 40% greater than the target 1 Gbps under the proposed model.

The main results of this chapter have been presented for a student poster competition at ACM MobiCom 2016 where we were rewarded the runner-up best poster award, and have been submitted as a conference paper (Hajir & Gagnon, 2017a) and a journal paper (Hajir & Gagnon, 2017b).

4.1.1 Motivations and prior work

The exponential growth of data traffic in mobile networks and the bandwidth shortage facing wireless carriers has motivated the exploration of higher frequency bands for the 5G mobile networks. To keep up with this rapid increase of mobile data growth massive densification of small cells has brought interest lately (Baldemair & al., 2015). With the huge available bandwidth, mmWave small-cells can provide multiple gigabit rates. The performance of mmWave cellular networks was simulated in prior works Akdeniz & al. (2014); Akdeniz *et al.* (2013); Rappaport & al. (2013) using insights from propagation channel measurements . In Bai *et al.* (2014) the authors propose a framework to evaluate the coverage and rate performances in mmWave cellular networks, where the coverage performances are examined as a function of the antenna geometry and base station density. In Mehrpouyan & al. (2015), a new hybrid Heterogeneous Network (HetNet) paradigm is introduced, that exploits the vast bandwidth and propagation characteristics in the 60 GHz and 70 – 80 GHz bands to reduce the impact of interference in HetNets.

Although the amount of bandwidth available in mmWave is very large, the propagation properties in these frequencies are challenging and vary greatly from lower to higher bands. Hence, these bands need to be allocated properly in order to exploit both the advantages and the limits of the four main mmWave frequency bands presented below. Moreover, interference management techniques are critical to the performance of dense heterogeneous cellular networks, since overlapping coverage areas experience high levels of interference Lopez-Perez & al. (2015).

Frequency partitioning is an attractive and low-complexity solution that has been widely used to reduce the downlink interference in the edge zones or among base stations from different tiers Chandrasekhar & Andrews (2009). In Novlan & al. (2012), the authors showed that the use of Strict Fractional Frequency Reuse (FFR) bands reserved for the users of each tier with the lowest average Signal-to-interference-plus-noise ratio (SINR) provides the highest gains in terms of coverage and rate. The different available bands in the mmWave spectrum makes it a natural fractionality that could be used not only to mitigate interferences but also to achieve a higher

spectrum efficiency and data rates in ultra dense small-cell deployment networks. Because of the high pathloss in the higher frequencies bands, the interferences among neighbouring smallcells are strongly mitigated and a better spatial reuse is allowed. We consider in this chapter four mmWave frequency bands explored in Ghosh & Tal. (2014) and described in the following:

- 28 GHz band: The 27.5 – 28.35 GHz (850 MHz) and 29.1 – 29.25 GHz (150 MHz) are licensed. This is the lower band of the mmWave spectrum and unlike at 60 GHz, atmospheric absorption does not significantly contribute to additional path loss, making it suitable for outdoor mobile communications;
- 38 GHz band: The 38.6 – 40 GHz band is licensed. Similar to the 28 GHz band, the outdoor cellular propagation measurements in NYC show that this band is suitable for outdoor mobile communications when coupled with the use of large antenna arrays and with the help of beamforming when directional antennas are used;
- E-band or the 70 GHz and 80 GHz bands: 71 – 76 GHz and 81 – 86 GHz respectively are lightly licensed and can be aggregated up to a total of 2×5 GHz. These bands can suffer from high rain attenuations at long distances but are suitable candidates for indoor communications and small-cell areas.

We do not consider the unlicensed 57 – 64 GHz band (V-band) which may not be the first choice for a cellular mmWave systems since it has a large amount of oxygen absorption and rain attenuation. Moreover, 802.11ad also known as WiGig (or 60GHz Wi-Fi), is designed to be used in this frequency band (Nitsche & al., 2014).

4.1.2 Main contributions and organization

In this chapter, we propose a spatial frequency reuse for ultra-dense heterogeneous networks, where each band of the 5G mmWave frequencies presented above is allocated to inner and outer regions of the macrocells and smallcells in a two-tier network. In section 4.2, we present

the system model of the proposed framework. In section 4.3, we propose a coverage analysis for a typical user under the proposed spatial reuse, where macrocells are modeled as a Hard-Core Point Process (HCPP) and the small cells as a Poisson Point Process (PPP). In section 4.4, we analyse the performances of the proposed spatial reuse model under a large-scale path loss model using the results of the recent millimeter-wave propagation measurements Rappaport & al. (2015); Sun *et al.* (2016). The analysis is performed in terms of achieved throughput and compared to traditional LTE systems. The most favourable small-cells density in an ultra-dense system are also obtained through simulations.

As depicted in Figure 4.1, the propagation conditions in higher frequency are more suitable for short distance transmission. For instance, a path loss of 135 dB is obtained at 100 m for transmissions in 28 GHz frequency band while it is reached at only 25 m for transmission in 73 GHz frequency band.

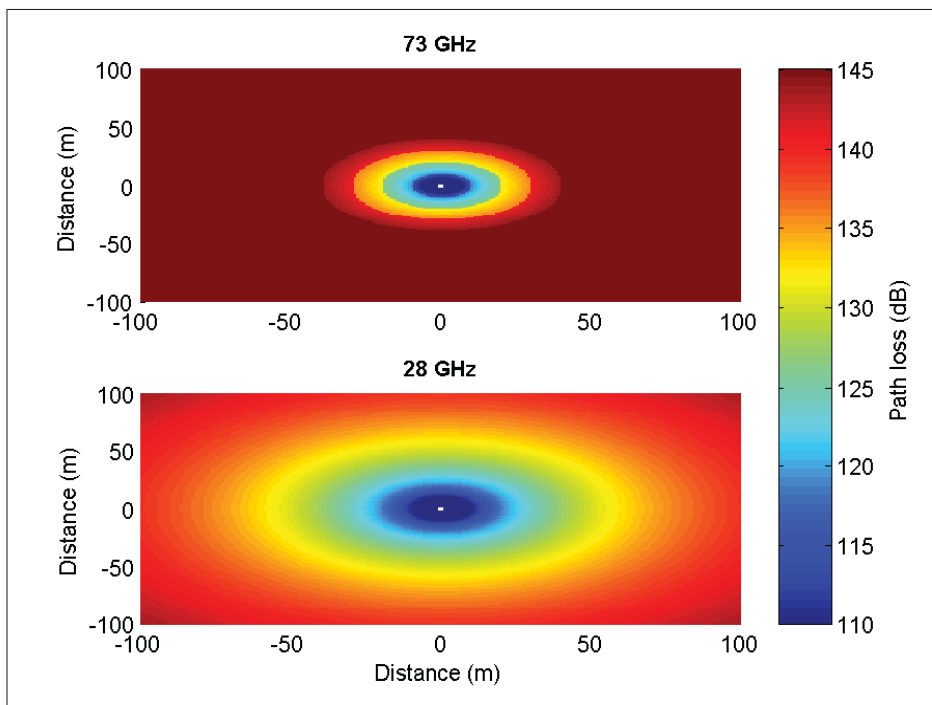


Figure 4.1 Propagation loss in mmWaves frequency bands 28 GHz and 73 GHz using large-scale path loss model

4.2 System model

As depicted in Figure 4.2, we consider an isolated macrocell overlaid by a dense network of small-cells under open access mode. The macrocell is divided into two regions: the inner region and outer region. The inner macro-area is allocated the 38 GHz band while the outer macro-area is allocated the 28GHz band. These bands could be aggregated with 4G bands in order to reach higher rates and achieve the requirements of 5G.

Similarly small cell coverage area is divided into two distinct regions : the inner and outer region. The inner zone being very close to the SBS, the users located in this region suffer from low interferences, the co-tier interferences are strongly mitigated given the higher path losses which makes it suitable for high frequency bands (above 83GHz). The outer region of small-cells can be considered as an extended coverage area where the circular ring can be used to offload the traffic from the macrocell and obtain higher data rates. This area is allocated the 73GHz frequency band which is less affected by distance-based attenuation than the 83GHz. Given the ultra-dense small cell deployment, downlink interference among neighbouring small-cells are likely to exist. However these interferences are considerably lower than what is experienced in 4G frequency bands given the propagation properties of millimeterwave bands. Nonetheless, even if they are not attenuated by the environment the large bandwidth in E-bands(10GHz) dedicated to smalls cells permits clustering-based frequency sharing or fractional frequency partitioning. As the inner and outer region of a given cell operates in different frequency bands, the power of transmission in the inner region can be slightly decreased by a factor δ compared to the outer region hence allowing energy consumption savings and interference mitigation in the proposed system.

4.3 Tractable framework on coverage probability

In this section, we derive the probability coverage in the downlink under the spatial frequency reuse model proposed. We analyze the small-cell tier and the macro-tier separately as we apply a split spectrum approach. In this analysis, the HetNet consists of two tiers, the macro and

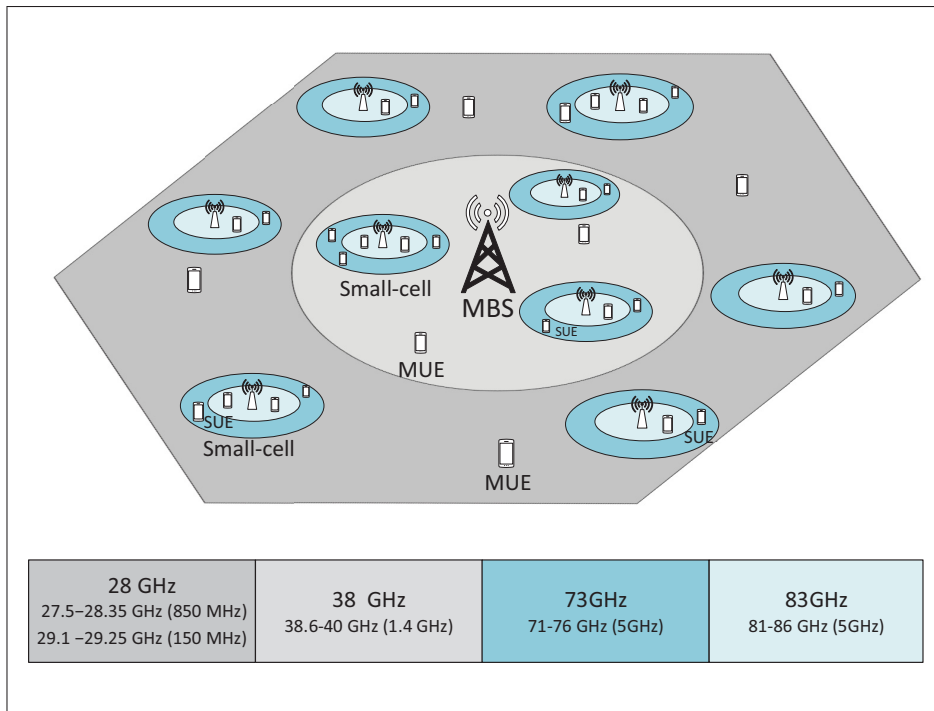


Figure 4.2 Frequency reuse for millimeterwave bands in small cells based networks

small cell tiers (otherwise called as the first and second tiers), which are spatially distributed as two-dimensional processes Φ_1 and Φ_2 , with different transmit powers P_m and P_s respectively. The macrocell tier process Φ_1 is modeled as a homogeneous HCPP with the density λ_1 and hard distance D_h . The small-cell tier process Φ_2 is modelled as a homogeneous PPP with density λ_2 . Furthermore, the collection of mobile users, located according to an independent homogeneous PPP Φ_u with the density λ_u , is assumed in this work. We consider the process $\Phi_u \cup \{0\}$ obtained by adding a user at the origin of the coordinate system, which is the typical user under consideration. This is allowed by Slivnyak's Theorem (Dietrich Stoyan, 1987), which states that the properties observed by a typical point of the PPP Φ_u , are identical to those observed by the origin in the process $\Phi_u \cup \{0\}$.

In the proposed two-tier HetNets, a typical user can be associated either with a macrocell or a smallcell BS and either located in the center or edge zone of the corresponding base station

coverage area. For a typical user the coverage probability is defined by:

$$p_c(\theta) = \sum_{i=1}^2 p_c^{i,c}(\theta) * \phi(i) * \mathbb{P},(i) + p_c^{i,e}(\theta) * \phi(i) * \mathbb{P}(i,e) \quad (4.1)$$

with $p_c^{i,c}$ and $p_c^{i,e}$ being the coverage probability of a typical user associated with the center and edge zone of i -th tier BS, respectively, $\phi(i)$ the probability that the user is associated with i -th tier BS, $\mathbb{P}(i,c), \mathbb{P}(i,e)$ the probability that the user is located in the center and edge zone of the i -th corresponding tier cell, respectively. For simplicity the index $i = 1$ corresponds to the macro-tier and $i = 2$ the smallcell-tier. The downlink SINR at the typical user u can be expressed as $SINR = \frac{P_u h R_u^{-\alpha}}{I + \sigma^2}$ where $I = \sum_{x \in \Phi \setminus \{k\}} P_x h_x \|x\|^{-\alpha}$. We assume that the small-scale fading between a BS and the typical user (serving BS or interfering) is i.i.d exponentially distributed with the unitary mean value (Rayleigh fading). The Rayleigh fading assumption might be discussable in the case of mmWave communications and some authors rather use more general fading model such as Nakagami. However, Gupta *et al.* (2016) show that considering Nakagami model does not provide any additional design insights, but it does complicate the analysis significantly. Therefore it justifies the use of Rayleigh fading in our analysis. The comparison of these two results obtained in the cited paper are presented in Appendix 1.

We assume that a user will always connect to the small-cell tier when located in its coverage area. This assumption is acceptable since a user has an advantage either in term of SINR or throughput to be associated with the closest SBS. Indeed, given the short range of the small-cells the SINR received from this tier is very likely to be greater than the SINR received from the closest MBS. In the case the received SINR is not greater, the frequency reuse applied in our model still makes the SBSs a better choice since the amount of bandwidth available for each SBS is very large and permits to achieve very high data rates. Therefore, we avoid one the inherent problem in HetNets of uneven distribution of the traffic loads among BSs when received signal power (RSP)-based user association is used.

Hence, we can define $\phi(2)$ the probability that a typical user is associated with the small-tier as:

$$\phi(2) = (1 - \exp(-\pi * \lambda_2 * c_2^2)) \quad (4.2)$$

where λ_2 is the density of every other user not associated with a close by small-cells will be then associated to the macro-tier, we hence obtain define $\phi(2)$ the probability that a typical user is associated with the macro-tier as:

$$\phi(1) = \exp(-\pi * \lambda_2 * c_2^2) \quad (4.3)$$

As regards the probability that a user is located in the center/edge zone of its corresponding tier (i.e., $\mathbb{P}(i, c)$, $\mathbb{P}(i, e)$), we assume that the radius of the inner regions are adequately set in order that these probabilities are the same and equal to 0.5 for a perfect load balancing.

4.3.1 Coverage analysis of the macro-tier

4.3.1.1 In the macro-tier center zone

Based upon the above-mentioned cell association model, we express the coverage probability of the typical user. Let $R_{i,c}$ be a random variable corresponding to the distance between a center typical user and its serving BS from the i -th tier, and α_k the path loss exponent (PLE) of the corresponding cell and zone (i.e. $k=1;2;3;4$ corresponding to the PLE associated with the frequencies allocated to the center macrocell; edge macrocell; center small-cell and edge small-cell respectively).

The cumulative distribution function of R_1 is obtained by:

$$\begin{aligned}
F_{R_{1,c}}(r) &= \mathbb{P}[R_{1,c} \leq r \mid u \in \mathcal{L}_{1,c}] \\
&= \mathbb{P}[R_{1,c} \leq r \mid R_{1,c} \leq C_1] \\
&= \frac{1 - \exp(-\pi\lambda_1 r^2)}{1 - \exp(-\pi\lambda_1 C_1^2)}
\end{aligned} \tag{4.4}$$

with C_1 being the radius of the macrocell inner region. We differentiate $F_{R_{1,c}}(r)$ and then obtain the probability density function (PDF) of $R_{1,c}$.

We differentiate $F_{R_{1,c}}(r)$ and then obtain the pdf of $R_{1,c}$.

$$f_{R_{1,c}}(r) = \frac{2\pi\lambda_1 r}{1 - \exp(-\pi\lambda_1 C_1^2)} \exp(-\pi\lambda_1 r^2) \tag{4.5}$$

The coverage probability for the typical user located in the center zone of the macrocell and associated with the corresponding MBS is (Wang *et al.*, 2014):

$$\begin{aligned}
p_c^{i,c}(\theta) &\approx \mathbb{P}[SINR > \theta \mid u \in \mathcal{L}_{1,c}] \\
&= \int_0^{C_1} \mathbb{P}[SINR > \theta \mid R_i = r, u \in \mathcal{L}_{1,c}] \cdot f_{R_{1,c}}(r) dr \\
&= \int_0^{C_1} \exp\left(-\frac{\theta\sigma^2 r^{\alpha_1}}{P_m}\right) \cdot \mathcal{L}_1(r^{\alpha_1} \theta) \cdot f_{R_{1,c}}(r) dr
\end{aligned} \tag{4.6}$$

with $\mathcal{L}_{1,c}$ being the center macro-area and C_1 the radius of the center macro-area, $\mathcal{L}_1(r^{\alpha_1} \theta)$ the Laplace transform of the interference suffered by a typical MUE defined as:

$$\mathcal{L}_1(r^{\alpha_1} \theta) \approx \exp\left(-\pi\lambda_1 D_h^2 \rho\left(\frac{\theta r^{\alpha_1}}{D_h}, \alpha_1\right)\right) \tag{4.7}$$

with ρ defined as $\rho(a, b) = a^{2/b} \int_{a^{-2/b}}^{\infty} (1/(1+v^{b/2})) dv$. It should be noted that $\exp(-\frac{\theta\sigma^2 r^{\alpha_1}}{P_m})$ and $\mathcal{L}_1(r^{\alpha_1} \theta)$ respectively represent the impact of noise and the interference.

Under the proposed split spectrum approach, a MU will only suffer from the interferences induced by the neighbouring MBSs. We assume that there is no interfering MBS within a radius D_h around a given MBS. Hence the macrocell tier process is modeled as a hard-core point process. This assumption is reasonable because unlike SBSs, MBSs are strategically deployed by the operators in order to cover a given geographical area.

4.3.1.2 In the macro-tier edge zone

Let us express here, the coverage probability of the edge macro-tier. The pdf of $R_{1,e}$ is expressed as:

$$\begin{aligned} F_{R_{1,e}}(r) &= \mathbb{P}[R_{1,e} \leq r \mid u \in \mathcal{Z}_{1,e}] = \mathbb{P}[R_{1,e} \leq r \mid R_{1,e} \geq C_1] \\ &= \frac{1 - \exp(-\pi\lambda_1 r^2)}{\exp(-\pi\lambda_1 C_1^2)} \end{aligned} \quad (4.8)$$

We differentiate $F_{R_{1,e}}(r)$ and then obtain the pdf of $R_{1,e}$.

$$f_{R_{1,e}}(r) = \frac{2\pi\lambda_1 r}{\exp(-\pi\lambda_1 C_1^2)} \exp(-\pi\lambda_1 r^2) \quad (4.9)$$

The coverage probability for the typical user located in the edge zone of the macrocell and associated with the corresponding MBS is expressed as Wang *et al.* (2014):

$$\begin{aligned} p_c^{i,e}(\theta) &\approx \mathbb{P}[SINR > \theta \mid u \in \mathcal{Z}_{1,e}] \\ &= \int_{C_1}^{\infty} \mathbb{P}[SINR > \theta \mid R_i = r, u \in \mathcal{Z}_{1,e}] \cdot f_{R_{1,e}}(r) dr \\ &= \int_{C_1}^{\infty} \exp\left(-\frac{\theta \sigma^2 r^{\alpha_2}}{P_m}\right) \cdot \mathcal{L}_1(r^{\alpha_2} \theta) \cdot f_{R_{1,e}}(r) dr \end{aligned} \quad (4.10)$$

4.3.2 Coverage analysis of the smallcell-tier

4.3.2.1 Center zone of small-cells

The pdf of $R_{2,c}$ is expressed similarly to $R_{1,c}$ in (5) by replacing C_1 with c_1 , the radius of the inner small-cell region. Hence we obtain:

$$f_{R_{2,c}}(r) = \frac{2\pi\lambda_2 r}{1 - \exp(-\pi\lambda_2 c_1^2)} \exp(-\pi\lambda_2 r^2) \quad (4.11)$$

The coverage probability of the typical user located in the center zone of the small-cell and associated with the corresponding SBS is then expressed as:

$$\begin{aligned} p_c^{i,c}(\theta) &\approx \mathbb{P}[SINR > \theta \mid u \in \mathcal{L}_{2,c}] \\ &= \int_0^{c_1} \mathbb{P}[SINR > \theta \mid R_i = r, u \in \mathcal{L}_{2,c}] \cdot f_{R_{2,c}}(r) dr \\ &= \int_0^{c_1} \exp\left(-\frac{\theta \sigma^2 r^{\alpha_3}}{P_s}\right) \cdot \mathcal{L}_{2,c}(r^{\alpha_3} \theta) \cdot f_{R_{2,c}}(r) dr \end{aligned} \quad (4.12)$$

with $\mathcal{L}_{2,c}$ being the center smallcell-area and P_s the transmission power of the SBS.

Under the proposed split spectrum approach, a SU will suffer from the interferences induced by the neighbouring SBSs. We assume that the coverage radius of a smallcell is c_2 and that the interferences come from the whole plans. Indeed the small-cell tier process is modeled as a poisson point process in this case. This assumption is reasonable since the smallcells are randomly deployed by the users . Hence, we define the Laplace transform of the interference I_2 induced to a typical user in the smallcell center zone as $\mathcal{L}_{2,c}(r^{\alpha_3} \theta) \approx \exp(-\pi\lambda_2 \rho(\theta, \alpha_3) r^2)$.

4.3.2.2 Edge zone of small-cells

The pdf of $R_{2,e}$ can be expressed as:

$$\begin{aligned} F_{R_{2,e}}(r) &= \mathbb{P}[R_{2,e} \leq r \mid u \in \mathcal{L}_{2,e}] = \mathbb{P}[R_{2,e} \leq r \mid c_1 \leq R_{2,e} \leq c_2] \\ &= \frac{1 - \exp(-\pi\lambda_2 r^2)}{\exp(-\pi\lambda_2 c_1^2) - \exp(-\pi\lambda_2 c_2^2)} \end{aligned} \quad (4.13)$$

We differentiate $F_{R_{2,e}}(r)$ and then obtain the pdf of $R_{2,e}$.

$$f_{R_{2,e}}(r) = \frac{2\pi\lambda_2 r}{\exp(-\pi\lambda_2 c_1^2) - \exp(-\pi\lambda_2 c_2^2)} \exp(-\pi\lambda_2 r^2) \quad (4.14)$$

The coverage probability for the typical user located in the edge zone of the small-cell and associated with the corresponding SBS is expressed as:

$$\begin{aligned} p_c^{2,e}(\theta) &\approx \mathbb{P}[SINR > \theta \mid u \in \mathcal{L}_{2,e}] \\ &= \int_{c_1}^{c_2} \mathbb{P}[SINR > \theta \mid R_i = r, u \in \mathcal{L}_{2,e}] \cdot f_{R_{2,e}}(r) dr \\ &= \int_{c_1}^{c_2} \exp\left(-\frac{\theta \sigma^2 r^{\alpha_4}}{P_s}\right) \cdot \mathcal{L}_{2,e}(r^{\alpha_4} \theta) \cdot f_{R_{2,e}}(r) dr \end{aligned} \quad (4.15)$$

We define the Laplace transform of the interference I_2 induced to a typical SU in the small-cell edge zone as:

$$\mathcal{L}_{2,e}(r^{\alpha_4} \theta) \approx \exp(-\pi\lambda_2 \rho(\theta, \alpha_4) r^2) \quad (4.16)$$

4.4 Single user-throughput analysis

The data throughput achievable at a single user is another important metric, especially when considering the deployment of small-cells as a capacity solution, and when this metric is determined by the small-cells density of the heterogeneous network (Andrews, 2013). We assume the users are distributed according to an independent homogeneous PPP of density λ_u . The

distribution of Voroni cell area formed by a homogeneous PPP has no closed form expression; however precise estimates have been obtained in (Hinde & Miles, 1980).

The CCDF of the throughput achieved at the typical user served by the i -th tier is provided by:

$$\begin{aligned} \mathbb{P}(R_i > \beta) = & \sum_{i=1}^2 \sum_{n=0}^{\infty} \mathbb{P}[N_{i,c} = n] \cdot p_c^{i,c} \cdot (2^{(n+1)\beta/W_{i,c}} - 1) + \\ & \sum_{i=1}^2 \sum_{n=0}^{\infty} \mathbb{P}[N_{i,e} = n] \cdot p_c^{i,e} \cdot (2^{(n+1)\beta/W_{i,e}} - 1) \end{aligned} \quad (4.17)$$

with $N_{i,c}$ and $N_{i,e}$ the number of users served by the i -th tier and located in the center and edge zone of the corresponding cell, respectively; $W_{i,c}$ and $W_{i,e}$ the bandwidth allocated to center and edge zone the i -th tier cells, respectively.

The number of other users sharing resource with the typical user served by the i -th tier and located in the j -th zone of its corresponding cell ($j \in \{c, e\}$) is denoted by $N_{i,j}$, and the probability mass function of $N_{i,j}$ can be derived as (Singh *et al.*, 2013):

$$\mathbb{P}[N_{i,j} = n] \approx \frac{b^q}{n!} \cdot \frac{\Gamma(n+q+1)}{\Gamma(q)} \cdot \left(\frac{\lambda_u}{\lambda_i / (0.5 * \phi(i))} \right)^n \quad (4.18)$$

$$\cdot \left(b + \frac{\lambda_u}{\lambda_i / (0.5 * \phi(i))} \right)^{-(n+q+1)} \quad (4.19)$$

4.5 Performance evaluation with accurate large-scale distant-dependent pathloss models

In the previous paragraph, we have used a simple exponential Rayleigh fading with path loss exponents approximated for each frequency bands to capture the propagation features of each frequency.

Although this method gives us a clear idea of the performances of the proposed spatial reuse for different incremental values of α capturing the propagation conditions of each mmWave bands, it is not taking into account the oxygen absorption, rain attenuation as well as beamforming to capture the effects of antenna gains in a real life environment. Hence, given the complexity of the propagation in the mmwaves, we use in this section the recent propagations measures and the related accurate large-scale distant-dependent path loss models in (Akdeniz & al., 2014) and (MacCartney *et al.*, 2013) , as well as antenna gains and environment attenuation values expressed in Table II to evaluate the performances of the proposed framework under real-life propagation conditions.

We consider the downlink of an Orthogonal Frequency Division Multiple Access (OFDMA) macrocell network overlaid by N small base stations (SBSs) and N' macrocell user equipments (MUEs). Let $\mathcal{F} = \{F_1, \dots, F_n, \dots, F_N\}$ be the set of FAPs and $\mathcal{M} = \{M_1, \dots, M_n, \dots, M_{N'}\}$ the set of MUEs in a given macrocell.

The downlink SINR achieved by a SUE n_u associated with small-cell S_n on a particular sub-channel k with I_{sbs} interfering small-cells is given by:

$$\gamma_{n_u, S_n} = \frac{P_{sbs}^k PL_{u,sbs}^k G_{u,sbs}^k}{\sum_{i \in I_{sbs}} P_i^k PL_{u,i}^k G_{u,i}^k + \sigma^2} \quad (4.20)$$

where $PL_{u,sbs}^k$ and $PL_{u,i}^k$ represent the channel gain including the path-loss and shadowing from the serving SBS sbs and the interfering SBSs i to SUE n_u respectively in smallcell S_n on subchannel k , $G_{u,sbs}^k$ and $G_{u,i}^k$ are the antenna gains from the serving and interfering SBSs respectively, σ^2 the noise power.

The SINR achieved by a MUE M_n associated with macrocell m on a particular suchannel k can be written as:

$$\gamma_{n,B_m}^k = \frac{P_{mbs}^k PL_{u,mbs}^k G_{u,mbs}^k}{\sum_{m \in I_{mbs}} P_m^k PL_{u,m}^k G_{u,m}^k + \sigma^2} \quad (4.21)$$

where $PL_{u,mbs}^k$ and $PL_{u,m}^k$ represent the channel gain including the path-loss and shadowing associated with k from the serving MBS mbs and the interfering MBS m to a MUE M_n respectively in macrocell B_m , $G_{u,mbs}^k$ and $G_{u,m}^k$ are the antenna gains from the serving and interfering MBSs respectively.

In order to mitigate co-tier interferences in the downlink for macro-edge users, SFFR (Strict fractional frequency reuse) with a factor of 3 might be used. A cooperative approach as clustering based resource allocation is suitable for the mitigation of these interference in the edge of the macrocell.

4.5.1 Path loss model for millimeterwave bands

We use here the alpha plus beta model given by the following expression:

$$PL(dB) = \alpha + \bar{\beta} * 10 \log_{10}(d) + X_{\sigma} \quad (4.22)$$

where α is the floating intercept in dB, $\bar{\beta}$ the linear slope, d the Rx-Tx distance and X_{σ} the shadow fading term, which values have been obtained from the recent measurements campaign in NYC and Austin presented in (MacCartney *et al.*, 2013; Rangan *et al.*, 2014; Ghosh & Tal., 2014) and denoted in Table 4.1.

Since we do not have the closed form path loss expression for the 83 GHz frequency band, we assume free space path loss for users located in the inner zone of small-cells, given by:

$$PL_{dB} = 92.4 + 20 * \log_{10}(f_{GHz}) + 20 * \log_{10}(d_{km}) \quad (4.23)$$

Table 4.1 Parameters for alpha plus beta model path loss model

Frequency bands	α	β	γ
28 GHz (Akdeniz & al., 2014)	72.0 dB	2.92	8.7 dB
38 GHz (MacCartney <i>et al.</i> , 2013)	115.17 dB	1.28	7.59 dB
73 GHz (Akdeniz & al., 2014)	86.6 dB	2.45	8 dB

This assumption is acceptable since the 83 GHz band is allocated to the center area of small cells, where the users located in this zone are at a very short distance from their serving SBS and are very probably in line of sight. We take account of the wall loss inside the building.

4.5.2 Proposed algorithm for BS association and SINR computation

Algorithm 4.1 describes the different steps for base station association and frequency band allocation for the purpose of system-simulations. We take into account the mobility of the users in this model, where only the slow mobility users are associated with a nearby SBS while fast users are served by the MBS. This avoids the multiple handovers that might severely penalize fast users.

4.5.3 Instantaneous rate computation of a typical user

Now, we assume that the scheduler of each BS gives $\frac{1}{n_{i,j}^u}$ fraction of the available bandwidth for BS i to each of the $n_{i,j}^u$ users attached to BS i and located in region j (i.e. center or edge of each cell). This assumption can be justified as most of the schedulers such as round robin or proportional fair give approximatively $\frac{1}{n_{i,j}^u}$ fraction of the resources to each user.

The achieved data rate of user $u^{i,j}$ associated with cell i and located in region j is expressed as:

$$r_u^{i,j} = \frac{n_k^i W_k}{n_{i,j}^u} * \log_2(1 + SINR_{i,j}^k) \quad (4.24)$$

Algorithm 4.1 Proposed algorithm for BS association and SINR computation

```

1: Random deployment of users  $n_u \{x_u, y_u\} \forall u \in \mathcal{U}$  and SBSs  $S_n \{x_n, y_n\} \forall n \in \mathcal{N}$  in macrocell  $B_m \{x_m, y_m\}$ 
2: for all  $n_u \in \mathcal{U}$  do
3:   if  $\|x_u - x_m\| < radius_{B,center}$  then
4:      $n_u.bs = B_{m,center}, PL_{n_u, B_m}^k = PL_{38GHz}$ 
5:   else
6:      $n_u.bs = B_{m,edge}, PL_{n_u, B_m}^k = PL_{28GHz}$ 
7:   end if
8:    $n_u.sinr^k = \gamma_{n_u, B_m}^k$ 
9:   for all  $n \in \mathcal{N}$  do
10:    if  $\gamma_{n_u, S_n} > \gamma_{n_u, B_m}$  and  $n_u.mobility = slow$  then
11:      if  $\gamma_{n_u, S_n} > \gamma_{n_u, S_{n-1}}$  then
12:        if  $\|x_u - x_n\| < radius_{n,center}$  then
13:           $n_u.bs = S_{n,center}, PL_{n_u, S_n}^k = PL_{83GHz}$ 
14:        else
15:           $n_u.bs = S_{n,edge}, PL_{n_u, S_n}^k = PL_{73GHz}$ 
16:        end if
17:         $n_u.sinr^k = \gamma_{n_u, S_n}^k$ 
18:      end if
19:    end if
20:  end for
21: end for

```

with W_k the bandwidth of subchannel k , n_k^i the number for subchannels available for cell i in zone j and $SINR_{i,j}^k$ the SINR achieved by user $u^{i,j}$ in channel k .

4.6 Numerical results

In this section, we present first the numerical results on the coverage for the proposed mmWave model. In a second part, we conduct Monte Carlo simulations for the throughput analysis of the proposed framework. Table II depicts the numerical values used for analytical evaluation and system simulations. We remind that the total link loss T_{loss} is the PL computed in (15) and (16) to which are added the environment attenuations, hence $T_{loss} = PL_{xGHz} + Rain\ attenuation + Oxygen\ absorption + n * Wall\ loss$, where n is the number of walls. We note that the worst case

of rain conditions is taken into account in Table II, where a heavy rain is occurring (200mm/hr). The use of highly-directional steerable horn antennas at the TX and RX provided the ability to capture directional azimuth and elevation plane measurements. The measurements in (Akdenez & al., 2014; MacCartney *et al.*, 2013) were conducted using narrowbeam TX and RX antennas, each with 24.5 dBi gain and 10.9 half-power beamwidth (HPBW) in the azimuth. The value of this gain is 6dB lower at RX and 9dB lower at TX for the interfering links. Although most of the gains might be seen as simply the result of the increase of bandwidth (1GHz for the mmWave and 20MHz+20MHz in LTE), we have considered a basic mmWave system in this work to show the great potential of the mmWave systems. Indeed, no spatial multiplexing nor MIMO or any advanced techniques have been considered here, hence we expect much higher gains when these techniques will be applied to the mmWave system.

4.6.1 Validation of the proposed model

We have developed in sections 4.3 and 4.4 expressions for the coverage and user throughput, respectively, and it is now important to see how these analytical results compare with the widely known hexagonal model. We compare the traditional hexagonal grid model to the proposed random SBSs PPP and MBSs HCPP model. We consider a MBS located at the origin and N surrounding interfering MBSs and overlaid by N' SBSs. The SINR of a typical user is obtained by:

$$SINR = \frac{P_u h R_u^{-\alpha}}{I_u + \sigma^2} \quad (4.25)$$

with $I_u = \sum_{i \in \mathcal{I}_u} P_i h_i r_i^{-\alpha}$, \mathcal{I}_u the set of user u interfering BSs, r_i the distance seen from the interfering BS i , and h_i its observed fading power. The channel fading power for the simulation is a Rayleigh fading $h \sim \exp(\mu)$. By implementing the locations of MBSs as a HCPP we alleviate the weakness of traditional PPP models where the artificially high probability of nearby and dominant interfering BSs.

We compare in Figure 4.3, the traditional hexagonal model with the proposed HCPP model for the macro-tier in both the center and edge region. We can see that the random model is slightly

Table 4.2 Numerical values for the analytical and system-simulation evaluation

Analytical evaluation	
C_1 (radius of the MBS inner region), D_h (distance of the HCPP), c_1 (radius of the SBSs inner region) c_2 (radius of the SBSs outer region)	150 m, 500 m, 10 m, 20 m
BSs densities	$\lambda_1 = 4 \text{ MBSs}/\text{km}^2$; $\lambda_2 = 100 * \lambda_1$
User density	$\lambda_u = 1000 \text{ users}/\text{km}^2$
PLE (2.4 GHz; 28 GHz; 38 GHz; 73 GHz; 83 GHz)	$\alpha = 3$; $\alpha_1 = 3.3$; $\alpha_2 = 3.7$; $\alpha_3 = 4.3$; $\alpha_4 = 4.7$
System-simulation	
Radius of macrocells outer region/inner regions	250 m/150 m
Radius of small-cells outer region/inner regions	10 m/20 m
Rain attenuation	27dB/km (28 GHz), 38dB/km (38 GHz), 50dB/km (73 and 83 GHz)
Oxygen absorption	0.18 dB/km (28 and 38 GHz) , 0.5 dB/km (73 and 83 GHz)
Antenna gain	24.5 dBi Tx and 24.5 dBi Rx
BW per band	1 GHz for mmWaves, 20MHz+20MHz for microwaves
MBS, SBS transmission power	40 W, 40 mW
Thermal Noise	-92.01 dBm
Density of users, probability of fast user mobility	$\lambda_u = 1000 \text{ users}/\text{km}^2$, $\rho = 0.2$

more optimistic at low SINR, since the minimum distance of two interfering MBSs might is greater or equal to D_h , while in the hexagonal grid model, the minimum distance between two interfering MBSs is always D_h . At high SINR, the user is located closer to the MBS, hence the effect of the interfering BSs is less corrupting, giving a random model slightly more pessimistic than the grid model.

Figure 4.4 depicts the probability of coverage for a typical small-cell user in the edge and center zone. We can observe that the analytical model is slightly more pessimistic and this can be explained by the fact that we consider the co-tier interferences from the whole plan while in the grid model we only consider the interferences from the SBSs of the underlying macrocell.

And finally, Figure 4.5 depicts the probability of coverage of a typical user in the system (from both tiers) and permits us to validate the proposed analytical model when compared to the hexagonal grid. The slight deviations being due to the deviation in small-tier and macro-tier explained above.

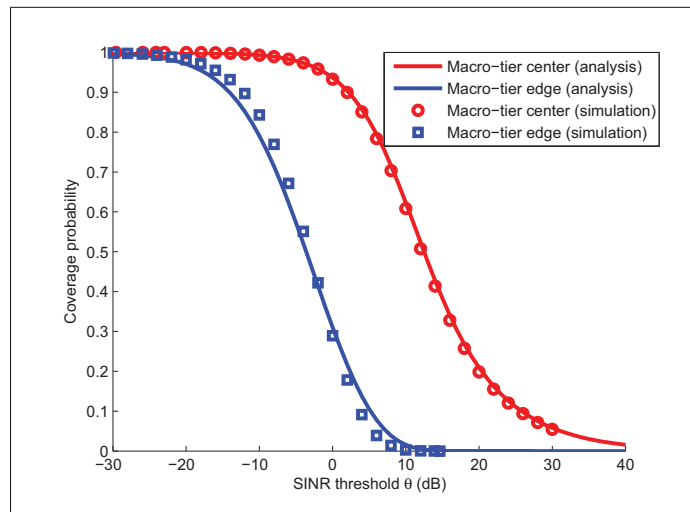


Figure 4.3 Validation of the proposed analytical model: Analytical coverage probability versus simulated coverage analysis in the macro-tier

4.6.2 Coverage comparison with other systems

In Figure 4.6, we compare the SINR coverage probability of our model in the center and edge macro-tier. We can see that the proposed framework offers a consistent increase of coverage probability of 20% for an SINR threshold greater than -5 dB compared to microwaves system and up to 60% of increase when compared to the mmWave system with no frequency reuse. In the edge zone, our model offers a consistent increase of coverage probability of about 30% compared to a mmWave system with no frequency reuse and an increase of 10% compared to microwave system. Although the propagation conditions are not as accurate as the system-simulation evaluation, the coverage analysis shows that increasing the path loss helps reach a

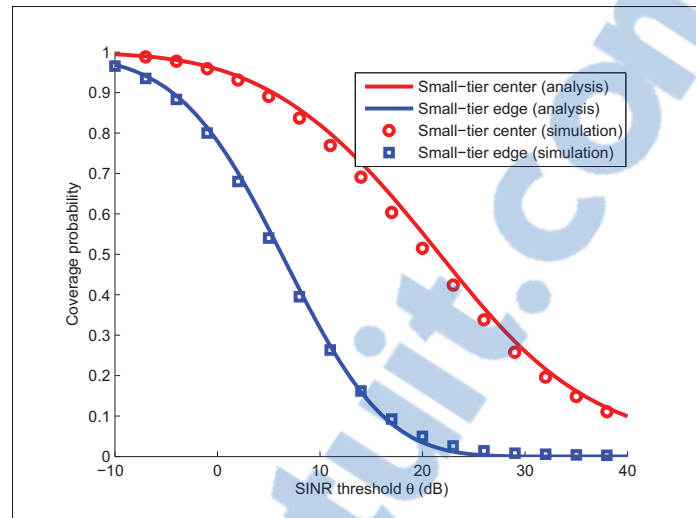


Figure 4.4 Validation of the proposed analytical model: Analytical coverage probability versus simulated coverage analysis in the small-tier

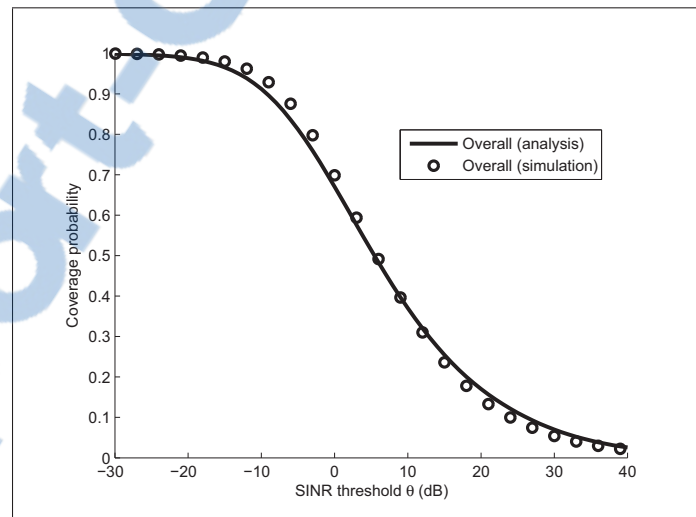


Figure 4.5 Validation of the proposed analytical model: Analytical coverage probability versus simulated coverage analysis for users from both tiers

better coverage probability in mmWave systems only when a proper frequency reuse is applied. Indeed, the performance of the microwave system outperforms the mmWave when all the bands

are available for every user no matter its location or its base station association (i.e., SBS or MBS). Thus, it is essential to allocate the frequencies the most sensitive to the path loss attenuation to small-cells, while the lower bands of the mmWave frequencies are dedicated to outdoor communications. In a system with no-interference, increasing the PLE decreases the received power, thus reduces the SNR. However, in the current setting where signals are also impaired by interference from a dense deployment of BSs, increasing the PLE decreases both the received power and the interference, resulting in an upwards shift in the optimum coverage probability curves.

In Figure 4.7, a similar comparison is performed for users located in the coverage area of a small-cell and connected to a SBS. In the edge and center zones the proposed model outperforms both the microwaves and mmWave with no reuse frameworks.

Figure 4.8 depicts the overall coverage probability and we observe an increase of 18% at an SINR threshold of 5 dB when the proposed fractional reuse is applied compared to the two other models of comparison.

4.6.3 Results on user throughput analysis

We present in Figure 4.9 the CCDF of a typical user for different small-cells densities. We notice that increasing the density of small-cells increases the overall throughput. However the gain of base station densification is high up to 200 BSs, specially for high throughput values. We can understand from this result that deploying more than 200 BSs per macrocell may be of a limited interest for the system throughput enhancement. This can be easily explained by the results in Figure 4.10. This figure depicts the CCDF of a small-cell user for different small-cells densities. We notice that increasing the density of small-cells decreases the throughput. This is due to the interferences inducted by neighbouring small-cells, since increasing the density of SBSs per area increase the number of interfering cells.

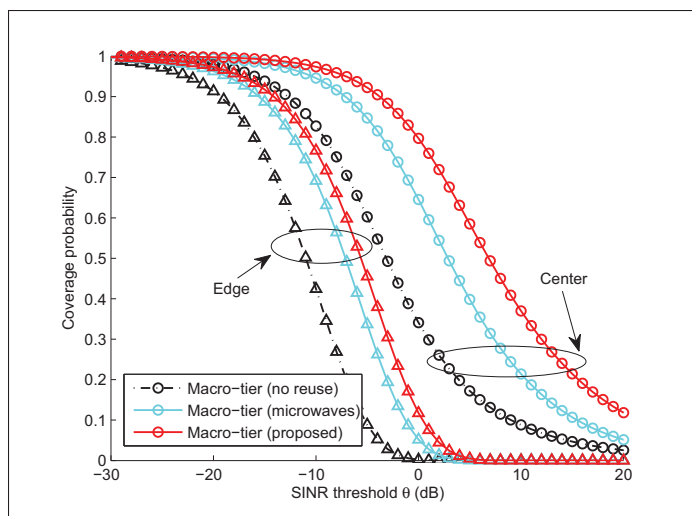


Figure 4.6 Coverage probability for macro-tier (center and edge) under the proposed model compared to no frequency reuse and microwaves systems $\lambda_2 = 100 * \lambda_1$ SBSs deployed

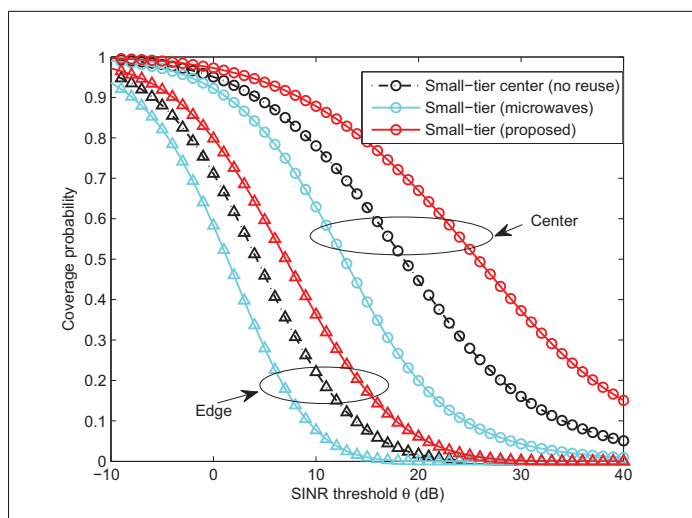


Figure 4.7 Coverage probability for smallcell-tier under the proposed model compared to no frequency reuse and microwaves systems $\lambda_2 = 100 * \lambda_1$ SBSs deployed



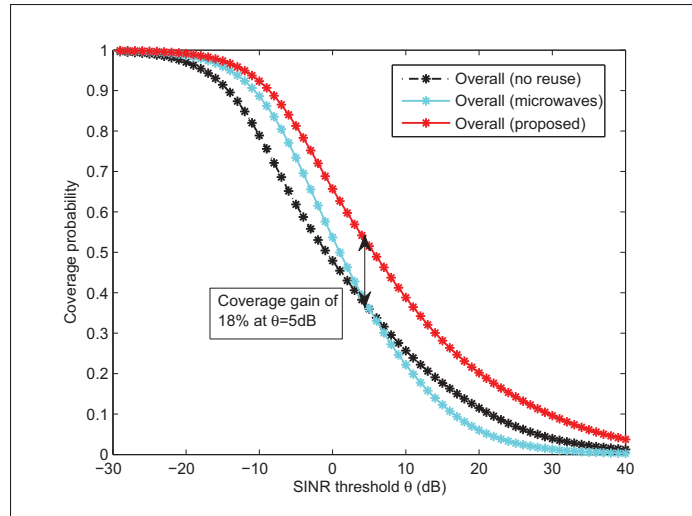


Figure 4.8 Overall coverage probability under the proposed model compared to no frequency reuse and microwaves systems.
 $\lambda_2 = 100 * \lambda_1$ SBSs deployed

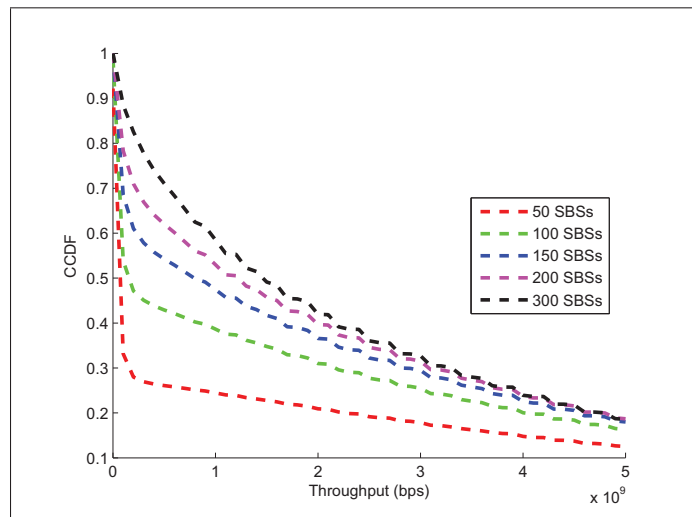


Figure 4.9 Overall user throughput distribution (CCDF curves) for different small-cells densities

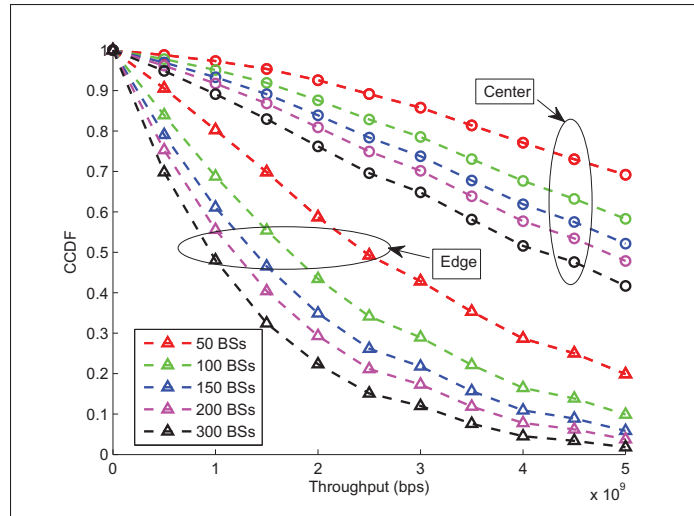


Figure 4.10 Small-cell user throughput distribution (CCDF curves) for different small-cells densities

4.6.4 Simulation results on throughput using the accurate path loss models

We consider an OFDMA hexagonal macrocell overlaid by a 100 or more SBSs. The simulation parameters are depicted in Table 4.2. The algorithm 4.1 is performed for BS association and resource allocation and the achieved data rate in equation 4.17 is computed. We assume that the available subchannels in each cell and zone are equally split among the active users of each corresponding area.

Figure 4.11 shows the throughput CDF of users from both tiers and compare the performances for multiple SBS densities. With 200 SBSs deployed per macrocell, 50% of the users reach a throughput of 500 Mbps when approximately 30% of the users reach a throughput greater than 1 Gbps. The 5% tile throughput is about 100 Mbps. When we densify more the network in terms of SBS we can reach up to 40% of probability that a user has a throughput greater than 1 Gbps and a 5% tile throughput of 200 Mbps. When compared to a traditional LTE system in Figure 4.12, we observe significant gains with the proposed model. Indeed, our model shows a gain of 50 times the throughput with a single antenna LTE system and 16 times with a 4×4 MIMO is LTE system.

An other interesting observation is that increasing the number of SBSs up to 500 SBSs per MBS increases significantly the throughput, however the gain in term of throughput when more bases stations are added slightly decreases after 300 BSs. If we compare this result with a traditional LTE system in Figure 4.12, we notice that increasing the number of SBSs does not necessarily increase the throughput as we reach a convergence after 300 SBSs deployed. This is explained by the different propagation nature of the two bands: in mmWave bands, the high pathloss helps decrease the downlink interference among neighbouring small cells while in the microwave increasing the number of SBSs severely harms the performance of small-cell tier users due to the high interferences induced. Although most of the gains might be seen as simply the result of the increase of bandwidth (1GHz for the mmWave and 20MHz+20MHz in LTE), we have considered a basic mmWave system in this work to show the great potential of the mmWave systems. Indeed, no spatial multiplexing nor MIMO or any advanced techniques have been considered here; hence we expect much higher gains when these techniques will be applied to the proposed mmWave system. Moreover, the coverage analysis performed in the previous section confirms that not only the increase of available bandwidth impacts positively the performances of the system but that also the SINR coverage is enhanced in the proposed framework.

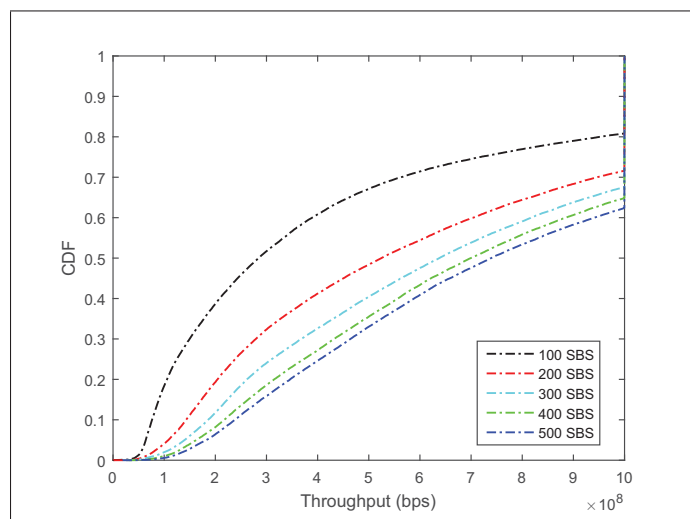


Figure 4.11 CDF of the achieved throughput for different small cells densities

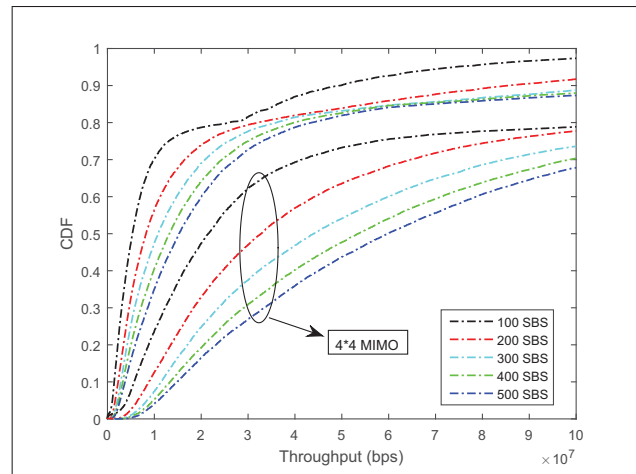


Figure 4.12 CDF of the achieved throughput for an LTE system (no mimo and mimo 4*4) for purpose of comparison with the performances of the proposed model Fig.9

Figure 4.13 depicts the medium throughput versus the inner/outer small-cell radius for different SBSs densities. We can see that the median throughput is maximized for a certain inner radius value according to the density of small-cells. We notice that this optimal radius value decreases with the density of SBSs. This can be explained by the fact that more the density of small-cells is high more the probability of a user being located in the inner zone is high as the SUEs connect to the closest SBS. However, when the number of users in the inner zone increases, the median throughput decreases since they share the same resources dedicated to this specific region. In this case, decreasing the radius of the inner zone allow more user to be located in the edge zone of the small-cells, hence obtaining a better load balancing among the inner and outer region of each small-cell. For a density of 150 small-cells, the optimal value of the inner radius should be about 30% the radius of the outer small-cell region.

The same evaluation is performed for the macro-tier in Figure 4.14. The density of small-cells only affects the median throughput of the system but the optimal value of the inner radius that maximizes the median throughput is constant and equal to 65% of the value of the outer region radius.

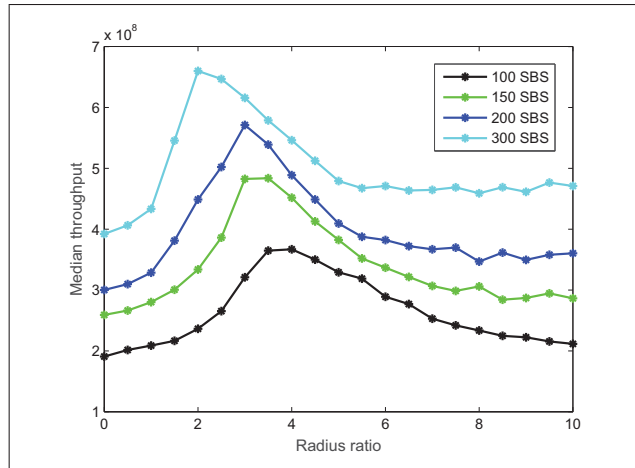


Figure 4.13 Median throughput achieved vs radius ratio (inner/outer) of small-cells

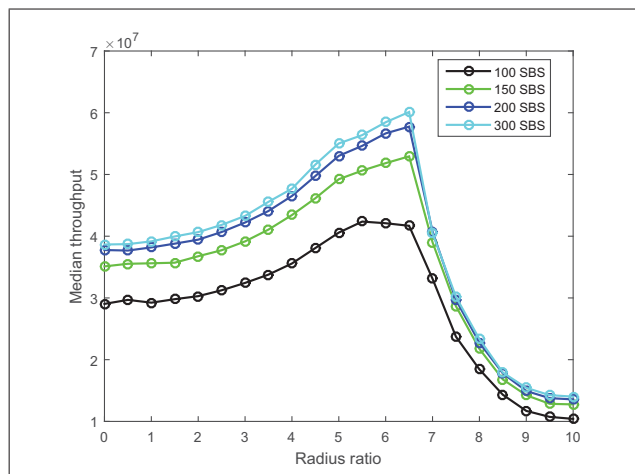


Figure 4.14 Median throughput achieved vs radius ratio(inner/outer) of macrocells

4.7 Conclusion

We demonstrate in this work that an adequate frequency allocation and reuse in 5G mmWave networks with the help of a dense small-cells deployment allows to reach very high throughputs and SINR coverage in ultra-dense systems. The proposed allocation results from natural properties of mmWave bandwidth allowing frequency reuse in small cells. The cross-tier interferences are suppressed under this framework and co-tier interferences strongly mitigated

thanks to the propagation properties of high mmWave frequencies. Moreover the large bandwidth available for E-bands and allocated to small-cells in our model allows very high data rates, hence strongly enhancing the overall capacity of a cell in ultra-dense networks. Finally, lower mmWave frequencies show very good performance for outdoor communication with the help of directional, high gain antennas that can be used at both the mobile device and base station to compensate the high pathloss. Hence, the combination of dense small-cells deployment and spatial frequency reuse in mmWave systems shows a great potential for the achievement of the 1 Gbps target in the next generation of mobile networks.

CHAPTER 5

DISCUSSION AND RECOMMENDATIONS

5.1 Discussion on future challenges for resource management in 5G networks

Evolving fifth generation cellular wireless networks are envisioned to overcome the fundamental challenges of existing cellular networks. Among these challenges, the most pressing are obtaining higher data rates, end-to-end performance, ubiquitous user-coverage, lower latency and energy consumption. To address these challenges, 5G systems will adopt a multi-tier architecture consisting of macrocells overlaid by different types of licensed cells. We have mainly investigated the small-cells case in this thesis, but several types of RATs are likely to co-exist in 5G networks, such as relays, device-to-device networks and backhaul connections, to serve an unprecedented number of smart and heterogeneous wireless devices with different QoS requirements in a spectrum and energy-efficient manner. This architectural shift along with advanced physical communications technology such as MIMO, full-duplex, beamforming and mmWave communications will strongly contribute in attaining key attributes of 5G.

Radio resource and interference management will be a key research challenge in heterogeneous 5G wireless networks. The traditional methods for radio resource and interference management may not be adequate for multi-tiers networks and new approaches are required to deal with these urging network aspects.

We have thoroughly investigated in this thesis the challenges of the radio resource management in the next generations of systems and proposed new solutions to address them. These challenges may be summarized in the 5 followings points:

- Efficient and fair resource allocation among nodes in the context of heterogeneity and dense deployment of wireless devices;
- Low complexity solutions for resource allocation among small-cells;

- Load balancing between macrocell and small-cells due to coverage and traffic load imbalance as a result of varying transmit powers of different BSs;
- Admission control and handover in ultra-dense small-cells networks and management of the different priorities in accessing channels of different frequencies;
- Interference management solutions taking into account the different types of BSs access: public or private access restrictions in different tiers lead to diverse interference levels.

The heterogeneity and dense deployment of small-cells strongly affects interference management in both the uplink and downlink transmissions. The varying transmission power of different types of BSs lead to strong interferences and to some extent network deadzones. The problem is compounded by the fact that different types of access co-exist, private access restrictions leading to high interferences and public access to unbalanced traffic loads.

The emergence of new solutions such as carrier aggregation and coordinated multi-point transmission (CoMP), allow simultaneous connections to multiple BSs and aggregation of subcarriers from the different spectrum bands, may further complicate the interference and resource management problems in 5G networks. The decoupling of downlink and uplink has also attracted increasing attention in the latest wireless communications system standards.

Coordination and cooperation among base stations and users from different tiers will be a key requirement to mitigate interferences in ultra-dense 5G networks. Several types of cooperation are emerging. For instance, in LTE release 12, the dual connectivity for simultaneous connectivity to the macrocell and smallcell has been introduced. However, these cooperation schemes will require reliable, fast and low latency backhaul connections, which is a major technical challenge for multi-tier 5G networks.

While device energy consumption has always brought a lot of interest in academic and industrial research, energy efficiency on the network is essential to ensure the viability of the network.

As we have investigated in the previous chapter, the need for more bandwidth will lead to the coexistence of spectrum bands from different frequencies (2GHz up to 83GHz), with drastically different propagation characteristics within the same network. The concept of *phantom cell* (Ishii *et al.*, 2012) is rising, where the data and control plane are not operated by the same node; the control data (C-plane) being sent by MBSs with a high power of transmission, while the essential data (U-plane) is transmitted by low power BSs in mmWave frequencies.

The cloud computing-based architecture referred to as Centralized-RAN (C-RAN) for radio access networks which supports 2G, 3G, 4G and future wireless communication standards has recently brought a lot of interest from academia and the telecommunications industry. The main idea behind C-RAN is to separate the base station into a radio unit and a signal processing unit. Moreover, the Base-Band Units (BBUs) from multiple base stations are gathered into a centralized BBU pool. The radio unit is called a Remote Radio Head (RRH). A centralized BBU pool enables an efficient utilization of hardware resources and reduces the cost of base station deployment and operation. The advanced features of LTE-A and 5G, such as CoMP described above and cooperative techniques for interference mitigation, can be efficiently supported by C-RAN, which is essential especially for ultra-dense small-cells deployment.

Furthermore, Heterogeneous-CRAN (H-CRAN) has been introduced recently to bring forth the advantage of ensuring SONs by incorporating the cloud computing into HetNets (Peng *et al.*, 2014). Different from C-RAN, the BBU pool in H-CRANs is interfaced to MBSs for mitigating the cross-tier interferences between RRHs (SBSs) and MBSs through the centralized cloud computing based cooperative processing techniques. The control signalling and system broadcasting information are delivered by MBSs to UEs, which simplifies the capacity and latency constraints in the fronthaul links between RRHs and the BBUs pool, and make RRHs active or sleep efficiently to save the energy consumption.

The base-station-centric architecture that we traditionally know may change in 5G. The new trends described above, such as the downlink-uplink decoupling, the control and data planes

separation and the C-RAN, lead to the concept of device-centric architecture characterizing the new architectural shift expected in 5G networks.

All these new factors, trends and network shifts may be translated into key objectives for interference mitigation and resource management in the next generation of systems. Designing optimized cell association and power control techniques, proposing efficient methods to support simultaneous association to multiple BSs and developing new practices for cooperation and coordination among multiple tiers, are the most critical objectives of research in this area.

5.2 Recommendations and potential approaches for further research

Although this research has already been discussed in detail in the previous chapters, the aim of this section is to review its main highlights and possible extensions. In the second chapter, we proposed a CAC to address the problem of deadzones due to strong cross-tier interferences suffered by edge users in two-tier networks. In further research, the co-existence of both private and public access modes could be considered and see how it affects the performances of the system in terms of call blocking probabilities. Differentiation among new calls and handoff calls for the access to the network resources can also be investigated and a higher level of priority applied to handovered on-going calls. The proposed fractional reuse scheme could be coupled with cooperative solutions to mitigate the co-tier interferences among the BSs from the same tier. Finally, the optimal network parameters such as density of small-cells, transmit power, under such frequency partitioning could be investigated.

In the third chapter, we proposed a game theoretic approach to cope up with co-tier and cross-tier interferences and to propose a more fair and robust resource allocation scheme among interfering entities forming a cluster. In future works, different levels of access priorities could be investigated by applying bias into the proposed game to cope up with these various requirements. In the research we have carried out, we have assumed that the BSs transmit at an equal power in all subchannels, and proposed a game that defines the number of RBs each player of the grand coalition should receive. In a future work, we may consider different levels of

transmission power to permit to reuse some subchannels in the same interfering set when the induced interference is acceptable. We have also expressed random demand of users, we could extend this study for real-life demands expressed by users according their location and the QoS requirement of the applications they are using (voice call, video game, virtual reality etc.).

Simultaneous connections to multiple BSs and different BS association for uplink and down-link transmissions would increase the degrees of freedom which can be exploited to further improve the network capacity and balance the load among different BSs in different tiers. The CoMP concept introduced in the previous section could be used in the proposed cooperative approach. Hence, the formed coalition will not only permit to find a common agreement for the resource sharing but also allow double association to boost the capacity of the system in constrained situations.

The proposed games can be easily applied to resource allocation in C-RAN with fronthaul capacity constraints which is an open research issue. The fronthaul in such networks, defined as the transmission link between the BBU and the RRH, requires a high capacity, but is often constrained. With the clustering of RRHs to access the common BBU resources, the proposed game may tackle the problem of resource allocation with the fronthaul constraint in a cooperative way.

In chapter IV, we have investigated the use of the standardized mmWave frequencies for cellular systems. There are many open questions and key extensions remaining in this topic of research. For instance, in our proposed model, mobile users connected to MBSs are considered in outdoor street level locations. Unfortunately, the crucial topic of outdoor-to-indoor coverage is essentially neglected in most of the work to date. When the mobile user is located indoor and have not been able to connect to an indoor SBS, user may be served either via multihop relaying or fallback to conventional microwave cells. Therefore, further study will be needed to quantify the performances of these systems.

The research topic on cell association with the co-existence of mmWave and sub-6GHz BSs is crucial. Given the possible lower-SINR at mmWave BSs than sub-6GHz BSs, bias-based cell

range expansion can be used to increase RSRP from mmWave BSs and allow more users to connect to the small-cells tier where huge bandwidth is available for short ranged communications, hence offering very high data rates to connecting users. Carrier aggregation may be investigated when coupled with dual connectivity with microwave BSs, to help reach the requirement of users if the transmissions on mmWave frequencies fail to offer the level of SINR and data rates necessary to satisfy user's demand.

Moreover, the two most important physical challenges in mmWave – susceptibility to blocking and the need for strong directionality – are not yet well investigated and analysis for mmWave systems accounting for these factors are needed to design the next generation of cellular networks. In short, we expect this new paradigm of mmWave cellular systems to challenge wireless engineers for some time. We expect that the model developed in chapter IV will continue to be improved and extended with the growing understanding of physical characteristics of mmWave communications.

Finally, quantifying and optimizing the densification gains in a wide variety of deployment scenarios and network models is a key area for continued small-cell research.

GENERAL CONCLUSION

We have investigated in this thesis, one of the most challenging technical issues in the deployment of dense small-cells overlaying the existing traditional macro-tier: radio interference and resource management. We have thoroughly presented in the first chapter small-cells technology, its features and success factors as well as its role in 5G systems. We have also presented the benefits of ultra-densification of small-cells and identified the key challenges that have to be addressed in order to fully exploit the advantages of these deployments.

We have presented in the second chapter the model we have developed for centralized, fractional-frequency based spectrum partitioning. This scheme permits to strongly mitigate the downlink interferences in the boundaries of macrocells, hence aiming to solve the problem of deadzones caused by the dense deployment of small-cells in the edge zones. An analytical model based on a Markov chains decision process has been used to evaluate the performances of the scheme in terms of blocking probabilities.

Although this scheme provides a significant improvement in terms of cross-tier interference mitigation and admitted calls, the problem of co-tier interferences becomes crucial under an ultra-dense deployment of small-cells and a cooperative approach becomes essential to enhance the overall capacity of the system.

Consequently, we have developed two game theoretic approaches for cooperative and distributed resource allocation in two-tier self-organized networks. The proposed model permits to jointly deal with the co-tier and cross-tier interference among the BSs forming clusters and able to find a common agreement on the available resource sharing that maximizes the throughput and fairness of the system while keeping the complexity of the framework low.

Driven by the recent mmWave standardizations, measurement campaigns and coverage analysis studies showing that roughly three times more small-cells are required to accommodate 5G

networks compared to existing 4G systems, we investigated the operation of two-tier cellular systems in these newly opened frequencies. We have shown that the proposed model permits to strongly mitigate the interferences and the large bandwidth available under the proposed model allow very high data rates, up to several tens of Gbps. We have shown that low mmWave frequencies are suitable for outdoor communication with the help of directional high gain antennas that can be used at both the mobile device and base station to compensate the high pathloss. We quantified and optimized the densification gains in a proposed deployment scenario for two-tier networks, exploiting the advantages and limits of the wide range of available mmWave frequency bands.

And finally, in the last chapter we have discussed the future challenges facing the problem of interference and resource management in the future generations of systems, and the technological opportunities and new trends that lead to further complicated schemes. Lastly, we have presented some of the future studies that might be conducted to complete or further investigate the solutions proposed in this thesis.

APPENDIX I

APPENDIX OF CHAPTER 3

1. Proof of the joint-monotonicity of the weighted Owen value

In order to prove that the coalitional weighted Owen value \bar{U} is joint-monotonic in convex games, (Vidal-Puga, 2005) has proved that:

$$\sum_{i \in P_u \cup P_v} \bar{U}_i^N(P) \leq \sum_{i \in P_u \cup P_v} \bar{U}_i^N(P^{u+v}) \quad (\text{A I-1})$$

The proof of this proposition is presented in this annex. We proceed by induction on m , the size of P . For $m = 2$, the result is straightforward. We assume the result is true for coalition structures of size $m - 1$. Let $P_q, P_r \in P$.

We assume without loss of generality that $q = m - 1$ and $r = m$. Let $P^* = \{P_1^*, P_2^*, \dots, P_{m-1}^*\}$ where $P_p^* = P_p$ for all $p < m - 1$ and $P_{m-1}^* = P_{m-1} \cup P_m$. Let $M^* = \{1, 2, \dots, m - 1\}$, and let $w \in \mathbb{R}^M$, $w^* \in \mathbb{R}^{N^*}$ be defined as $w_p = w_p^* = \frac{|P_u|}{|N|}$ for all $u < m - 1$, $w_{m-1} = \frac{|P_{m-1}|}{|N|}$, $w_m = \frac{|P_m|}{|N|}$ and $w - m - 1^* = w_{m-1} + w_m$.

It follows from the definition of the weighted Owen value that each coalition gets its weighted Shapley value of the game between coalitions with weights given by their size. Therefore, for any $\forall P_u \in P$, $\sum_{i \in P_u} \bar{U}_i^N = Sh_i^{wM}(v/P)$. Hence, we obtain:

$$Sh_{m-1}^{wM}(v/P) + Sh_m^{wM}(v/P) \leq Sh_{m-1}^{w^*M^*}(v/P^*) \quad (\text{A I-2})$$

For simplicity, we denote $q = v/P$ and $r^* = v/C^*$. Castrillo & Wettstein (2001) proved that $Sh_q^{wM}(v) = w_q v(M) - w_q v(M \setminus q) + \sum_{p \in M \setminus q} w_p Sh_q^{wM \setminus p}(v)$. Hence,

$$\begin{aligned}
Sh_{m-1}^{wM}(u) + Sh_m^{wM}(v) &= w_{m-1}u(M) - w_{m-1}u(M \setminus (m-1)) + \sum_{p \in M \setminus (m-1)} w_p Sh_{m-1}^{wM \setminus p}(u) + w_m u(M) - \\
&w_m u(M \setminus m) + \sum_{p \in M \setminus m} w_p Sh_m^{wM \setminus p}(u) \\
&= w_{m-1}u(M) - w_{m-1}u(M \setminus m) + w_m u(M) - w_m u(M \setminus m) \\
&+ w_m Sh_{m-1}^{wM \setminus m}(u) + w_{m-1} Sh_m^{wM \setminus (m-1)}(u) \\
&+ \sum_{p < m-1} w_p \left(Sh_{m-1}^{wM \setminus p}(u) + Sh_m^{wM \setminus p}(u) \right)
\end{aligned} \tag{A I-3}$$

and

$$\begin{aligned}
Sh_{m-1}^{w^*M^*}(u^*) &= w_{m-1}^* u^*(M^*) - w_{m-1}^* u^*(M^* \setminus (m-1)) \\
&+ \sum_{p < m-1} w_p^* Sh_{m-1}^{w^*M^* \setminus p}(u^*) \\
&= (w_{m-1} + w_m) u(M) - (w_{m-1} + w_m) \times u(M \setminus \{m-1, m\}) \\
&+ \sum_{p < m-1} w_p^* Sh_{m-1}^{w^*M^* \setminus p}(u^*)
\end{aligned} \tag{A I-4}$$

Under the induction hypothesis, $Sh_{m-1}^{wM \setminus p}(u) + Sh_m^{wM \setminus p}(u) \leq Sh_{m-1}^{w^*M^* \setminus p}(u^*)$ for all $p < m-1$.

Hence, it is enough to prove,

$$\begin{aligned}
&w_{m-1}u(M) - w_{m-1}u(M \setminus (m-1)) + w_m u(M) - w_m u(M \setminus m) + w_m Sh_{m-1}^{mM \setminus m}(u) + w_{m-1} Sh_m^{wM \setminus (m-1)}(u) \\
&\leq (w_{m-1} + w_m) u(M) - (w_{m-1} + w_m) u(M \setminus \{m-1, m\})
\end{aligned} \tag{A I-5}$$

Simplifying and rearranging terms,

$$\begin{aligned}
 & w_{m-1} \left[u(M \setminus (m-1)) - u(M \setminus \{m-1, m\}) - Sh_m^{wM \setminus (m-1)}(u) \right] \\
 & + w_m \left[u(M \setminus (m)) - u(M \setminus \{m-1, m\}) - Sh_m^{wM \setminus (m)}(u) \right] > 0
 \end{aligned} \tag{A I-6}$$

Hence, both terms must be non-negative. The first is analogous. To prove that the second term is non-negative, we need to prove that $Sh_m^{wM \setminus (m)}(u) \leq u(M \setminus (m)) - u(M \setminus \{m-1, m\})$ we know from Kalai & Samet (1987), that the weighted Shapley value is a weighted average of marginal contributions. Since the game under study (\mathcal{N}, v) is convex, the TU game $(M \setminus m, u)$ is convex too. This implies that the maximal marginal contribution of $m-1$ in $(M \setminus m, u)$ is $u(M \setminus (m)) - u(M \setminus \{m-1, m\})$. This concludes the proof.

APPENDIX II

APPENDIX OF CHAPTER 4

1. Comparison of Nakagami and Rayleigh fading models in mmWave bands

In the recent research studies conducted by Gupta *et al.* (2016), it has been shown that considering a general fading model such Nakagami to evaluate the channel fading in mmWave systems, does not provide any additional design insights, while significantly complicating the analysis of such models. The two essential results obtained in the paper are presented in this annex to justify the assumption of Rayleigh fading used in Chapter 4. Figure II-1 depicts the rate coverage in a two-tier network mmWave system with Rayleigh fading while Figure II-2, depicts the rate coverage of the same system with Nakagami fading. When this two results are compared, the insights are similar which justifies the Rayleigh fading assumption for analysis.

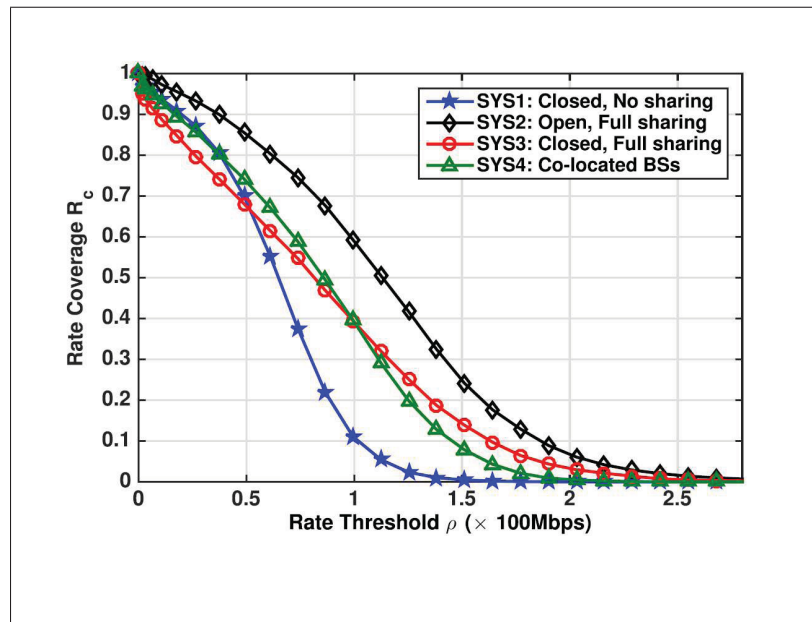


Figure-A II-1 Rate coverage in a two-network mmWave system with Rayleigh fading for different cases analysed

Taken from Gupta *et al.* (2016)



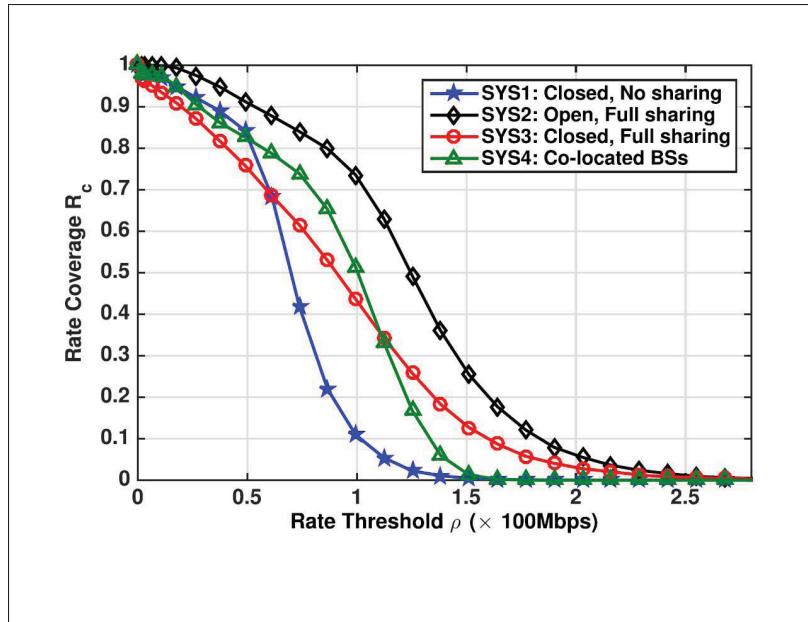


Figure-A II-2 Rate coverage in a two-network mmWave system with Nakagami fading (with parameter 10) and BS antenna half beamwidth for different cases. When compared to Rayleigh fading (Fig. II-1), the insights are similar which justifies the Rayleigh fading assumption for our analysis
Taken from Gupta *et al.* (2016)

BIBLIOGRAPHY

- AboulHassan, M. A., Yassin, M., Lahoud, S., Ibrahim, M., Mezher, D., Cousin, B. & Sourour, E. A. (2015, July). Classification and comparative analysis of inter-cell interference coordination techniques in lte networks. *2015 7th international conference on new technologies, mobility and security (ntms)*, pp. 1-6. doi: 10.1109/NTMS.2015.7266476.
- Akdeniz, M. R. & al. (2014). Millimeter wave channel modeling and cellular capacity evaluation. *IEEE journal on selected areas in commun.*, 32(6), 1164-1179. doi: 10.1109/JSAC.2014.2328154.
- Akdeniz, M. R., Liu, Y., Rangan, S. & Erkip, E. (2013, Dec). Millimeter wave picocellular system evaluation for urban deployments. *2013 IEEE globecom workshops*, pp. 105-110. doi: 10.1109/GLOCOMW.2013.6824970.
- Akkarajitsakul, K., Hossain, E., Niyato, D. & Kim, D. I. (2011). Game theoretic approaches for multiple access in wireless networks: A survey. *IEEE communications surveys tutorials*, 13(3), 372-395. doi: 10.1109/SURV.2011.122310.000119.
- Alpcan, T. & Basar, T. (2005a). A globally stable adaptive congestion control scheme for internet-style networks with delay. *Networking, IEEE/acm transactions on*, 13(6), 1261-1274. doi: 10.1109/TNET.2005.860099.
- Alpcan, T. & Basar, T. (2005b). A globally stable adaptive congestion control scheme for internet-style networks with delay. *IEEE/acm trans. netw.*, 13(6), 1261-1274. doi: 10.1109/TNET.2005.860099.
- Alpcan, T., Başar, T., Srikant, R. & Altman, E. (2002a). Cdma uplink power control as a noncooperative game. *Wirel. netw.*, 8(6), 659-670. doi: 10.1023/A:1020375225649.
- Alpcan, T., Başar, T., Srikant, R. & Altman, E. (2002b). Cdma uplink power control as a noncooperative game. *Wirel. netw.*, 8(6), 659-670. doi: 10.1023/A:1020375225649.
- Americas, G. (2013). *Meeting the 1000x challenge: The need for spectrum, technology and policy innovation*. Consulted at http://www.4gamericas.org/documents/2013_4G%20Americas%20Meeting%20the%201000x%20Challenge%2010%204%2013_FINAL.pdf.
- Andrews, J. G. (2013). Seven ways that hetnets are a cellular paradigm shift. *IEEE communications magazine*, 51(3), 136-144. doi: 10.1109/MCOM.2013.6476878.
- Andrews, J. G., Buzzi, S., Choi, W., Hanly, S. V., Lozano, A., Soong, A. C. K. & Zhang, J. C. (2014). What will 5g be? *IEEE journal on selected areas in communications*, 32(6), 1065-1082. doi: 10.1109/JSAC.2014.2328098.

- Anpalagan, A., Bennis, M. & Vannithamby, R. (Eds.). (2015). *Design and deployment of small cell networks*. Cambridge: Cambridge University Press. doi: 10.1017/CBO9781107297333.
- Assaad, M. (2008, Sept). Optimal fractional frequency reuse (ffr) in multicellular ofdma system. *Vehicular technology conference, 2008. vtc 2008-fall. IEEE 68th*, pp. 1-5. doi: 10.1109/VETECONF.2008.381.
- Aumann, R. J. & Dreze, J. H. Cooperative games with coalition structures. *International journal of game theory*, 3(4), 217–237. doi: 10.1007/BF01766876.
- Aumann, R. & Dreze, J. (1974). Cooperative games with coalition structures. *International journal of game theory*, 3(4), 217-237. doi: 10.1007/BF01766876.
- Azar, Y., Wong, G. N., Wang, K., Mayzus, R., Schulz, J. K., Zhao, H., Gutierrez, F., Hwang, D. & Rappaport, T. S. (2013a, June). 28 ghz propagation measurements for outdoor cellular communications using steerable beam antennas in new york city. *2013 IEEE international conference on communications (icc)*, pp. 5143-5147. doi: 10.1109/ICC.2013.6655399.
- Azar, Y., Wong, G. N., Wang, K., Mayzus, R., Schulz, J. K., Zhao, H., Gutierrez, F., Hwang, D. & Rappaport, T. S. (2013b, June). 28 ghz propagation measurements for outdoor cellular communications using steerable beam antennas in new york city. *2013 IEEE international conference on communications (icc)*, pp. 5143-5147. doi: 10.1109/ICC.2013.6655399.
- Başar, T. & Olsder, G. (1998). *Dynamic noncooperative game theory, 2nd edition*. Society for Industrial and Applied Mathematics. doi: 10.1137/1.9781611971132.
- Bai, T., Alkhateeb, A. & Heath, R. W. (2014). Coverage and capacity of millimeter-wave cellular networks. *IEEE commun. mag.*, 52(9), 70-77. doi: 10.1109/MCOM.2014.6894455.
- Baldemair, R. & al. (2015). Ultra-dense networks in millimeter-wave frequencies. *IEEE commun. mag.*, 53(1), 202-208. doi: 10.1109/MCOM.2015.7010535.
- Barbarossa, S., Sardellitti, S., Carfagna, A. & Vecchiarelli, P. (2010, June). Decentralized interference management in femtocells: A game-theoretic approach. *Cognitive radio oriented wireless networks communications (crowncom), 2010 proceedings of the fifth international conference on*, pp. 1-5.
- Bonald, T., Borst, S., Hegde, N., Jonckheere, M. & Proutiere, A. (2009). Flow-level performance and capacity of wireless networks with user mobility. *Queueing systems*, 63(1), 131. doi: 10.1007/s11134-009-9144-7.
- Borst, S., Proutiere, A. & Hegde, N. (2006, April). Capacity of wireless data networks with intra- and inter-cell mobility. *Proceedings IEEE infocom 2006. 25th IEEE international conference on computer communications*, pp. 1-12. doi: 10.1109/INFOCOM.2006.175.

- c. Hong, W. & Tsai, Z. (2010, May). On the femtocell-based mvno model: A game theoretic approach for optimal power setting. *2010 IEEE 71st vehicular technology conference*, pp. 1-5. doi: 10.1109/VETECS.2010.5493800.
- CALVO, E. & GUTIRREZ, E. (2013). The shapley-solidarity value for games with a coalition structure. *International game theory review*, 15(01), 1350002. doi: 10.1142/S0219198913500023.
- Castrillo, D. & Wettstein, D. (2001). Bidding for the surplus : A non-cooperative approach to the shapley value. *Journal of economic theory*, 100(2), 274 - 294. doi: <http://dx.doi.org/10.1006/jeth.2000.2704>.
- Chandrasekhar, V. & Andrews, J. G. (2009). Spectrum allocation in tiered cellular networks. *IEEE transactions on communications*, 57(10), 3059-3068. doi: 10.1109/T-COMM.2009.10.080529.
- Chandrasekhar, V., Andrews, J., Muharemovict, T., Shen, Z. & Gatherer, A. (2009). Power control in two-tier femtocell networks. *Wireless communications, IEEE transactions on*, 8(8), 4316-4328. doi: 10.1109/TWC.2009.081386.
- Chen, Y., Zhang, J. & Zhang, Q. (2012). Utility-aware refunding framework for hybrid access femtocell network. *Wireless communications, IEEE transactions on*, 11(5), 1688-1697. doi: 10.1109/TWC.2012.031212.110002.
- Chen, Y., Teo, K. H., Kishore, S. & Zhang, J. (2008). Inter-cell interference management in wimax downlinks by a stackelberg game between bss. *Communications, 2008. icc '08. IEEE international conference on*, pp. 3442-3446. doi: 10.1109/ICC.2008.647.
- Cisco. (2015). Cisco visual networking index:forecast and methodology, 2014-2019. *Technical report, cisco systems inc., san jose ca, white paper*.
- Cisco. (2016). *Cisco visual networking index: Global mobile data traffic forecast update, 2015–2020 white paper*.
- Cisco. (Feb. 2014). Cisco visual networking index: Global mobile data traffic forecast update, 2013-2018. *Technical report, cisco systems inc., san jose ca, white paper*.
- Clerckx, B., Kim, Y., Lee, H., Cho, J. & Lee, J. (2011). Coordinated multi-point transmission in heterogeneous networks: A distributed antenna system approach. 1-4. doi: 10.1109/MWSCAS.2011.6026627.
- Curiel, I. J., Maschler, M. & Tijs, S. H. Bankruptcy games. *Zeitschrift für operations research*, 31(5), A143–A159. doi: 10.1007/BF02109593.
- de la Roche, G., Valcarce, A., Lopez-Perez, D. & Zhang, J. (2010). Access control mechanisms for femtocells. *Communications magazine, IEEE*, 48(1), 33-39. doi: 10.1109/M-COM.2010.5394027.

- Deng, X. & Papadimitriou, C. H. (1994). On the complexity of cooperative solution concepts. *Mathematics of operations research*, 19(2), 257-266. doi: 10.1287/moor.19.2.257.
- Dietrich Stoyan, Wilfrid Kendall, J. M. S. N. C. (1987). Stochastic geometry and its application. mathematische monographien. *Crystal research and technology*, 22(12), 1510–1510. doi: 10.1002/crat.2170221215.
- ElSawy, H., Hossain, E. & Kim, D. I. (2013). Hetnets with cognitive small cells: user offloading and distributed channel access techniques. *Communications magazine, IEEE*, 51(6), 28-36. doi: 10.1109/MCOM.2013.6525592.
- Estrada, R., Jarray, A., Otrok, H., Dziong, Z. & Barada, H. (2013). Energy-efficient resource-allocation model for ofdma macrocell/femtocell networks. *Vehicular technology, IEEE transactions on*, 62(7), 3429-3437. doi: 10.1109/TVT.2013.2253693.
- Fang, Y. & Zhang, Y. (2002). Call admission control schemes and performance analysis in wireless mobile networks. *Vehicular technology, IEEE transactions on*, 51(2), 371-382. doi: 10.1109/25.994812.
- Farbod, A. & Liang, B. (2007). Efficient structured policies for admission control in heterogeneous wireless networks. *Mob. netw. appl.*, 12(5), 309–323. doi: 10.1007/s11036-008-0045-5.
- Ghosh, A. & Tal. (2014). Millimeter-wave enhanced local area systems: A high-data-rate approach for future wireless networks. *IEEE journal on selected areas in commun.*, 32(6), 1152-1163. doi: 10.1109/JSAC.2014.2328111.
- Ghosh, A., Zhang, J., Andrews, J. & Muhamed, R. (2010). *Fundamentals of lte*. Pearson Education. Consulted at <http://books.google.ca/books?id=HjxmKq5MABcC>.
- Ghosh, A., Mangalvedhe, N., Ratasuk, R., Mondal, B., Cudak, M., Visotsky, E., Thomas, T. A., Andrews, J. G., Xia, P., Jo, H. S., Dhillon, H. S. & Novlan, T. D. (2012). Heterogeneous cellular networks: From theory to practice. *IEEE communications magazine*, 50(6), 54-64. doi: 10.1109/MCOM.2012.6211486.
- Gummalla, A. C. V. & Limb, J. O. (2000). Wireless medium access control protocols. *IEEE communications surveys tutorials*, 3(2), 2-15. doi: 10.1109/COMST.2000.5340799.
- Gupta, A. K., Andrews, J. G. & Heath, R. W. (2016). On the feasibility of sharing spectrum licenses in mmwave cellular systems. *IEEE transactions on communications*, 64(9), 3981-3995. doi: 10.1109/TCOMM.2016.2590467.
- Guruacharya, S., Niyato, D., Hossain, E. & Kim, D. I. (2010, Dec). Hierarchical competition in femtocell-based cellular networks. *2010 IEEE global telecommunications conference globecom 2010*, pp. 1-5. doi: 10.1109/GLOCOM.2010.5683278.

- Guvenc, I., Jeong, M.-R., Watanabe, F. & Inamura, H. (2008). A hybrid frequency assignment for femtocells and coverage area analysis for co-channel operation. *Communications letters, IEEE*, 12(12), 880-882. doi: 10.1109/LCOMM.2008.081273.
- Guvenc, I., Jeong, M.-R., Sahin, M., Xu, H. & Watanabe, F. (2010, Sept). Interference avoidance in 3gpp femtocell networks using resource partitioning and sensing. *Personal, indoor and mobile radio communications workshops (pimrc workshops), 2010 IEEE 21st international symposium on*, pp. 163-168. doi: 10.1109/PIMRCW.2010.5670354.
- Ha, V. N. & Le, L. B. (2014). Fair resource allocation for ofdma femtocell networks with macrocell protection. *IEEE transactions on vehicular technology*, 63(3), 1388-1401. doi: 10.1109/TVT.2013.2284572.
- Hajir, M. & Gagnon, F. (2015, May). Qos-aware admission control for ofdma femtocell networks under fractional frequency-based allocation. *Vehicular technology conference (vtc spring), 2015 IEEE 81st*, pp. 1-6. doi: 10.1109/VTCSpring.2015.7146036.
- Hajir, M., Langar, R. & Gagnon, F. (2016a). Coalitional games for joint co-tier and cross-tier cooperative spectrum sharing in dense heterogeneous networks. *IEEE access*, 4, 2450-2464. doi: 10.1109/ACCESS.2016.2562498.
- Hajir, M., Langar, R. & Gagnon, F. (2016b, May). Solidarity-based cooperative games for resource allocation with macro-users protection in hetnets. *2016 IEEE international conference on communications (icc)*, pp. 1-7. doi: 10.1109/ICC.2016.7511562.
- Hajir, M. & Gagnon, F. (2017a). Spatial reuse model for mmwave frequencies in Ultra-Dense Small-Cells networks. *Submitted to 2017 IEEE 28th annual international symposium on personal, indoor, and mobile radio communications (pimrc)*.
- Hajir, M. & Gagnon, F. (2017b). Towards 1gbps in ultra-dense systems : A spatial frequency reuse model for small-cells based mmwave networks. *Submitted to IEEE transactions on wireless communications*, 1, 1-12.
- Hajir, M., Langar, R. & Gagnon, F. (2016c). Solidarity-based cooperative games for resource allocation with macro-users protection in HetNets. *IEEE icc 2016 - mobile and wireless networking symposium (icc'16 mwn)*, pp. 5429-5435.
- Han, Z. & Poor, H. V. (2009). Coalition games with cooperative transmission: a cure for the curse of boundary nodes in selfish packet-forwarding wireless networks. *IEEE transactions on communications*, 57(1), 203-213. doi: 10.1109/TCOMM.2009.0901.060661.
- Han, Z. & Liu, K. J. R. (2008). *Resource allocation for wireless networks: Basics, techniques, and applications*. New York, NY, USA: Cambridge University Press.
- Han, Z., Niyato, D., Saad, W., Baar, T. & Hjrungnes, A. (2012). *Game theory in wireless and communication networks: Theory, models, and applications* (ed. 1st). New York, NY, USA: Cambridge University Press.

- Hatoum, A., Aitsaadi, N., Langar, R., Boutaba, R. & Pujolle, G. (2011). Fcra: Femtocell cluster-based resource allocation scheme for ofdma networks. *Communications (icc), 2011 IEEE international conference on*, pp. 1-6. doi: 10.1109/icc.2011.5962705.
- Hinde, A. & Miles, R. (1980). Monte carlo estimates of the distributions of the random polygons of the voronoi tessellation with respect to a poisson process. *Journal of statistical computation and simulation*, 10(3-4), 205-223. doi: 10.1080/00949658008810370.
- Hong, E. J., Yun, S. Y. & Cho, D. H. (2009, Sept). Decentralized power control scheme in femtocell networks: A game theoretic approach. *2009 IEEE 20th international symposium on personal, indoor and mobile radio communications*, pp. 415-419. doi: 10.1109/PIMRC.2009.5449782.
- Hoteit, S., Secci, S., Langar, R., Pujolle, G. & Boutaba, R. (2012, Dec). A bankruptcy game approach for resource allocation in cooperative femtocell networks. *Global communications conference (globecom), 2012 IEEE*, pp. 1800-1805. doi: 10.1109/GLOCOM.2012.6503376.
- Huang, J. W. & Krishnamurthy, V. (2011). Cognitive base stations in lte/3gpp femtocells: A correlated equilibrium game-theoretic approach. *IEEE transactions on communications*, 59(12), 3485-3493. doi: 10.1109/TCOMM.2011.093011.100693.
- Ishii, H., Kishiyama, Y. & Takahashi, H. (2012, Dec). A novel architecture for lte-b :c-plane/u-plane split and phantom cell concept. *2012 IEEE globecom workshops*, pp. 624-630. doi: 10.1109/GLOCOMW.2012.6477646.
- Jain, R., Chiu, D.-M. & Hawe, W. R. (1984). *A quantitative measure of fairness and discrimination for resource allocation in shared computer system*.
- Jang, J. & Lee, K. B. (2003). Transmit power adaptation for multiuser ofdm systems. *IEEE journal on selected areas in communications*, 21(2), 171-178. doi: 10.1109/JSAC.2002.807348.
- Jo, H. S., Sang, Y. J., Xia, P. & Andrews, J. G. (2012). Heterogeneous cellular networks with flexible cell association: A comprehensive downlink sinr analysis. *IEEE trans. on wireless commun.*, 11(10), 3484-3495. doi: 10.1109/TWC.2012.081612.111361.
- Jo, H.-S., Mun, C., Moon, J. & Yook, J.-G. (2009). Interference mitigation using uplink power control for two-tier femtocell networks. *Wireless communications, IEEE transactions on*, 8(10), 4906-4910. doi: 10.1109/TWC.2009.080457.
- Kalai, E. & Samet, D. (1987). On weighted shapley values. *International journal of game theory*, 16(3), 205-222. doi: 10.1007/BF01756292.
- Kang, X., Zhang, R. & Motani, M. (2012). Price-based resource allocation for spectrum-sharing femtocell networks: A stackelberg game approach. *Selected areas in communications, IEEE journal on*, 30(3), 538-549. doi: 10.1109/JSAC.2012.120404.

- Kishiyama, Y., Benjebbour, A., Nakamura, T. & Ishii, H. (2013). Future steps of lte-a: evolution toward integration of local area and wide area systems. *IEEE wireless communications*, 20(1), 12-18. doi: 10.1109/MWC.2013.6472194.
- Kivanc, D., Li, G. & Liu, H. (2003). Computationally efficient bandwidth allocation and power control for ofdma. *IEEE transactions on wireless communications*, 2(6), 1150-1158. doi: 10.1109/TWC.2003.819016.
- Ko, C.-H. & Wei, H.-Y. (2011). On-demand resource-sharing mechanism design in two-tier ofdma femtocell networks. *Vehicular technology, IEEE transactions on*, 60(3), 1059-1071. doi: 10.1109/TVT.2011.2106171.
- La, R. & Anantharam, V. (2003). *A game-theoretic look at the gaussian multiaccess channel*. Electronics Research Laboratory, College of Engineering, University of California. Consulted at <https://books.google.ca/books?id=yiPvtgAACAAJ>.
- Langar, R., Secci, S., Boutaba, R. & Pujolle, G. (2015). An operations research game approach for resource and power allocation in cooperative femtocell networks. *Mobile computing, IEEE transactions on*, 14(4), 675-687. doi: 10.1109/TMC.2014.2329835.
- Larew, S. G., Thomas, T. A., Cudak, M. & Ghosh, A. (2013, Dec). Air interface design and ray tracing study for 5g millimeter wave communications. *2013 IEEE globecom workshops (gc wkshps)*, pp. 117-122. doi: 10.1109/GLOCOMW.2013.6824972.
- Lau, V. & Maric, S. (1998). Mobility of queued call requests of a new call-queueing technique for cellular systems. *Vehicular technology, IEEE transactions on*, 47(2), 480-488. doi: 10.1109/25.669086.
- Le, L. & Hossain, E. (2007). Multihop cellular networks: Potential gains, research challenges, and a resource allocation framework. *Communications magazine, IEEE*, 45(9), 66-73. doi: 10.1109/MCOM.2007.4342859.
- Le, L. B., Hossain, E., Niyato, D. & Kim, D. I. (2013a, June). Mobility-aware admission control with qos guarantees in ofdma femtocell networks. *Communications (icc), 2013 IEEE international conference on*, pp. 2217-2222. doi: 10.1109/ICC.2013.6654857.
- Le, L. B., Niyato, D., Hossain, E., Kim, D. I. & Hoang, D. T. (2013b). Qos-aware and energy-efficient resource management in ofdma femtocells. *Wireless communications, IEEE transactions on*, 12(1), 180-194. doi: 10.1109/TWC.2012.120412.120141.
- Lee, C., Huang, J.-H. & Wang, L.-C. (2010a, May). Distributed channel selection principles for femtocells with two-tier interference. *Vehicular technology conference (vtc 2010-spring), 2010 IEEE 71st*, pp. 1-5. doi: 10.1109/VETECS.2010.5493938.
- Lee, K., Jo, O. & Cho, D. H. (2011). Cooperative resource allocation for guaranteeing intercell fairness in femtocell networks. *IEEE communications letters*, 15(2), 214-216. doi: 10.1109/LCOMM.2011.010311.101238.

- Lee, P., Lee, T., Jeong, J. & Shin, J. (2010b, Feb). Interference management in lte femtocell systems using fractional frequency reuse. *Advanced communication technology (icact), 2010 the 12th international conference on*, 2, 1047-1051.
- Lee, Y. L., Chuah, T. C., Loo, J. & Vinel, A. (2014a). Recent advances in radio resource management for heterogeneous lte/lte-a networks. *IEEE communications surveys tutorials*, 16(4), 2142-2180. doi: 10.1109/COMST.2014.2326303.
- Lee, Y. L., Chuah, T. C., Loo, J. & Vinel, A. (2014b). Recent advances in radio resource management for heterogeneous lte/lte-a networks. *IEEE communications surveys tutorials*, 16(4), 2142-2180. doi: 10.1109/COMST.2014.2326303.
- Li, G. & Liu, H. (2006). Downlink radio resource allocation for multi-cell ofdma system. *IEEE transactions on wireless communications*, 5(12), 3451-3459. doi: 10.1109/TWC.2006.256968.
- Li, H., Xu, X., Hu, D., Qu, X., Tao, X. & Zhang, P. (2010). Graph method based clustering strategy for femtocell interference management and spectrum efficiency improvement. *Wireless communications networking and mobile computing (wicom), 2010 6th international conference on*, pp. 1-5. doi: 10.1109/WICOM.2010.5601236.
- Lien, S.-Y., Lin, Y.-Y. & Chen, K.-C. (2011). Cognitive and game-theoretical radio resource management for autonomous femtocells with qos guarantees. *Wireless communications, IEEE transactions on*, 10(7), 2196-2206. doi: 10.1109/TWC.2011.060711.100737.
- Lopez-Perez, D. & al. (2015). Towards 1 gbps/ue in cellular systems: Understanding ultra-dense small cell deployments. *IEEE commun. surveys tutorials*, 17(4), 2078-2101. doi: 10.1109/COMST.2015.2439636.
- Lopez-Perez, D., Valcarce, A., de la Roche, G. & Zhang, J. (2009). Ofdma femtocells: A roadmap on interference avoidance. *IEEE communications magazine*, 47(9), 41-48. doi: 10.1109/MCOM.2009.5277454.
- Luo, Z. Q. & Zhang, S. (2008). Dynamic spectrum management: Complexity and duality. *IEEE journal of selected topics in signal processing*, 2(1), 57-73. doi: 10.1109/JSTSP.2007.914876.
- Ma, B., Cheung, M. H., Wong, V. & Huang, J. (2015). Hybrid overlay/underlay cognitive femtocell networks: A game theoretic approach. *Wireless communications, IEEE transactions on*, 14(6), 3259-3270. doi: 10.1109/TWC.2015.2403363.
- MacCartney, G. R. & Rappaport, T. S. (2014, June). 73 ghz millimeter wave propagation measurements for outdoor urban mobile and backhaul communications in new york city. *2014 IEEE international conference on communications (icc)*, pp. 4862-4867. doi: 10.1109/ICC.2014.6884090.

- MacCartney, G. R., Zhang, J., Nie, S. & Rappaport, T. S. (2013, Dec). Path loss models for 5g millimeter wave propagation channels in urban microcells. *2013 IEEE global commun. conf.*, pp. 3948-3953. doi: 10.1109/GLOCOM.2013.6831690.
- Maheshwari, K. & Kumar, A. (2000). Performance analysis of microcellization for supporting two mobility classes in cellular wireless networks. *IEEE transactions on vehicular technology*, 49(2), 321-333. doi: 10.1109/25.832964.
- Mathur, S., Sankar, L. & Mandayam, N. B. (2008). Coalitions in cooperative wireless networks. *IEEE journal on selected areas in communications*, 26(7), 1104-1115. doi: 10.1109/JSAC.2008.080908.
- Mehrpouyan, H. & al. (2015). Hybrid millimeter-wave systems: a novel paradigm for hetnets. *IEEE commun. mag.*, 53(1), 216-221. doi: 10.1109/MCOM.2015.7010537.
- Moon, J.-M. & Cho, D.-H. (2009). Efficient handoff algorithm for inbound mobility in hierarchical macro/femto cell networks. *Communications letters, IEEE*, 13(10), 755-757. doi: 10.1109/LCOMM.2009.090823.
- Mustika, I., Yamamoto, K., Murata, H. & Yoshida, S. (2011, May). Potential game approach for self-organized interference management in closed access femtocell networks. *Vehicular technology conference (vtc spring), 2011 IEEE 73rd*, pp. 1-5. doi: 10.1109/VETECS.2011.5956517.
- Myerson, R. (1997). *Game theory*. Harvard University Press. Consulted at <https://books.google.ca/books?id=E8WQFRCsNr0C>.
- Naranjo, J., Viering, I. & Friederichs, K.-J. (2012). A cognitive radio based dynamic spectrum access scheme for lte heterogeneous networks. *Wireless telecommunications symposium (wts), 2012*, pp. 1-7. doi: 10.1109/WTS.2012.6266099.
- Ng, D. & Schober, R. (2011). Resource allocation and scheduling in multi-cell ofdma systems with decode-and-forward relaying. *Wireless communications, IEEE transactions on*, 10(7), 2246-2258. doi: 10.1109/TWC.2011.042211.101183.
- Nie, S., MacCartney, G. R., Sun, S. & Rappaport, T. S. (2013, Sept). 72 ghz millimeter wave indoor measurements for wireless and backhaul communications. *2013 IEEE 24th annual international symposium on personal, indoor, and mobile radio communications (pimrc)*, pp. 2429-2433. doi: 10.1109/PIMRC.2013.6666553.
- Nitsche, T. & al. (2014). IEEE 802.11ad: directional 60 ghz communication for multi-gigabit-per-second wi-fi. *IEEE commun. mag.*, 52(12), 132-141. doi: 10.1109/MCOM.2014.6979964.
- Novlan, T. D. & al. (2012). Analytical evaluation of fractional frequency reuse for heterogeneous cellular networks. *IEEE trans. on commun.*, 60(7), 2029-2039. doi: 10.1109/T-COMM.2012.061112.110477.

- Nowak, A. & Radzik, T. (1994). A solidarity value for non-person transferable utility games. *International journal of game theory*, 23(1), 43-48. doi: 10.1007/BF01242845.
- Owen, G. (1982). *Game theory*. Academic Press.
- Pan, J.-L. & Djuric, P. (2002). Multibeam cellular mobile communications with dynamic channel assignment. *Vehicular technology, IEEE transactions on*, 51(5), 1252-1258. doi: 10.1109/TVT.2002.801745.
- Pantisano, F., Bennis, M., Saad, W. & Debbah, M. (2012). Spectrum leasing as an incentive towards uplink macrocell and femtocell cooperation. *Selected areas in communications, IEEE journal on*, 30(3), 617-630. doi: 10.1109/JSAC.2012.120411.
- Pantisano, F., Bennis, M., Saad, W., Debbah, M. & Latva-aho, M. (2013). Interference alignment for cooperative femtocell networks: A game-theoretic approach. *Mobile computing, IEEE transactions on*, 12(11), 2233-2246. doi: 10.1109/TMC.2012.196.
- Pao, W.-C., Chen, Y.-F. & Chan, C.-Y. (2013). Power allocation schemes in ofdm-based femtocell networks. *Wirel. pers. commun.*, 69(4), 1165-1182. doi: 10.1007/s11277-012-0626-2.
- Pedersen, K. I., Wang, Y., Soret, B. & Frederiksen, F. (2012). eicic functionality and performance for lte hetnet co-channel deployments. 1-5. doi: 10.1109/VTCFall.2012.6399106.
- Peng, M., Li, Y., Jiang, J., Li, J. & Wang, C. (2014). Heterogeneous cloud radio access networks: a new perspective for enhancing spectral and energy efficiencies. *IEEE wireless communications*, 21(6), 126-135. doi: 10.1109/MWC.2014.7000980.
- Qingling, Z. & Li, J. (2006, Oct). Rain attenuation in millimeter wave ranges. *2006 7th international symposium on antennas, propagation and theory*, pp. 1-4. doi: 10.1109/IS-APE.2006.353538.
- Rangan, S., Rappaport, T. S. & Erkip, E. (2014). Millimeter-wave cellular wireless networks: Potentials and challenges. *Proc. of the IEEE*, 102(3), 366-385. doi: 10.1109/JPROC.2014.2299397.
- Rappaport. (2009). *Wireless communications: Principles and practice*. Dorling Kindersley. Consulted at <https://books.google.co.uk/books?id=11qEWkNFFwQC>.
- Rappaport, T. S. & al. (2013). Millimeter wave mobile communications for 5g cellular: It will work! *IEEE access*, 1, 335-349. doi: 10.1109/ACCESS.2013.2260813.
- Rappaport, T. S. & al. (2015). Wideband millimeter-wave propagation measurements and channel models for future wireless communication system design. *IEEE trans. on commun.*, 63(9), 3029-3056. doi: 10.1109/TCOMM.2015.2434384.

- Rappaport, T. S., Murdock, J. N. & Gutierrez, F. (2011). State of the art in 60-ghz integrated circuits and systems for wireless communications. *Proceedings of the IEEE*, 99(8), 1390-1436. doi: 10.1109/JPROC.2011.2143650.
- Rappaport, T. S., Gutierrez, F., Ben-Dor, E., Murdock, J. N., Qiao, Y. & Tamir, J. I. (2013). Broadband millimeter-wave propagation measurements and models using adaptive-beam antennas for outdoor urban cellular communications. *IEEE transactions on antennas and propagation*, 61(4), 1850-1859. doi: 10.1109/TAP.2012.2235056.
- Rappaport Stephen, S. & Hu, L.-R. (1994). Microcellular communication systems with hierarchical macrocell overlays: traffic performance models and analysis. *Proceedings of the IEEE*, 82(9), 1383-1397. doi: 10.1109/5.317084.
- Rose, L., Le Martret, C. & Debbah, M. (2012). Channel and power allocation algorithms for ad hoc clustered networks. *Communications and information systems conference (mcc), 2012 military*, pp. 1-8.
- Saad, W., Han, Z., Debbah, M., Hjørungnes, A. & Basar, T. (2009a). Coalitional game theory for communication networks. *Signal processing magazine, IEEE*, 26(5), 77-97. doi: 10.1109/MSP.2009.0000000.
- Saad, W., Han, Z., Debbah, M., Hjørungnes, A. & Basar, T. (2009b). Coalitional game theory for communication networks: A tutorial. *Corr*, abs/0905.4057. Consulted at <http://arxiv.org/abs/0905.4057>.
- Samimi, M., Wang, K., Azar, Y., Wong, G. N., Mayzus, R., Zhao, H., Schulz, J. K., Sun, S., Gutierrez, F. & Rappaport, T. S. (2013, June). 28 ghz angle of arrival and angle of departure analysis for outdoor cellular communications using steerable beam antennas in new york city. *2013 IEEE 77th vehicular technology conference (vtc spring)*, pp. 1-6. doi: 10.1109/VTCSpring.2013.6691812.
- Saquib, N., Hossain, E., Le, L. B. & Kim, D. I. (2012). Interference management in ofdma femtocell networks: issues and approaches. *Wireless communications, IEEE*, 19(3), 86-95. doi: 10.1109/MWC.2012.6231163.
- Saquib, N., Hossain, E. & Kim, D. I. (2013). Fractional frequency reuse for interference management in lte-advanced hetnets. *Wireless communications, IEEE*, 20(2), 113-122. doi: 10.1109/MWC.2013.6507402.
- Semasinghe, P., Hossain, E. & Zhu, K. (2015). An evolutionary game for distributed resource allocation in self-organizing small cells. *Mobile computing, IEEE transactions on*, 14(2), 274-287. doi: 10.1109/TMC.2014.2318700.
- Sen, S., Arunachalam, A., Basu, K. & Wernik, M. (1999). A qos management framework for 3g wireless networks. *Wcnc. 1999 IEEE wireless communications and networking conference (cat. no.99th8466)*, pp. 1273-1277 vol.3. doi: 10.1109/WCNC.1999.796942.

- Shapley, L. S. Cores of convex games. *International journal of game theory*, 1(1), 11–26. doi: 10.1007/BF01753431.
- Shapley, L. S. (1952). *A value for n-person games*.
- Shen, Z., Andrews, J. G. & Evans, B. L. (2005). Adaptive resource allocation in multiuser ofdm systems with proportional rate constraints. *IEEE transactions on wireless communications*, 4(6), 2726-2737. doi: 10.1109/TWC.2005.858010.
- Singh, S., Dhillon, H. S. & Andrews, J. G. (2013). Offloading in heterogeneous networks: Modeling, analysis, and design insights. *IEEE transactions on wireless communications*, 12(5), 2484-2497. doi: 10.1109/TWC.2013.040413.121174.
- Song, G. & Li, Y. (2005a). Cross-layer optimization for ofdm wireless networks-part i: theoretical framework. *IEEE transactions on wireless communications*, 4(2), 614-624. doi: 10.1109/TWC.2004.843065.
- Song, G. & Li, Y. (2005b). Cross-layer optimization for ofdm wireless networks-part ii: algorithm development. *IEEE transactions on wireless communications*, 4(2), 625-634. doi: 10.1109/TWC.2004.843067.
- standard3gpp. Telecommunication management; self-organizing networks (SON) ; concepts and requirements.
- Sulyman, A. I., Nassar, A. T., Samimi, M. K., Maccartney, G. R., Rappaport, T. S. & Alsanie, A. (2014a). Radio propagation path loss models for 5g cellular networks in the 28 ghz and 38 ghz millimeter-wave bands. *IEEE communications magazine*, 52(9), 78-86. doi: 10.1109/MCOM.2014.6894456.
- Sulyman, A. I., Nassar, A. T., Samimi, M. K., Maccartney, G. R., Rappaport, T. S. & Alsanie, A. (2014b). Radio propagation path loss models for 5g cellular networks in the 28 ghz and 38 ghz millimeter-wave bands. *IEEE communications magazine*, 52(9), 78-86. doi: 10.1109/MCOM.2014.6894456.
- Sun, S., MacCartney, G. R. & Rappaport, T. S. (2016, April). Millimeter-wave distance-dependent large-scale propagation measurements and path loss models for outdoor and indoor 5g systems. *2016 10th european conf. on antennas and propagation (eucaP)*, pp. 1-5. doi: 10.1109/EuCAP.2016.7481506.
- Sun, Y., Jover, R. & Wang, X. (2012). Uplink interference mitigation for ofdma femtocell networks. *Wireless communications, IEEE transactions on*, 11(2), 614-625. doi: 10.1109/TWC.2011.120511.101794.
- Urgaonkar, R. & Neely, M. (2012). Opportunistic cooperation in cognitive femtocell networks. *Selected areas in communications, IEEE journal on*, 30(3), 607-616. doi: 10.1109/JSAC.2012.120410.

- Venturino, L., Prasad, N. & Wang, X. (2009). Coordinated scheduling and power allocation in downlink multicell ofdma networks. *IEEE transactions on vehicular technology*, 58(6), 2835-2848. doi: 10.1109/TVT.2009.2013233.
- Vidal-Puga, J. (2005). *The Harsanyi paradox and the 'right to talk' in bargaining among coalitions* (Report n°0501005). Consulted at <https://ideas.repec.org/p/wpa/wuwpga/0501005.html>.
- Wang, H., Zhou, X. & Reed, M. C. (2014). Coverage and throughput analysis with a non-uniform small cell deployment. *IEEE trans. on wireless commun.*, 13(4), 2047-2059. doi: 10.1109/TWC.2014.022014.130855.
- Wang, T. & Vandendorpe, L. (2011). Iterative resource allocation for maximizing weighted sum min-rate in downlink cellular ofdma systems. *IEEE transactions on signal processing*, 59(1), 223-234. doi: 10.1109/TSP.2010.2078811.
- Wang, Y. & Pedersen, K. I. (2012). Performance analysis of enhanced inter-cell interference coordination in lte-advanced heterogeneous networks. 1-5. doi: 10.1109/VETECS.2012.6240233.
- Wells, J. (2009). Faster than fiber: The future of multi-g/s wireless. *IEEE microwave magazine*, 10(3), 104-112. doi: 10.1109/MMM.2009.932081.
- Wong, C. Y., Cheng, R. S., Lataief, K. B. & Murch, R. D. (1999). Multiuser ofdm with adaptive subcarrier, bit, and power allocation. *IEEE journal on selected areas in communications*, 17(10), 1747-1758. doi: 10.1109/49.793310.
- Wu, Y., Zhang, D., Jiang, H. & Wu, Y. (2009, Sept). A novel spectrum arrangement scheme for femto cell deployment in lte macro cells. *Personal, indoor and mobile radio communications, 2009 IEEE 20th international symposium on*, pp. 6-11. doi: 10.1109/PIMRC.2009.5450296.
- Zahir, T., Arshad, K., Nakata, A. & Moessner, K. (2013). Interference management in femtocells. *Communications surveys tutorials, IEEE*, 15(1), 293-311. doi: 10.1109/SURV.2012.020212.00101.
- Zhang, H., Jiang, C., Beaulieu, N., Chu, X., Wen, X. & Tao, M. (2014). Resource allocation in spectrum-sharing ofdma femtocells with heterogeneous services. *Communications, IEEE transactions on*, 62(7), 2366-2377. doi: 10.1109/TCOMM.2014.2328574.
- Zhang, L., Yang, L. & Yang, T. (2010). Cognitive interference management for lte-a femtocells with distributed carrier selection. *Vehicular technology conference fall (vtc 2010-fall), 2010 IEEE 72nd*, pp. 1-5. doi: 10.1109/VETEFCF.2010.5594585.
- Zhao, H., Mayzus, R., Sun, S., Samimi, M., Schulz, J. K., Azar, Y., Wang, K., Wong, G. N., Gutierrez, F. & Rappaport, T. S. (2013, June). 28 ghz millimeter wave cellular communication measurements for reflection and penetration loss in and around buildings in new

york city. *2013 IEEE international conference on communications (icc)*, pp. 5163-5167.
doi: 10.1109/ICC.2013.6655403.